CHALMERS

Decentralized Thermal Energy Storage for District Cooling

A techno-economic case study on the feasibility of small scale latent thermal energy storage in Gothenburg

Master's Thesis in Sustainable Energy Systems

FELICIA HÄGGSTRÖM
ISA WESSÉN

DEPARTMENT OF ARCHITECTURE AND CIVIL ENGINEERING
CHALMERS UNIVERSITY OF TECHNOLOGY
Gothenburg, Sweden 2026
www.chalmers.se

Master's Thesis 2026

Decentralized Thermal Energy Storage for District Cooling

A techno-economic case study on the feasibility of small scale latent thermal energy storage in Gothenburg

FELICIA HÄGGSTRÖM
ISA WESSÉN

CHALMERS

Department of Architecture and Civil Engineering
Chalmers University of Technology
Göteborg 2026

Decentralized Thermal Energy Storage for District Cooling
A techno-economic case study on the feasibility of small scale latent thermal energy storage in Gothenburg
Felicia Häggström, Isa Wessén

Supervisor: Rikard Edland, Göteborg Energi AB
Examinor: Angela Sasic Kalagasidis, Institution of Architecture and Civil Engineering

Master's thesis 2026
Department of Architecture and Civil Engineering
Chalmers University of Technology
SE-412 96 Gothenburg
Telephone +46 31 772 1000

Typeset in LaTeX
Gothenburg, Sweden 2026

Decentralized Thermal Energy Storage for District Cooling
A techno-economic case study on the feasibility of small scale latent thermal energy storage in Gothenburg
Felicia Häggström, Isa Wessén
Department of Architecture and Civil Engineering
Chalmers University of Technology

Abstract

District cooling (DC) networks are expanding. To accommodate future network expansion and mitigate increasing peak demand, thermal energy storage (TES) can be incorporated into the DC networks. Decentralized storage has the potential to relieve production and network capacity during peak demand hours by storing cooling energy at individual customer sites. This thesis investigates the theoretical potential of decentralized TES containing phase change materials, called latent thermal energy storage (LTES), both from the perspective of the customer and producer. The analysis uses mixed integer linear programming (MILP) together with operational data from a critical section of Gothenburg's DC network (2025). The results indicated that peak demand in the Almedal area could be reduced by 6.1% using measured data, and by 10.0% with optimized operating conditions. Network flow reductions were also evaluated, showing a decrease of around 3.2% using measured data, creating potential for new customers to connect to the network. Optimizing operating conditions alone reduced the flow by 34.9%, while the addition of storage provided a reduction by 10.0%. The economic analysis showed that profitability is highly case-dependent and primarily driven by achieved peak reduction. While customers generally benefit more economically from LTES implementation than producers, a cost-sharing approach improved the profitability for both parties if sufficient peak reduction is achieved. With the calculated investment cost of 2149 SEK/kWh, the producer would be willing to cover between 45-81% of the investment to remain profitable, depending on discount rate. In contrast, the customer could, independently of discount rate, pay for the full storage and still remain profitable over a 10 year project period.

Key Words: PCM, district cooling, latent thermal energy storage, cooling storage, Gothenburg, energy system modeling, linear programming, mixed-integer linear programming, storage optimization, peak reduction, HVAC

Acknowledgements

We would first like to thank our supervisor at Göteborg Energi, Rikard Edland, for his continuous support, guidance, and availability throughout this thesis project. Without his help, this thesis would not have been possible. We would also like to thank Angela Sasic Kalagasidis, our examiner at Chalmers, for her encouragement, support, and belief in us throughout the project. We are sincerely grateful to both of them for trusting us, giving us the freedom to shape the thesis according to our ambitions, and guiding us all the way to the finish line.

We would also like to express our gratitude to Anders Strand for his support and expertise regarding the district cooling network. In addition, we would like to thank everyone at Göteborg Energi, especially within the district cooling network department, who contributed to, showed interest in and supported us throughout this thesis work.

(From Felicia) I would like to sincerely thank Isa for these six months together. Your contribution, positive energy, and constant encouragement have been invaluable to me throughout this project. I truly could not have wished for a better thesis partner.

(From Isa) I want to say thank you to Felicia as well. I am so grateful for you as a thesis partner. With your determined, ambitious and positive spirit, writing this thesis has been incredibly rewarding. I know there is no one I would have laughed with more, and I could not have wished for anyone better.

Felicia Häggström & Isa Wessén, Gothenburg, June 2026

List of Acronyms

Below is the list of acronyms and abbreviations that have been used throughout this thesis listed in alphabetical order:

DC	District Cooling
DH	District Heating
DHC	District Heating and Cooling
FLH	Full Load Hours
HTF	Heat Transfer Fluid
HX	Heat Exchanger
LP	Linear Programming
LTES	Latent Thermal Energy Storage
MILP	Mixed Integer Linear Programming
NPV	Net Present Value
PBP	Payback Period
PCM	Phase Change Material
SOC	State of Charge
STES	Sensible Thermal Energy Storage
TCES	Thermochemical Energy Storage
TES	Thermal Energy Storage

Nomenclature

Below is the nomenclature of indices, sets, parameters, and variables that have been used throughout this thesis.

Indices & Notation

t	Index for hourly time step
d	Index for daily time step
i	Index for customer

Sets

$\mathcal{T}$	Set of all time steps
$\mathcal{D}$	Set of number of days
$\mathcal{T}_{charge}$	Subset to $\mathcal{T}$ for all time steps when charging is permitted
$\mathcal{T}_{discharge}$	Subset to $\mathcal{T}$ for all time steps when discharging is permitted
$\mathcal{I}$	Set of all customers

Parameters

$T^{sup,s}_{i,t}$	Supply water temperature on secondary side for customer i at timestep t $[°C]$
$T^{sup,p}_{i,t}$	Supply water temperature on primary side for customer i at timestep t $[°C]$
$T^{ret,s}_{i,t}$	Return water temperature on secondary side for customer i at timestep t$[°C]$
$T^{ret,p}_{i,t}$	Return water temperature on primary side for customer i at timestep t $[°C]$
N^{unit}_{i}	Number of units installed for customer i

CAP_i	Installed LTES capacity for customer i $[kWh]$
$\dot{m}^{charge}$	Maximum mass flow rate for charging the LTES $[kg/s]$
$load_{i,t}$	load for customer i at timestep t $[kWh/h]$
α	Charging penalty weight
c_p	Specific heat capacity for water $[J/kgK]$
$T^{LTES}_{discharge}$	Minimum outlet water temperature during discharging of the LTES $[°C]$
T^{LTES}_{charge}	Outlet water temperature during charging of the LTES $[°C]$
$\dot{m}_{i,t}$	flow for customer i at timestep t $[kg/s]$
T^{LTES}_{melt}	Melting temperature for the PCM in the LTES $[°C]$
w^{max}	Maximum fraction of mass flow rate
M	Big-M parameter for discharge
ϵ	Small positive constant used in binary activation constraints
$load^{max}_{i,d}$	Daily maximum load for customer i for day d $[kW]$
$\dot{m}^{new,s}_{i,t}$	New mass flow after discharging for customer i at timestep t $[kg/s]$
$\dot{m}^{LTES}_{i,t}$	Mass flow rate going into the LTES for customer i at timestep t $[kg/s]$
$T^{mixed,s}_{i,t}$	New supply water temperature on secondary side for customer i at timestep t $[°C]$
c^{PCM}_i	Investment cost of the PCM material for customer i $[SEK]$
c^{energy}_i	Energy cost for customer i $[SEK]$
$c^{capacity}_i$	Capacity cost for customer i $[SEK]$
c^{flow}_i	Flow cost for customer i $[SEK]$
c^{tot}_i	Total cost for customer i $[SEK]$
c^{inv}_i	Total investment cost of LTES for customer i $[SEK]$
PBP_i	Payback period for customer i $[years]$
NPV^{cust}_i	Net Present Value for each customer $[SEK]$
FLH	Full load hours for new customers in the DC network $[h]$
$c^{avg\ inc}$	Calculated average income for new customers in the DC network $[SEK/kWh]$
c^{loss}	Loss of income from customers for producer $[SEK/year]$
c^{inc}	Total yearly income for producer based on new customers in the DC network $[SEK/year]$
$c^{connect}$	Connection cost for producer from implementing new customers $[SEK]$
NPV^{prod}	Net Present Value for producer $[SEK]$

Variables

$SOC_{i,t}$	State of charge for LTES for customer i at timestep t $[kWh]$
$charge_{i,t}$	Charging of storage for customer i at timestep t $[kW]$
$discharge_{i,t}$	Discharging of storage for customer i at timestep t $[kW]$
$peak_{i,d}$	Peak load for customer i for day d $[kW]$
$w_{i,t}$	Fraction of mass flow rate for discharging at timestep t
$on_{i,t}$	Binary variable indicating activation of LTES for customer i at timestep t

Contents

List of Figures

List of Tables

1
Introduction

Rising global temperatures and increasing urban densification are increasing the demand for cooling[5][6]. Cooling currently accounts for approximately 20% of global electricity demand, a share expected to grow due to the continued urbanization, increased living standards and economic development[7]. Today, most cooling in EU-countries is provided by on-site systems, resulting in a high dependence on electricity for appliances and compressors such as air conditioners [8]. District cooling (DC) networks offer an alternative approach by utilizing efficient energy conversion technologies as well as natural cooling sources if temperatures allow it, therefore providing an energy-efficient and cost-effective method of distributing cooling[9][7].

Gothenburg, the second-largest city of Sweden, has an expanding DC network in response to growing demand. The network currently uses three production methods: natural cooling from the Göta River, absorption chillers, and compression chillers[10]. However, the operational mix varies with weather conditions and seasonal variations. During warmer periods, the temperature of the Göta River becomes too high to be effectively utilized, this increases the reliance on absorption and compressor chillers[11]. Similarly, during periods where high district heating (DH) demand increases, there is a low supply of excess heat available for absorption chillers. During these periods, additional cooling production from electrically driven compressors is required to meet the cooling demand.

To improve and expand DC networks, peak-shaving strategies can be used. One approach is thermal energy storage (TES), which allows excess cooling capacity to be stored during periods of low demand and utilized when demand peaks, typically during daytime hours[12]. Traditionally, centralized TES solutions such as large accumulator tanks have been used to manage daily demand variations and improve overall energy efficiency. Although, decentralized storage solutions located at the consumer sites offers additional benefits compared to centralized ones, by reducing flow and pressure constraints in the network, enabling greater utilization of existing infrastructure[2]. Among TES technologies, latent thermal energy storage (LTES), using phase change materials (PCM) is particularly suitable for decentralized cooling applications due to its high energy density and operation within narrow temperature ranges.

This thesis aims to investigate the use of decentralized storage within the DC network of Gothenburg that is owned and operated by Göteborg Energi AB. The case study consists of the Almedal area which is a critical part of the DC network. This area accounts for 4.95% of the annual production of cooling, and 6.20% of the total network flow[2]. The area has 11 customers connected as of now and is likely to expand in the future. Almedal is deemed critical since it is located far away from production sites and is a branching section that does not form a loop.

In addition, pipe flow capacity constraints limit the DC system and restrict the connection of additional customers[2]. If more customers want to connect to the pipeline, the flow rate during peak hours will become a limiting factor until the network is expanded or demand is reduced. When constructing new urban development areas, connections to the DC network could be designed with storage integration in mind, to potentially reduce the original peak flow rate. The planned Arena district in Gothenburg is one of these areas, where decentralized storage potentially could enable reduced flow rates and, consequently, allow smaller pipe dimensions in the district cooling network[13].

1.1 Aim and Scope

The aim of this thesis is to investigate to what extent LTES can benefit the current network with the Almedal area as a case study. The research questions are presented below.

1. **To what extent is LTES a feasible decentralized cold storage solution for Gothenburg?**
    - Is LTES a suitable storage solution?
    - What parameters are important when designing and fitting a LTES and choosing PCM?
    - What PCM melting temperatures are compatible with Gothenburg's DC temperatures?
    - What is a reasonable storage size for decentralized implementation, considering cost and operational impact?
    - How can a LTES unit be connected to a substation?

2. **How would decentralized LTES have affected operation in Almedal during the summer period of 2025?**
    - How would peak loads and demand profiles have changed with storage?
    - What economic benefits could decentralized storage have provided for connected customers?

3. **What are the theoretical possibilities of installed LTES in DC networks?**
    - What system requirements are of importance to effectively utilize LTES in DC networks?
    - To what extent can LTES increase available capacity and enable new customers to connect to the DC network?
    - What economic benefits can storage provide from a producer perspective, through network expansion?

1.2 System Boundary and Delimitations

The geographical boundary of the analysis consists of the Almedal area, located in the southeastern part of Gothenburg and includes 11 connected customers. The analysis is primarily based on measured data obtained from this area. However, operational data related to cooling production and electricity use are, where necessary, evaluated from a broader system perspective including the complete Gothenburg DC network.

This study includes several delimitations. The first concerns the evaluation of PCM. No specific PCM is selected or experimentally validated. Instead, the analysis is based on a generalized PCM representing materials that are technologically feasible and meet the defined performance criteria. No laboratory testing has been conducted to determine the chemical composition or thermophysical properties of a specific PCM. Consequently, the PCM used in the modeling is based on averaged properties derived from literature for a suitable category of PCM.

Furthermore, this study is based on a case study of the Gothenburg DC network and is therefore tailored to its specific operational conditions. As a result, the findings are not directly generalizable to other DC systems with different supply temperatures, return temperatures, operating strategies, or system constraints.

The analysis is limited to the period between the first of May and the last of September, corresponding both to the availability of operational data and the period during which cooling demand occurs and typically reaches its highest levels.

1.3 Methodology Overview

The theoretical foundation of the study is established through a literature review of TES, PCM and DC networks, presented in chapter 2 and chapter 3. The review focuses on the operational principles, advantages and limitations of PCM-based storage systems, together with the characteristics and operational conditions of the Gothenburg DC network. Due to PCM storage in DC networks being an emerging technology, there are limited availability of large-scale operational data and theoretical studies. Therefore, pilot projects and simulation-based research were prioritized over extensive empirical operational studies. Relevant literature was identified through targeted searches in academic databases including Scopus, ScienceDirect, Web of Science and Google Scholar.

The modeling methodology is presented in chapter 4, where the literature findings are combined with operational data obtained through collaboration with *Göteborg Energi AB*. Based on this, LTES configurations were developed and implemented in a linear optimization (LP) model and a mixed integer linear optimization (MILP) model. Further, the methodology includes assumptions regarding PCM- and the DC network-properties as well as thermal calculations.

The obtained results are presented and analyzed in chapter 5, including the reduction potential of the configurations, optimized operating conditions for the Almedal area and economic performance. The results are then further discussed and analyzed in chapter 6, where the sensitivity analyses are presented along with further evaluations of the results and the data. Finally, the main findings and conclusions of the study are summarized in chapter 7.

2

Literature Review of Thermal Energy Storage

This chapter provides an overview of the relevant TES technologies. The literature review has a particular focus on LTES using PCM, which is the primary technology investigated in this study. The chapter also presents PCM material characteristics, system designs, and key design considerations relevant to DC applications.

2.1 Thermal Energy Storage

TES systems provide a method for storing energy used in cooling applications[12]. Cooling storage has the potential to reduce peak load in DC networks, thereby limiting the use of electrically driven compressors that are currently used to meet peak demand.[14]. Additionally, when used as a complement to a DC system, these can help balance the gap between demand and supply, and ultimately increase the maximal number of customers due to the peak flow rate being reduced with the help of storage. The idea is to make use of available cooling capacity and charge the storage during nighttime, when demand is lower, and then discharge the stored cooling during daytime at higher demands.

There are three main types of TES that can be used; sensible thermal energy storage, latent thermal energy storage and thermochemical energy storage[15]. In the following section, each type of TES will broadly be described.

2.1.1 Sensible Energy

Sensible thermal energy storage (STES) is a commercially available technology that exists today in different scales[16]. STES consists of thermal energy being stored as a medium without undergoing any phase change, thus remaining in one phase while varying in temperature[17]. STES can vary from short term to long term, and a general example could be a large insulated tank with availability to store water and maintaining its temperature through insulation. The amount of thermal energy stored or released for a sensible storage process is given by Equation 2.1.

$$Q = m \cdot c_p \cdot (\Delta T) \tag{2.1}$$

Q equals the amount of thermal energy $[J]$, m the mass of storage material $[kg]$, c_p the specific heat capacity that is averaged in the equation to be applicable for a wide temperature range $[J/(kg \cdot K)]$, and ΔT is the difference in temperatures T_{charge} and $T_{discharge}$, in $[K]$ or $[°C]$. Therefore, to get a higher amount of thermal energy (Q), either m or ΔT needs to be increased.

The energy efficiency of STES can be very high for shorter periods thanks to a high proportion of the stored energy being available to use[17]. The energy loss in STES is dependent on factors such as the time the energy is planned to be stored, the ambient temperature, and insulation of the storage container itself. For STES, a wide selection of materials are available. When deciding upon a suitable one, properties such as cost effectiveness, low corrosiveness, climate impact and flammability are important to consider. Other important aspects are high energy density and high thermal conductivity. The operating temperature ranges can be tailored to meet the system requirements, however they are constrained by the phase change temperatures.

2.1.2 Latent Energy

Latent thermal energy storage (LTES) is a type of thermal energy storage where the energy is stored in the phase change of a material[12]. This could be liquid to gas and vice versa, or solid to liquid and vice versa. Latent energy is characterized by large changes in enthalpy whereas the temperature remains near constant. This makes LTES attractive when working with smaller temperature differences between charging and discharging. Some requirement for suitable LTES system materials include a small temperature phase change window that is compatible and chosen to fit the existing equipment. Furthermore, thermal conductivity is important, along with the chemical suitability and physical compatibility of the PCM with the encapsulating materials.

The definition of latent energy is defined in Equation 2.2. In this equation, it is assumed that the entire mass of PCM will phase change, thus representing an ideal phase change process[18]. Q is the latent energy $[J]$, m is the mass of the PCM $[kg]$ and Δh_m the enthalpy difference per kilogram $[J/kg]$.

$$Q = m \cdot \Delta h_m \tag{2.2}$$

The phase changing consists of different steps. Looking at Figure 2.1, there are two sensible energy zones and one latent energy zone during the complete phase change of the PCM[19]. The sensible ones consists of the heating/cooling of the solid phase as well as the liquid phase. The full representation of the phase change process is thus a combination of the latent energy and sensible energy equation, and are defined in Equation 2.3[18]. In this equation, there is a c_p for both the solid and the liquid phase. The integrals are calculated with respect to the temperature at inlet of the heat transfer fluid (HTF) and the material melting point temperature, as well as the melting temperature and the outlet temperature.

$$Q = \int_{T_i}^{T_m} m \cdot c_{p,s}\, dT + m \cdot \Delta h_m + \int_{T_m}^{T_f} m \cdot c_{p,l}\, dT \tag{2.3}$$

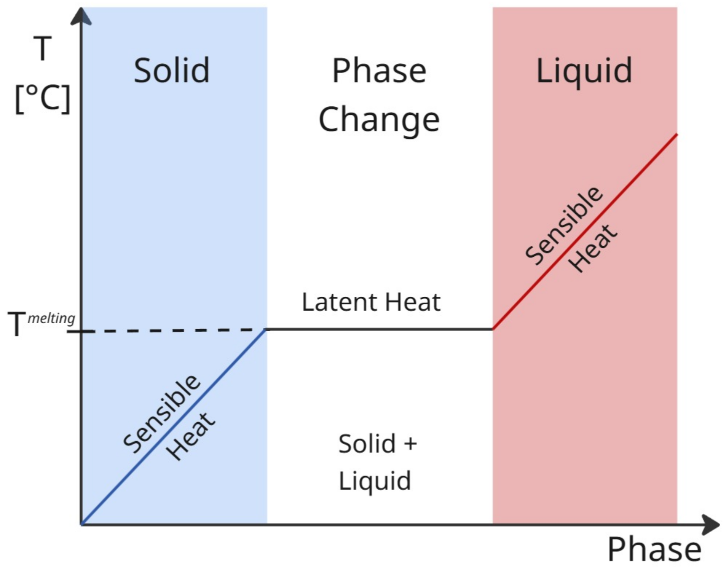

Figure 2.1: PCM diagram of how the temperature varies during phase change.

Compared to STES, LTES has a higher energy density. Consequently, for the same amount of stored energy, a STES system must be significantly larger to provide an equivalent cooling capacity [20]. LTES releases and absorbs energy during the phase change process, meaning that the temperature remains nearly constant when absorbing or releasing the energy. This makes LTES achieve a narrow operating temperature range, combined with higher energy density[12]. LTES is therefore presumed to be better suited for control-oriented strategies and small-scale applications[20].

2.1.3 Thermochemical Energy

Thermochemical energy storage (TCES) is currently in the formative phase[16]. Therefore, the market of TCES over the past years is limited, and consists mostly of research and development projects as well as demonstration projects. This storage method utilizes thermochemical materials as a way of storing or releasing heat[21]. This is done through a reversible thermochemical reaction and strong chemical bonds, which provides a high energy density of the storage[22].

The different TCES alternatives are generally categorized as thermochemical absorption storage, thermochemical adsorption storage and chemical reaction storage[22]. The first two, absorption and adsorption, are the ones suitable for lower temperature applications. However, the working temperatures for charging the material are often much higher, and often require temperatures above 50 °C. Consequently, this type of storage is considered unsuitable in this context. The discharge can however provide temperatures as cold as 5 °C.

2.2 Phase Change Materials

Phase change materials have gained attraction in TES applications due to their high energy density[23]. They are also highly customizable, as they have both various melting points and characteristics that depends on the choice of material[23]. However, using PCM at large scale for TES is not yet commercial, and designing one still has no guidelines and remains within the field of research[16]. Two of the most important factors when choosing the PCM is its heat of fusion $[kJ/kg]$, which is the potential of energy that the material can store or release during the phase change, as well as the thermal conductivity $[W/(m \cdot K)]$, which is how fast the material can absorb and release heat. These properties are important because the heat of fusion determines how much thermal energy the PCM can store and release during the phase change, while the thermal conductivity determines how quickly the material can transfer heat. Both of these properties directly affect the effectiveness and utilization availability of the storage.

2.2.1 PCM Classification

Based on their chemical composition, PCMs can be classified as organic, inorganic and eutectic[24][15]. Each type have its range of temperatures and characteristics, along with its advantages and drawbacks. The classifications are illustrated in figure 2.2.

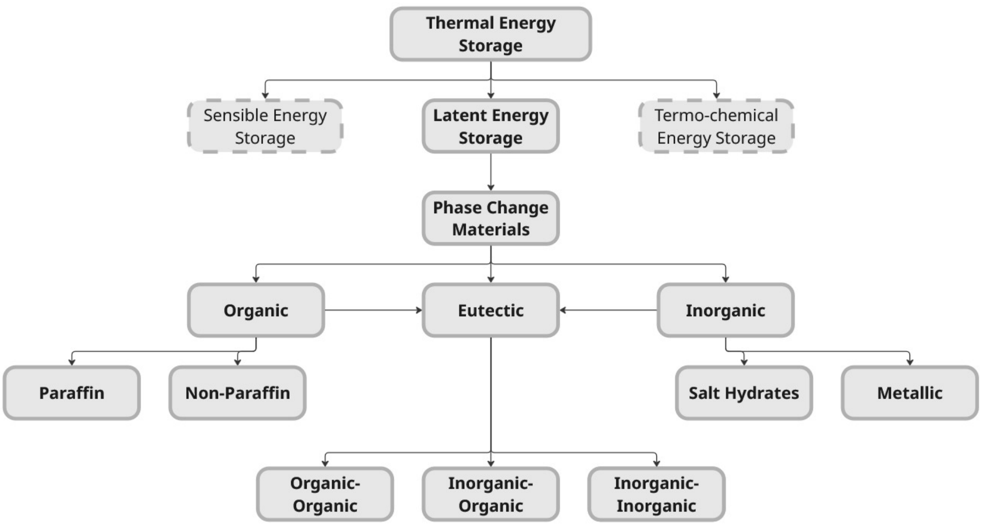

Figure 2.2: TES categorization with focus on PCM.

Organic PCMs can broadly be described as either paraffin or non-paraffin based. Paraffin materials have similar properties, while non-paraffins each have their own properties resulting in different characteristics[23]. However, there are several similarities between the two types. They are all characterized by congruent melting, meaning that the material can melt and freeze repeatedly without phase segregation or degradation of their latent heat of fusion. They also exhibit self-nucleation meaning they do not suffer from supercooling, and have low corrosiveness. However, these materials also present several drawbacks. Paraffins suffer from low thermal conductivity[24], and many of them have melting points way higher than the desired temperatures for district cooling. Non-paraffins also suffer from low thermal conductivity, and show potential issues such as toxicity and flammability[15]. Organic PCMs are likely to require additional flame retardants or encapsulation to ensure that the flammability risk is low[25].

Inorganic PCMs are classified as salt hydrates and metallic. They both have high thermal conductivity and latent heat of fusion[23][24]. Salt hydrates are notable for their low melting temperatures and high energy storage densities, but suffer from corrosiveness towards metals which in turn increases system costs and reduces the lifespan of the storage[15]. Furthermore, salt hydrates can suffer from supercooling due to the low rate of nucleation[23]. These characteristics need to be taken into consideration, especially since they both affect the long-term capacity and cycling performance of the storage[26]. Metallic materials have a very high thermal conductivity, however require melting temperatures above the desired range of district cooling and is therefore not applicable for this study[24]. Inorganic PCMs both display a non-combustibility and a thermal stability[25].

Eutectic PCMs are a combination of either organic or inorganic materials, making them highly customizable depending on the requirements[15]. They can be divided into three subgroups respectively; organic-organic, inorganic-organic and inorganic-inorganic.

2.2.2 Current Research and Applications

While few large-scale LTES are currently in operation, several studies and pilot projects have been conducted on this topic. These can provide valuable insights and guidelines that should be considered when designing LTES for large-scale applications.

Tan [16] investigated the performance of a PCM made out of commercial salt hydrates, as its high heat of fusion makes it a good contestant for storing energy. However, it showed that the LTES using this material was limited by material and device behavior. Experiments showed that phase separation, supercooling, and lower-than-expected charging rates significantly reduced the usable storage capacity compared to theoretical values.

Lamrani et al. [27] compared STES and LTES for building cooling using a validated dynamic model. The chosen PCM-based systems showed superior performance over chilled water storage, delivering longer periods of stable cooling and higher effectiveness. An increase of the PCM tank volume further improved performance. These results demonstrated that, based on their developed model, high-energy-density LTES were more effective for sustained cooling in district cooling networks.

Bourne and Novoselac [12] developed and experimentally tested a PCM-based TES for small to medium sized cooling systems. The PCM was macro-encapsulated into cylindrical tubes and packed into a containment tank. The PCM consisted of 99% tetradecane, and the freezing and melting temperature range was found using water at 2 °C and 9 °C respectively. The experiment showed that freezing of the PCM occurred between 5.4 °C - 5.5 °C, while melting occurred over a larger temperature range of 4.5 °C - 6.5 °C. Furthermore, the PCM experienced supercooling during solidification, and reached a temperature of 5.2 °C before freezing occurred. As for cooling performance, water at 17 °C was used, and different flow rates were measured. Results showed that the storage discharged faster as the mass flow rate increased, and the water temperature increased faster as well.

Shao et al. [28] investigated a cascaded packed-bed tank system using two PCM mixtures with different ratios of materials. The tanks were charged at 5 °C and discharged at 12 °C, and both had the same energy storage capacity. They found that one of the mixtures, with lower melting temperature consisting of 50%-50% tetradecane-hexadecane, performed poorly during charging, while the latter, consisting of 30%-70% tetradecane-hexadecane, performed poorly during discharging. However, by combining the two mixtures in a cascaded arrangement, the system achieved better overall efficiency during both charging and discharging, while still storing the same amount of energy. This showed that using complementary PCMs in sequence can optimize the thermodynamic performance of the tank.

Jokiel [29] analyzed a large-scale PCM storage system located at the University of Bergen in Norway. The storage system consisted of four tanks, each with a volume of 57 m^3 and a storage capacity of 2810 kWh, making it the largest LTES system in Europe. The storage was charged using chillers during off-peak hours and discharged during periods of high demand, with the aim of reducing peak loads and smoothing the load curve. Tests of the storage system showed that, during a 12-hour charging and discharging cycle representing the standard operating mode, only around 50% of the storage capacity was utilized. However, when the charging and discharging periods were extended and the mass flow rate was increased, the PCM utilization increased to almost 90%.

Cheng and Zhai [30] used a simulation model to analyze a cascaded packed bed PCM unit and its thermal performance on charging, accumulated cold, and exergy stored. They compared the results with those of a single-stage unit and found that the temperature difference between the HTF and the PCM decreased over time, causing the heat transfer rate to decline. In the cascaded unit, however, the hot fluid continuously encountered cooler PCM throughout the heat transfer process. As a result, the temperature difference remained relatively high, maintaining efficient heat transfer. The cascaded unit was also found to be preferable, as it reduced the charging time and increased the charging rate while storing nearly the same amount of cold energy. It was therefore concluded that integrating cascaded cooling TES with air-conditioning systems could help stabilize grid loads and thereby reduce operating costs.

Alam et al. [31] evaluated the energy-saving performance of an active PCM system installed in a building in Melbourne. The system used macro-encapsulated PCM with a phase change temperature of 15 °C to reduce daytime cooling loads on chillers. Over 25 months of monitoring, the system reduced chiller cooling load by 12–37% during colder months but remained largely inactive in summer. This was due to ambient temperatures being insufficient for effective charging during the warmer months. The study found that only a small portion of the storage capacity was utilized. Operational inefficiencies were also identified, including suboptimal control strategies and high pump energy consumption during charging which limited overall performance.

At ThumbsUp, which is part of RISE, several small-scale PCM storage units are currently being installed for testing purposes [32]. The project aims to integrate PCM storage with a building's domestic hot water system in order to improve energy efficiency. The storage system is connected to the domestic hot water supply and can be used for applications such as showering. According to the project description, one of the main challenges is designing a modular, efficient, easy-to-install, and easy-to-operate system while maintaining high performance. In total, three LTES units have been installed at the site [33].

Alam et al. [34] experimentally investigated the thermal performance of a PCM storage system under varying water inlet temperatures and flow rates. The study concluded that the PCM solidification rate is highly dependent on the inlet water temperature, while it in contrast is less sensitive to the flow rate. However, it was shown that during higher flow rates, the PCM solidifies more uniformly but also suffer from a higher degree of supercooling. For a PCM with a melting temperature of 13 °C, a water inlet temperature of 8 °C was recommended. It was also shown that the solidification and melting time of the PCM differed, where the time for solidification was longer than of melting. Finally, the PCM did never solidify or melted fully, and the study stated that a loss factor should be considered when designing a PCM tank.

2.2.3 Designs of PCM Storage

There are different ways a LTES can be designed. This thesis will investigate three different configurations[35]. These are presented in Figure 2.3.

The first design method is defined as a LTES with a HTF passing through the PCM medium in a vessel, e.g. through tubes. This is visualized in Figure 2.3a[16][36]. This type of storage completely surrounds the HTF with the PCM of choice. The storage unit could be a basin or tank filled with PCM, with the HTF flowing through pipes inside of it. The second method consists of the HTF surrounding the PCM instead. This is visualized in Figure 2.3b and Figure 2.3c.

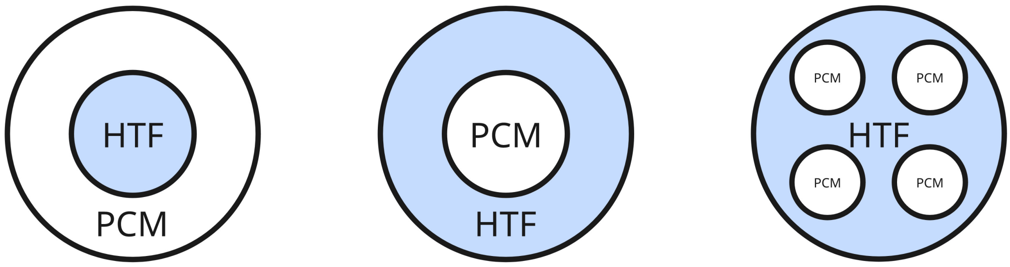

(a) A container with PCM and the HTF passing through.

(b) PCM in a closed vessel inside a container with the HTF.

(c) Several PCM vessels inside a container with the HTF.

Figure 2.3: Different LTES types.

The most common of the two is the later design, where several PCM units are stored in the HTF. These can be encapsulated in shapes such as balls, pipes or oval pods[37][38][39]. The advantages of this technique include more effective utilization of the entire PCM volume, ensuring better solidification and liquefaction of the material. One alternative is the use of tubular encapsulations, which consist of pipe-shaped elements that can be stacked [40][41]. The spacing between the tubes forms flow channels with a low pressure drop. Another alternative is spherical encapsulations, which can be manufactured in various diameters. These also allow the HTF to flow between the encapsulated units. In addition, the encapsulations can be stacked within flat containers, provided that sufficient space is maintained for HTF flow. There are commercial PCM companies providing these, such as PCM Products Ltd. Their rectangular blocks, called FlatICE, feature a self-stacking design that forms a self-assembling heat exchanger (HX) within the tank. The structure creates gaps between blocks, enabling flow paths and a large heat transfer area.

Different types of PCMs can be utilized and combined in an LTES design to form a cascaded storage system [37][30]. Studies have shown that cascaded storage can improve performance during both charging and discharging. Increasing the number of PCM types from one to two results in a significant performance improvement, whereas increasing the number from two to three provides a smaller additional benefit. In general, using more than three PCM types is not considered advantageous, as the increased cost and system complexity tend to outweigh the marginal performance gains. Another advantage of encapsulated LTES systems is the improved safety they offer when handling flammable PCMs, such as paraffin [38].

2.2.4 Design Complications

One risk when designing LTES includes the occurrence of unutilized zones that is not within reach of the thermal diffusion[16][42]. This problem is mostly seen when using the design presented in Figure 2.3a. This occur due to low thermal conductivity of most PCMs and estimations prove that only a thin layer around the tube with the HTF is actively storing the latent energy[16]. This along with the active cooling/heating time are central limiting factors of the energy storage. It is therefore important in the design to make sure to efficiently utilize the PCM by considering the effective area of heat transfer within the given time frame. Appropriate scaling and positioning of both tank walls and pipes must also be taken into consideration. One way to reduce the risk is to ensure that the PCM tank is sufficiently small, to ensure effective thermal diffusion through the tubes.[36]. Another way is to use several shallow tanks of PCM, such as the design visualized in Figure 2.3c.

Another problem with some types of PCM is the occurrence of phase separation. This occurred during testing of inorganic salt hydrates at Chalmers, and the effect caused a need for the mixture to be stirred after only a few cycles since the heavy molecules moved to the bottom of the tank over time[16]. The heavy molecules also happened to be the more effective thermal carriers of the bunch, causing uneven solidification of the material in the tank. This problem can be mitigated in the same way as for the low thermal conductivity, i.e. by using smaller containers and increase the heat transfer area.

Previous testing of different PCMs has shown that the materials do not melt and solidify at identical temperatures. Furthermore, the fraction of the total latent energy that is available for heating or cooling is not uniformly released or absorbed throughout the phase transition. Pluss Advanced Technologies, a supplier of commercial PCMs at various phase change temperatures, has characterized the thermal performance of PCM materials and reported temperature gliding behavior [43][44]. This temperature glide implies that, although a PCM is assigned a designated melting and freezing temperature, the phase transition occurs over a temperature interval rather than at a single isothermal point as shown in Figure 2.1. Consequently, the latent heat is distributed across a finite temperature range, meaning that the energy available at any specific temperature within the phase change region is not constant. As stated in previous sections, many PCMs suffer from a phenomenon called supercooling. Supercooling occurs when the material remains in a liquid state at a temperature below its melting temperature [45]. This has several disadvantages. First, the effective melting temperature may deviate from the designed operating range, as the phase change is delayed to lower temperatures. Second, more energy is required to initiate solidification, since the system must first remove additional sensible heat before the phase change can begin [46]. As a result, the phase change duration may also be delayed. Supercooling is more commonly observed in inorganic and eutectic PCMs, however it may also occur in organic PCMs when the encapsulation volume is small. This is because smaller containers contain fewer nuclei, i.e. initial sites where crystallization begins, which increases the risk of this phenomenon.

3
Theoretical Framework for District Cooling

This chapter begins with an overview of DC systems, including technical descriptions and equations. It then introduces the DC network in Gothenburg along with relevant technical details. Finally, the chapter presents the specific case study area of Almedal.

3.1 District Cooling Systems

In a DC system, chilled water is distributed through pipelines from cooling production facilities to buildings[9]. Broadly described, it consists of a cooling source, a distribution network, and substations where the buildings are connected to the system. The substations, also referred to as energy transfer stations, deliver either direct or indirect cooling. Direct cooling means that the DC water is distributed directly to the building, while indirect cooling uses HXs between the DC water and the building's internal cooling system[47]. An overview of a DC system with an indirect cooling substation is presented in Figure 3.1. In the DC system in Gothenburg, all buildings are supplied with cooling indirectly. For this reason, the following analysis in this thesis will be based on indirect cooling.

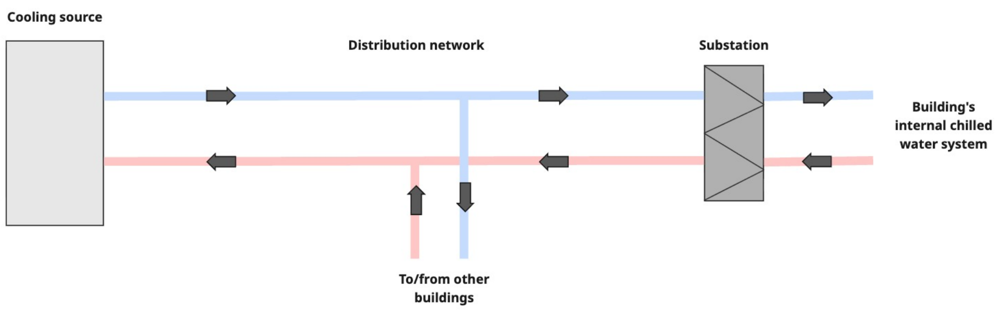

Figure 3.1: Overview of a DC system

DC systems can make use of available cooling from the surroundings, which is referred to as free cooling. These include sources such as oceans, deep lakes or aquifers[47]. The utilization of such sources depends on their temperature, which varies with the outdoor temperature[1]. Therefore, when the temperature of the free cooling source is too high and the system is not able to utilize it, alternative production methods must be implemented to meet demand. These methods can be either absorption chillers or compression chillers[48]. Absorption chillers produce cooling from excess heat, whereas compression chillers solely rely on electricity[1]. These machines are located at production sites, and are designed to receive water with a supply temperature of 14 °C or higher[2].

3.1.1 Technical Description of a District Cooling substation

At the substation, water from the DC network is delivered to the buildings indirectly through a HX, usually a plate HX[9]. The HXs acts as an interface between the primary side, the producer of cooling, and the secondary side, the customer[1]. If assuming steady flow, constant specific heat and negligible losses to the surrounding, the heat transfer between the two sides in the HX are[49]:

$$\dot{Q}_{producer} = \dot{Q}_{customer} \tag{3.1}$$

or, if expanding:

$$\dot{m}_{producer} \cdot c_p \cdot \Delta T_{producer} = \dot{m}_{customer} \cdot c_p \cdot \Delta T_{customer} \tag{3.2}$$

$\dot{m}$ is the mass flow, which is equal to the fluid density ρ multiplied by the volumetric flow $\dot{V}$. c_p is the specific heat capacity and ΔT is the temperature difference between the supply and return temperature on the respective side of the HX. It should be noted that, in this thesis, the density and specific heat are assumed to be unaffected by temperature and pressure, and are therefore considered constant.

A schematic of a DC substation is visualized in Figure 3.2. The DC network water enters the HX from the primary side and cools the water on the secondary side before returning to the production site. The amount of heat transfer needed is determined by the temperature difference between the secondary side supply and return water, as well as the mass flow rate. In other words, the customer's cooling demand depends on how much heat must be removed to keep its supply water at the desired temperature. If the supply temperature on the secondary side does not reach the desired level, the cooling delivered by the producer is increased by adjusting the mass flow rate. The mass flow rate is controlled by the control valves. These are connected to the supply temperature on the secondary side via a control unit, and can therefore be adjusted according to demand[2].

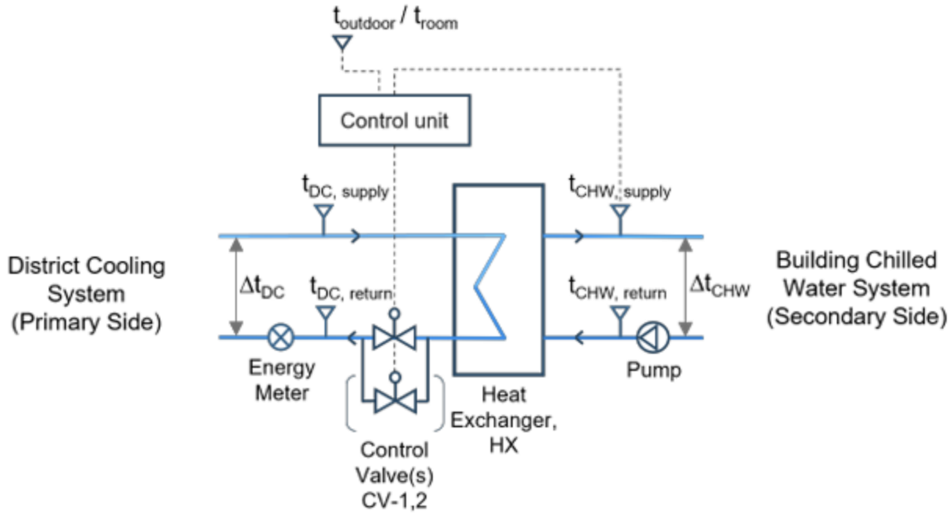

Figure 3.2: Schematic of a DC substation[1].

The thermal interaction between the primary side and the secondary side of the HX can be described in terms of the heat capacity rates of the two fluids[49]. The heat capacity rate represents the ability of a fluid stream to absorb or release heat per unit temperature change, and is defined as:

$$C_p = \dot{m}_p c_{p,p} \tag{3.3}$$

$$C_s = \dot{m}_s c_{p,s} \tag{3.4}$$

where $C_{p,p}$ is the heat capacity rate on the primary side and $C_{p,s}$ is the heat capacity rate on the secondary side.

A substation's pressure difference is typically regulated using pumps or control valves to compensate for and control the pressure losses that occur across the HX[50]. On the secondary side, pumps are the more common design choice.

3.1.2 Low delta-T syndrome

The design guidelines for a DC substation recommend that the flow rates on the primary and secondary sides should be balanced[50]. However, in practice, the secondary-side flow rate often exceeds that of the primary side, causing the supply temperature on the secondary side to increase[51]. As a result, the system temperature difference decreases, a phenomenon referred to as the "low delta-T syndrome." This syndrome negatively affects the DC network by requiring higher flow rates on the primary side to provide the same cooling load, leading to additional pumping demand and increased cooling production and thereby reducing the overall system efficiency. This can be caused by several factors. However, issues such as non-optimized secondary side supply temperatures and low secondary side return temperatures have been identified as some of the issues[52].

3.2 District Cooling Network in Gothenburg

The DC network in Gothenburg, managed by Göteborg Energi AB, currently consists of 8 production facilities connected to the DC grid. These are indicated by green dots in Figure 3.4 and listed in Table 3.1[2]. The total system capacity is 78.5 MW, and the annual demand is approximately 90 GWh. The Rosenlund production facility is the largest in the system, accounting for over 40% of the total capacity. The pipeline network spans roughly 50 km and is distributed across the city.

Table 3.1: The producers of the DC network, in order of size.

Producers	Installed Capacity [MW]
Rosenlund	32
Lindholmen	15.6
Gullbergsvass	11
Ceres	5.6
Odin	4.2
Svenska Mässan	4.1
Arkaden	3
Sahlgrenska	3
Total	**78.5**

Due to the climate and seasonal variations in Gothenburg, its cooling demand changes throughout the year. It reaches its peak in the summer months, usually between May and August, whereas production is at its minimum between December and February[2]. This is visualized in Figure 3.3, which shows the monthly variation of cooling demand between the years 2020-2025. Customers in DC systems are most often office buildings, industrial facilities, and commercial buildings[53]. In Gothenburg, the majority of customers are office- and commercial buildings, resulting in daily peak demand during daytime hours and reduced demand at night.

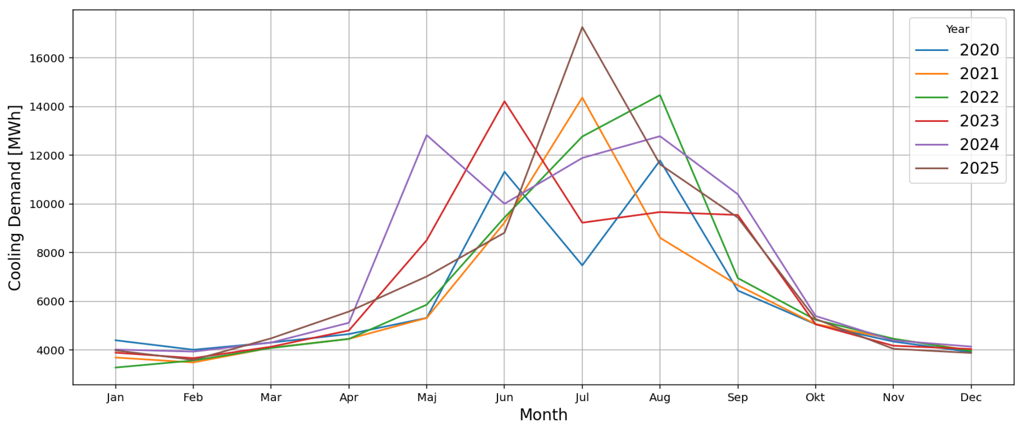

Figure 3.3: Monthly variation of cooling demand across different years.

3.2.1 Almedal Area

The Almedal area, the case study of this thesis, is far away from the DC production sites as shown in Figure 3.4. This results in hydraulic limitations within the network, since pumping is required to ensure sufficient supply temperatures and flow rates to the customers[2]. As the cooling demand increases and more customers are connected, water flow capacity may become a critical limiting factor that could hinder future network expansion. As of now, the maximum flow rate possible in the system is 600 m^3/h with the current pumps and pipe system[2].

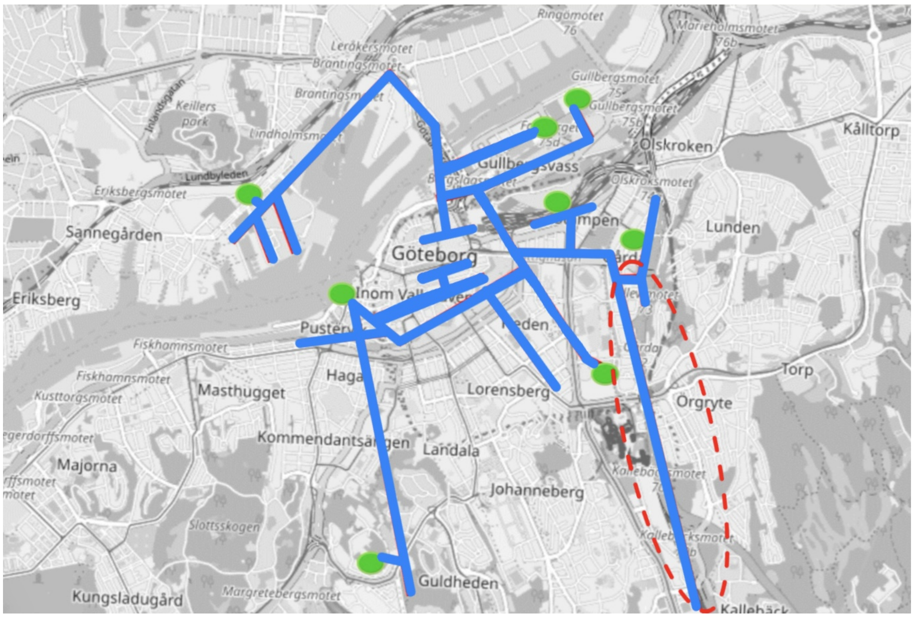

Figure 3.4: DC network in Gothenburg with the Almedal area within the red dotted line, green dots are production sites[2].

The area consists of 11 customers of different sizes and varying cooling demand. In Figure 3.5, the peak load between 1st of May and 30th of September for each customer is presented, alongside with the total cooling demand over the whole period.

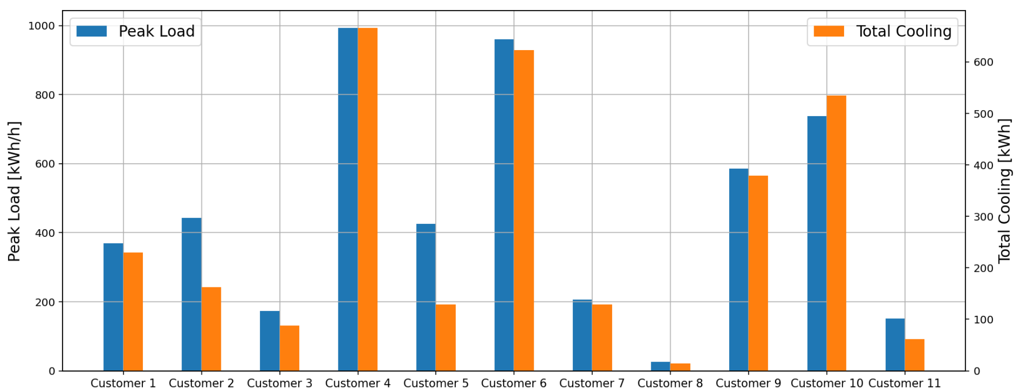

Figure 3.5: Peak load along with seasonal total cooling for each customer.

The average temperature difference, average supply water temperature and average return water temperature on the primary side are presented in Table 3.2. It is worth noting that the averages are calculated using the operating hours during which cooling is active.

Table 3.2: Average temperature difference, supply temperature, and return temperature on the primary side for each customer over the study period.

Customer Number	ΔT $[°C]$	**Supply Water** $[°C]$	**Return Water** $[°C]$
1	13.9	7.0	20.9
2	7.0	6.5	13.5
3	7.2	7.1	14.3
4	4.7	6.3	11.0
5	8.3	7.2	15.5
6	7.4	7.9	15.3
7	5.7	6.4	12.1
8	8.1	7.7	15.8
9	9.0	7.1	16.1
10	8.5	6.4	14.9
11	7.7	6.9	14.6

3.2.2 Arena area

Göteborgs Stad is currently planning a new area around Valhallagatan[13]. The construction plan includes a new arena, sports halls, housing, and office buildings, with the intention of making Gothenburg a more attractive option for both events and the citizens. Göteborg Energi intends to supply the area with district cooling, with an estimated cooling requirement of 4.2 MW. To supply the new area with cooling, a new pipeline would have to be built which is proposed to be connected to the Almedal pipeline.

The current proposal from Göteborg Energi is to use an outer pipe dimension of 315 mm, which would run approximately 250 m[54]. Additionally, a control valve would have to be installed. The pipe dimensions have been calculated based on estimations of the demand. The costs and maximum allowable mass flow rate for the 315 mm as well as the smaller size of 280 mm are presented in Table 3.3.

Table 3.3: Costs for different pipe dimensions and control valves.

Pipe dimension $[mm]$	**Maximum mass flow** $[m^3/h]$	**Cost for pipe** $[SEK/m]$	**Cost for control valve** $[SEK]$
315	408	21 735	82 426
280	300	20 261	74 793

3.2.3 Cooling Production

The DC system in Gothenburg uses free cooling, absorption chillers and compression chillers in order to meet their demand[3]. Their respective share for 2024 and 2025 is presented in table 3.4, where production with absorption chillers has the largest share and free cooling the smallest. Furthermore, the absorption and compression chiller load between 1st of May and 30th of September is presented in Figure 3.6.

Table 3.4: Production share of cooling methods for 2024 and 2025[3][4].

Production source	Share 2025 [%]	Share 2024 [%]
Free cooling (Göta river)	16	20
Absorption	53	58
Compression	31	22

Even if free cooling is preferable due to its low electricity consumption and cost, it only accounts for 20% of the total annual cooling supply. This is largely due to Sweden's climate, which creates seasonal variations in not just cooling demand but also source availability. During winter, when temperatures are low, the Göta River is sufficiently cold to provide most of the required cooling. This is also due to the demand being lower during winter. Free cooling from the Göta River can be used when its temperature is around 5 °C or lower. In contrast, during summer and warmer periods when cooling demand reaches its peak, the Göta River is too warm to be used as a primary cooling source. This is the reason why free cooling is not represented in Figure 3.6. During these periods however, the Göta River can instead be used to precool the returning DC water before it enters the chillers, if the river temperature is below the return temperature. This reduces the load on the absorption and compression chillers, which must then meet the remaining cooling demand[1]. Additionally, during summer, available excess heat from industrial and waste facilities is at its peak due to low demand in the district heating system, meaning a large amount of heat is available for the absorption chillers.

In terms of efficiency, absorption and compression chillers require different amounts of electricity to produce cooling[2]. Absorption chillers generally consume less electricity than compression chillers, making a reduction in the use of compression chillers the more desirable option. To compare the different electricity inputs, the energy efficiency ratio (EER) can be used[55][56]. EER is equivalent to coefficient of performance (COP), but specifically used for cooling systems. Furthermore, the seasonal energy efficiency ratio (SEER) is used to provide a more representative measure of day-to-day operation[57]. To account for entire production sites and supporting systems within the network, such as pumps, a network SEER is considered. The system EER includes both the chiller itself and supporting systems, such as the pump and its cooling tower. The standard system EER for absorption chillers and compression chillers are presented in Table 3.5.

Critical periods occur in May and October. This is due to warmer outdoor temperatures, causing the Göta River to become too warm for cooling use, while district

Table 3.5: Standard system EER for different cooling production sources.

Production source	System EER
Absorption chiller	30
Compression chiller	5

heating demand remains relatively high[2]. This results in limited excess heat availability, and the lack of absorption chiller production can be seen in Figure 3.6. The combination results in peak production from compression chillers, that reduces the network SEER. Also, during the warmest periods, when cooling demand peaks, excess heat is available but insufficient to cover the total demand. Consequently, compression chillers account for a large share of the cooling production, which likewise decreases the network SEER. In contrast, during the winter months, the system can be supplied with free cooling, increasing the network SEER significantly due to the low electricity consumption. This is visualized in Figure 3.7.

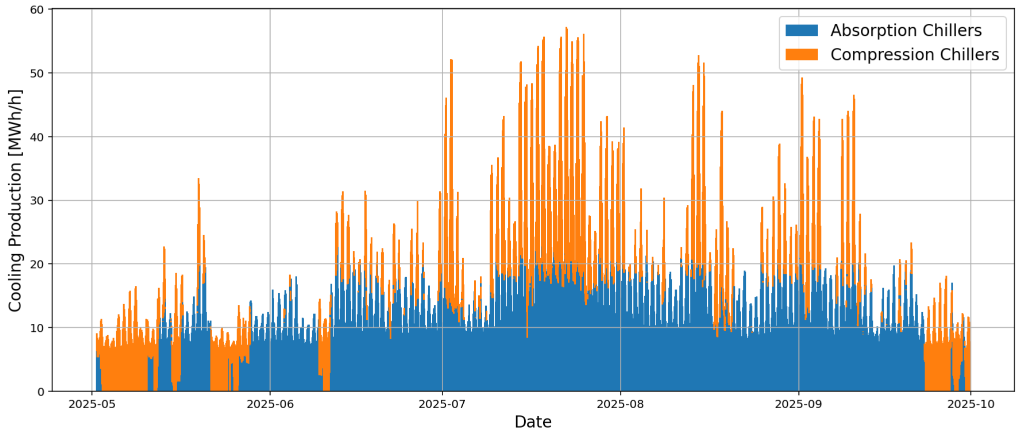

Figure 3.6: Cooling share produced by compression and absorption chillers.

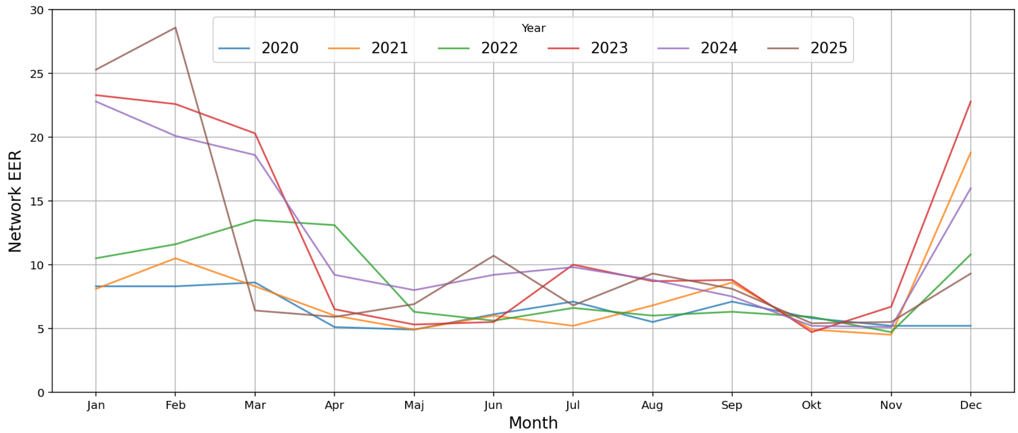

Figure 3.7: Monthly variation of the Network SEER across several years.

In addition to the undesirable increase in electricity consumption associated with compression chillers, the maximum cooling capacity of the DC network also constrains the system [2]. As stated in chapter 1, the cooling demand in Gothenburg is increasing as more customers seek connection to the district cooling network. During periods of high demand, customers require higher flow rates, which can lead to areas of the network where the flow cannot be further increased due to excessive pressure losses. This limitation is particularly problematic because many potential new customers are located far from pumping stations and production facilities. Such a situation exists in the Almedal area, where hydraulic constraints have resulted in the network almost reaching its maximum allowable mass flow rate during high demand periods, preventing further increases in cooling delivery.

3.2.4 Technical Description of a District Cooling Substation in Gothenburg

As stated in subsection 3.1.1, customers are supplied with cooling through substations located along the DC network. The DC supply water has a temperature requirement of 6 ± 1 °C, and the return temperature is designed to be ≥ 16 °C[58]. However, in practice, the return temperature is more likely to be around 14 °C due to different characteristics of individual substations (e.g. automation, fouling on HXs etc)[2]. In the district cooling network, the pressure is expected to reach a maximum of approximately 10 bar, although the actual pressure varies considerably depending on elevation and the distance to the network pumps. The pressure on the secondary side is generally lower.

The secondary side supply temperature has a requirement of 8 °C, but may vary depending on the supply temperature on the primary side. The customer supply temperature can physically never be lower than the supply temperature on the primary side. The HXs are dimensioned to deliver a minimum temperature difference of 2 °C, which means that if the supply temperature at the primary side exceeds 6 °C, the supply water on the secondary side will adjust correspondingly[59]. This function can be regulated at the control unit and is preferred to avoid short circuits in the system. If the control function is not in place, then the control valve on the primary side would increase the mass flow rate to try to obtain the desired temperature of 8 °C. Since the HX is not dimensioned to fulfill this requirement, the mass flow rate would therefore become excessively high which results in unnecessary pumping requirements as well as problem with meeting the design properties of the chillers. The chillers are designed for a maximum flow rate as well as incoming temperature. This results in higher costs for both the customer and producer. As for the customer return temperature, a desired temperature is 18 °C, but can differ depending on the building's demand[60].

There are three different agreements that the customer can choose between when connecting to the DC network[58].

- Göteborgs Energi owns the substation alongside with the control equipment (FK21)
- Göteborg Energi owns the substation but not the control equipment (FK22)
- The customer owns both the substation and the control equipment (FK30)

Currently, FK22 and FK30 are the most common agreements, meaning that the customer is responsible for the control unit. This gives the customer full control and responsibility for operating the substation. Under these agreements, the customer must ensure that the substation operates according to Göteborg Energi's technical requirements, such as regulating the supply temperature and managing the mass flow rate[58].

3.2.5 Cost Calculations

The pricing of DC bought from Göteborg Energi AB is divided into three sections: energy, capacity and flow[61]. The energy price states the total energy usage throughout the year. It is calculated by multiplying the total energy usage with the energy price, which varies monthly. Equation 3.5 states the calculation while the specific values of the monthly energy price is specified in Table 3.7.

$$c^{energy,tot} = \sum_{k=1}^{month} (c_k^{energy} \cdot E_k^{tot}) \tag{3.5}$$

The capacity cost depends on the maximum capacity usage, which either corresponds to the maximum measured capacity over a 12-month period or a pre-defined contracted value, representing the maximum capacity the customer can access[61]. The capacity cost is divided into two price components: a fixed component and a variable component. Both components depend on the maximum power usage, and the price categories are presented in Table 3.6. The total capacity cost is calculated according to Equation 3.6.

$$c^{capacity,tot} = (c^{capacity,fixed}(P^{max})) + (c^{capacity,variable} \cdot P^{max}) \tag{3.6}$$

Table 3.6: DC capacity cost.

P^{max} $[kW]$	$c^{capacity,fixed}$ $[SEK/year]$	$c^{capacity,variable}$ $[SEK/kW\ year]$
0 - 100	23 670	1 020
100 - 250	40 270	854
250 - 500	80 020	695
500 - 1 000	120 020	615
> 1 000	149 020	586

The flow price depends on the total flow[61]. The total flow is, similar to the energy price calculation, accumulated monthly and multiplied with a flow price that varies monthly. The flow is given in cubic meters, and the prices are stated in Table 3.7. The flow price is calculated through Equation 3.7.

$$c^{flow,tot} = \sum_{k=1}^{month} (c_k^{flow} \cdot V_k^{tot}) \tag{3.7}$$

Table 3.7: DC energy and flow price.

$month$	E_k^{tot} $[SEK/MWh]$	c_k^{flow} $[SEK/m^3]$
Jan	111	0.50
Feb	111	0.50
Mar	111	0.50
Apr	205	1.20
May	280	1.35
Jun	298	1.35
Jul	298	1.35
Aug	298	1.35
Sep	298	1.20
Oct	291	0.50
Nov	234	0.50
Dec	111	0.50

In addition to what the customer pays for cooling, Göteborg Energi must cover the electricity costs required to operate both compression and absorption chillers[2]. These costs include the grid usage fee, electricity tax, and the variable electricity price of the specific price region in Sweden. Together, these components form a combined electricity cost, evaluated on an hourly basis, and covers both electricity energy consumption and power demand. The total electricity cost is given by Equation 3.8.

$$\sum_{k=1}^{month} c_k^{electricity} = \sum_{k=1}^{month} (c_k^{grid\ fee} + c_k^{energy\ tax} + c_k^{el\ price}) \tag{3.8}$$

3.3 Integration of TES in the District Cooling System

Integrating TES into a DC system can be implemented either though a central storage or decentralized storage. In centralized configurations, storage units are installed at a main plant and serve the entire distribution network. In contrast, decentralized integration places storage units closer to end-users, such as within buildings or at substations[14][62]. This thesis will exclusively focus on decentralized thermal energy storage solutions located at the substation level.

Short-term TES in DC systems is particularly valuable due to daily variations in cooling demand, especially during peak summer periods when temperatures can fluctuate significantly between daytime and nighttime[63]. By storing excess cooling capacity during low-demand periods and releasing it during peak demand, TES can reduce peak loads and maintain a more stable and efficient network operation throughout the day. Daily TES systems generally do not require large storage volumes, as their primary purpose is to shift energy over short timescales, such as from daytime production to evening consumption.

Decentralized TES is typically implemented at the substation level to handle daily variations[64]. Placing TES at substations eliminates the need to transport cooling over long distances from a central source. This reduces pipe sizing requirements, and avoids modifications to the existing network infrastructure[62]. In addition, during peak load, decentralized placement reduces the demand for circulation pumps, as lower mass flow rates are required to meet the energy needs of the system. Instead, the load is expected to become more evenly distributed as demand is shifted. Therefore, decentralized TES does not only improve operational efficiency but also contributes to energy savings during peak hours in the network, providing both operational flexibility and cost efficiency. Consequently, the electricity usage is increased during during off peak hours.

The implementation of TES also involves several drawbacks that must be considered when integrating it into DC systems. First, TES requires a capital investment, regardless of its size or efficiency. The investment cost is strongly influenced by the complexity and type of TES technology selected[14]. Another important consideration is the physical space required for installation. Although decentralized TES units are smaller than large centralized systems, having multiple units across substations can be time-consuming and costly to implement. Consequently, careful planning is needed to balance the benefits of decentralized TES with the associated financial and spatial constraints.

3.3.1 Substation-Level LTES Integration in District Cooling Networks

There are several ways to implement a TES at the substation level. However, one of the main challenges in DC networks is the narrow temperature difference between the supply and return water[63]. Even though LTES is attractive due to its high latent heat capacity which allows a significant amount of energy to be stored or released over a small temperature range, the integration introduces specific operational and design requirements.

To effectively charge the storage, the heat transfer fluid from the network must be colder than the phase change temperature of the PCM[65]. In contrast, during discharge, the heat transfer fluid that is to be cooled must be warmer than the PCM temperature to extract the stored cooling. Furthermore, if additional HXs were used to separate the LTES from the main flow, the heat exchange would result in even smaller temperature differences. This, in combination with the already narrow temperature difference in DC networks, creates a critical design challenge. The PCM material must satisfy the temperature criteria to be effectively utilized, while at the same time fulfill both cost and spatial requirements in order to be advantageous and favorable.

4
Model Methodology

This chapter presents the methodology used to develop the model in this thesis. It begins with a description of the data collection and processing procedures. The chapter then introduces the mathematical model developed for the analysis, including its formulation, objective function, and constraints, as well as the methods used for model validation. The economic assessment method and the key assumptions underlying the study are also presented. Finally, a sensitivity analysis is conducted.

4.1 Data Collection and Handling

To enable scenario comparison and assess potential system improvements, measurement data from Göteborg Energi AB was used as input for modeling. The datasets include customer data and measurement from Almedal, total production data of the whole system, output parameters of the provided cooling to Almedal and electricity prices. Furthermore, datasets including yearly cooling production, electrical requirements and EER were provided.

The data included load, volume flow as well as supply and return temperature for each customer. The production data file contained total production of district cooling, added electrical power, absorption cooling production output and compression cooling production output. The electricity price file included the electricity grid fee, energy tax of electricity and the electricity price of the specific area SE3 in Sweden.

All the dataset provided was time-aligned and reported at one hour intervals, covering the period from first of May to last of September of 2025. These dates were of interest since this is when district cooling demand increases as well as when Göta river becomes too warm to exclusively cool the DC water.

4.2 Configuration Setup

To evaluate whether LTES in the DC system in Gothenburg can help reduce peak demand and smoothen the load curve, two different configurations was investigated. The first configuration involved the storage system pre-cooling the return water from the customer by being connected to the return pipe. The second configuration was connected in parallel, cooling a fraction of the return water from the customer before being mixed with the fully cooled water from the HX. The configurations are visualized in Figure 4.1a and Figure 4.1b. For configuration 1, a linear optimization model was constructed. For configuration 2, a mixed-integer linear optimization model was used.

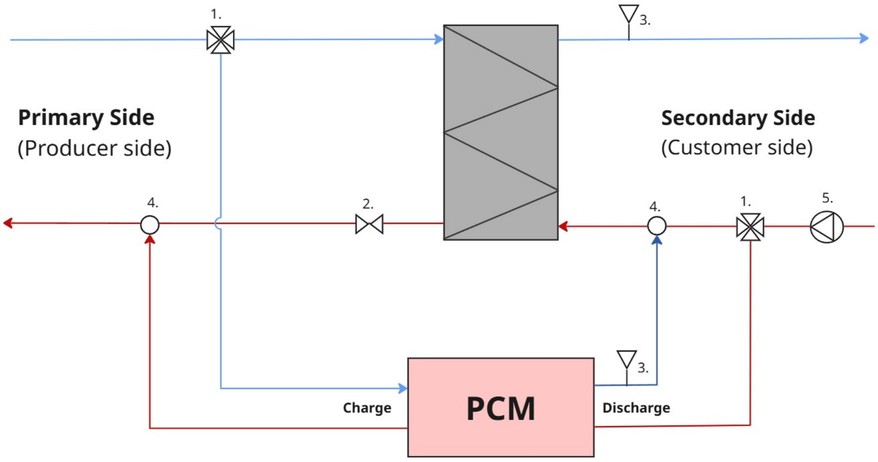

(a) Configuration 1: Pre cooling serial connected LTES configuration.

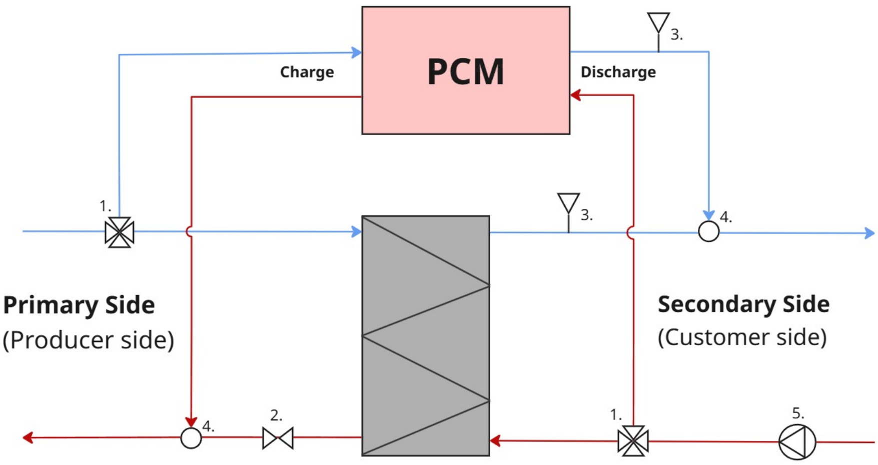

(b) Configuration 2: Parallel connected LTES configuration.

Figure 4.1: Components: 1. Splitter & Throttle Valve, 2. Throttle Valve, 3. Thermometer, 4. Mixer, 5. Pump.

4.3 Model Construction

Both models were created in Python using PuLP, a python library package designed for supporting different type of modeling[66]. It is an open source library that uses solvers such as Computational Infrastructure for Operations Research (COIN-OR). COIN-OR's branch cut solver, CBC, was used as the linear programming and mixed integer linear programming solver[67]. Both models were based upon the same framework, with modifications introduced to meet the specific requirements of each configuration.

For both models, the mass flow rates on the primary side and secondary side were assumed equal. This is due to lack of data regarding the temperatures and mass flows on the secondary side, and to it being recommended by the design guidelines for DC substations[50]. Consequently, since both sides have water as their HTF, the specific heat capacity will be similar and thus their respective heat capacity rates will be equal (from Equation 3.3 and Equation 3.4). This will result in that ΔT throughout the heat transfer will be constant, which means that the temperature difference between the cold inlet fluids will be the same as the hot outside fluids. This is visualized in Figure 4.2.

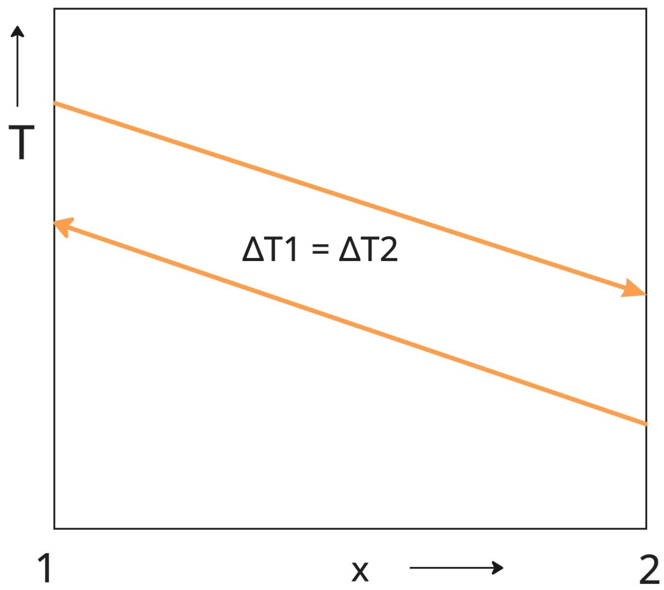

Figure 4.2: Visualization of the temperature changes of two fluids with equal heat capacity rates during heat exchange.

ΔT was assumed to be 2 °C. That is, the supply temperature coming out of the heat exchanger on the secondary side will always be 2 degrees higher than the supply temperature on the primary side. The same is valid for the return water temperatures.

$$T_{i,t}^{sup,s} = T_{i,t}^{sup,p} + 2 \tag{4.1}$$

$$T_{i,t}^{ret,s} = T_{i,t}^{ret,p} + 2 \tag{4.2}$$

For sizing the LTES, the FlatICE design described in subsection 2.2.3 was used as a reference. This since it is a commercial product that has been tested in several studies, such as those by Jokiel [29] and Alam et al. [34]. One FlatICE container is scaled at 500 mm x 250 mm x 40 mm, or 0.005 m^3. In this thesis, the PCM type S10 will be used[40]. This material has a melting temperature of 10 °C. One container weigh 5.59 kg and has an energy storage capacity of 0.220 kWh. In Table 4.1, the properties for one LTES unit used are presented.

Table 4.1: Properties for the LTES used.

No. of LTES $[-]$	**No. of FlatICE** $[-]$	**Volume** $[m^3]$	**Weight** **[kg]**	**Capacity** $[kWh]$
1	200	1	1 118	44

Each customer is evaluated with between 0 and 10 LTES units to determine the most suitable storage capacity. The total storage capacity is assumed to be proportional to the number of LTES units. Let CAP_i denote the storage capacity for customer i. Since each unit provides 44 kWh, the total storage capacity is given by

$$CAP_i = 44 \cdot N_i^{unit} \tag{4.3}$$

where

$$N_i^{unit} \in \{0, 1, 2, \ldots, 10\} \tag{4.4}$$

denotes the number of LTES units assigned to customer i. Furthermore, the total maximum production flow used for charging the LTES is defined as:

$$\dot{m}^{charge} = N_i^{unit} \tag{4.5}$$

The maximum mass flow rate used for charging the LTES is equal to the number of storage units assigned to each customer. For example, if a customer has one storage unit, the maximum mass flow rate for charging will be 1 kg/s, which equals 3.61 m^3/h. This value was chosen to ensure that the storage can be fully charged during the night, using a supply water temperature of 7 °C, while avoiding a significant increase in cooling production during this period. The choice of 7 °C also ensures that the storage can still be charged even if the supply water temperature on the primary side does not reach its optimal value of 6 °C.

The models have an hourly time resolution and operates between first of May and last of September to match the provided data given for analysis. They simulate the daily operation of a customer-level TES system, with the objective of minimizing the daily peak load which is determined by the net load after charging and discharging of the LTES. Both models have the following decision variables:

$$SOC_{i,t} \tag{4.6}$$

$$charge_{i,t} \tag{4.7}$$

$$discharge_{i,t} \tag{4.8}$$

$$peak_{i,d} \tag{4.9}$$

The objective function of both models is to minimize the daily peak load. That is:

$$min\ peak_{i,d} + \alpha \cdot \sum_{t=1}^{24} charge_{i,t} \cdot load_{i,t} \tag{4.10}$$

where:

$$\alpha = 0.001 \tag{4.11}$$

α is a small weight, which act as a penalty for charging the storage during high load. This is implemented to ensure charging is done during the hours of lowest load. Otherwise, the solver charges in the beginning or the end of the charging window, as long as it does not affect the peak of the day.

$SOC_{i,t}$ is the state of charge of the LTES, $charge_{i,t}$ and $discharge_{i,t}$ is the hourly charging and discharging power and $peak_{i,d}$ is the daily peak load. $SOC_{i,t}$ evolves according to the following constraint:

$$SOC_{i,t+1} = SOC_{i,t} + charge_{i,t} - discharge_{i,t} \tag{4.12}$$

The constraint states that the state of charge in the following hour is determined by the current storage level and the added or subtracted charge or discharge. Furthermore, to ensure that the storage does not undergo zero and never exceeds maximum capacity, the following constraints are added:

$$SOC_{i,t} \geq 0 \tag{4.13}$$

$$SOC_{i,t} \leq CAP_i \tag{4.14}$$

The models also have to make sure that the peak load have to be at least as large as the load, charge and discharge at each hour combined. Furthermore, the load, charge and discharge at each hour also have to make sure never to undergo zero.

$$load_{i,t} + charge_{i,t} - discharge_{i,t} \geq 0 \tag{4.15}$$

$$peak_{i,d} \geq load_{i,t} + charge_{i,t} - discharge_{i,t} \tag{4.16}$$

In addition to the decision variable constraints, the charging and discharging variables are further constrained to be available during certain hours. Due to the load curve of the customers, the charging is said to be done during nighttime (20:00 - 07:00) and discharging during daytime (08:00 - 19:00).

$$\text{charge}_{i,t} = \begin{cases} \text{charge}_{i,t} \geq 0 & \forall t \in \mathcal{T}_{\text{charge}} \\ 0, & \forall t \notin \mathcal{T}_{\text{charge}} \end{cases} \tag{4.17}$$

$$\text{discharge}_{i,t} = \begin{cases} \text{discharge}_{i,t} \geq 0 & \forall t \in \mathcal{T}_{\text{discharge}} \\ 0, & \forall t \notin \mathcal{T}_{\text{discharge}} \end{cases} \tag{4.18}$$

It is assumed that the storage system has knowledge of the daily load profile. Specifically, at the end of each day (20:00), the storage is assumed to know the load for the entire upcoming 24-hour period. Based on this information, the model can determine the optimal schedule for charging and discharging.

T^{LTES}_{charge} and $T^{LTES}_{discharge}$ are the temperatures of the water exiting the PCM storage after charging or discharging. The outlet temperatures of the water during charging and discharging of the storage are set to be 2 °C above or below the storage's melting temperature.

$$T^{LTES}_{charge} = T^{LTES}_{melt} - \ 2 \tag{4.19}$$

$$T^{LTES}_{discharge} = T^{LTES}_{melt} + \ 2 \tag{4.20}$$

$$T^{LTES}_{melt} = 10 \tag{4.21}$$

4.3.1 Configuration 1 - Serial

In configuration 1, both charging and discharging variables are constrained with respect to temperatures. The following constraints were added to simulate the charging and discharging behavior of the system. $\dot{m}_{i,t}$ is the mass flow rate of the return water on the secondary side.

$$\text{charge}_{i,t} = \begin{cases} \text{charge}_{i,t} \leq \dot{m}^{charge} \cdot c_p \ \cdot (T^{LTES}_{charge} - T^{sup,p}_{i,t}) & \textit{if} \ \ T^{sup,p}_{i,t} \leq T^{LTES}_{charge} \\ 0 & \textit{if} \ \ T^{sup,p}_{i,t} > T^{LTES}_{charge} \end{cases} \tag{4.22}$$

$$\text{discharge}_{i,t} = \begin{cases} \text{discharge}_{i,t} \leq \dot{m}_{i,t} \cdot c_p \ \cdot (T^{ret,s}_{i,t} - T^{LTES}_{discharge}) & \textit{if} \ \ T^{ret,s}_{i,t} \geq T^{LTES}_{discharge} \\ 0 & \textit{if} \ \ T^{ret,s}_{i,t} < T^{LTES}_{discharge} \end{cases} \tag{4.23}$$

Equation 4.22 ensures that charging only can occur if the supply temperature on the primary side is less than or equal to the outlet temperature of the LTES during charging. If the water temperature is higher than this, the temperature would not be low enough to allow efficient charging of the storage. This value was chosen with respect to the study made by Alam et al. [34], which concluded that the tested PCM was able to solidify when the inlet water temperature was 3 °C lower than the melting temperature, but not when only 1 °C lower than the melting temperature. The constraint was therefore set in between these values. Similarly, from Equation 4.23, if the temperature of the secondary side return water is too low, the LTES would not be able to pre-cool the water effectively and thus no discharging can be made. No previous studies was found regarding the effectiveness on discharging with respect to water inlet temperature, and therefore a similar temperature of 2 °C above melting temperature was set.

In this model, the amount of charging and discharging is assumed to depend on the temperature difference. That is, the mass flow rates are kept constant at each time step, so changes in the amount of charge or discharge directly affect the outlet temperature. However, the outlet temperature will never be lower or exceed the values stated in Equation 4.19 and Equation 4.20.

The first configuration will always be able to provide the customer with the desired temperature, i.e. $T_{i,t}^{sup,s}$. This since the full fraction of mass flow will be pre-cooled, and later fully cooled by the HX at the substation.

4.3.2 Configuration 2 - Parallel

For configuration 2, the idea is to redirect a part of the return water on the secondary side into the LTES, cool it fully, and later be mixed with the rest of the water from the HX. In this model, two additional decision variables were introduced.

$$w_{i,t} \tag{4.24}$$

$$on_t \in \{0, 1\} \tag{4.25}$$

$w_{i,t}$ is a continuous decision variable and represents the fraction of flow that is redirected into the storage during discharging. $on_{i,t}$ is a binary decision variable and simulate the discharging behavior of the storage. It states that discharging is allowed if set to 1 and 0 if it is not. To ensure that the fraction of flow is not exceeded, the following constraint were added:

$$w_{i,t} \leq w^{max} \cdot on_{i,t} \tag{4.26}$$

where:

$$w^{max} = 0.3 \tag{4.27}$$

The flow going into the LTES is thus:

$$m_{i,t}^{LTES} = \dot{m}_{i,t} \cdot w_{i,t} \tag{4.28}$$

Equation 4.26 states that if discharging is allowed, the fraction of flow rate into the storage can at maximum be w^{max}. In this model, w^{max} is set to be 0.3. This value was chosen to ensure that the new supply temperature to the customer would not become too high after mixing, since the outlet temperature of the LTES will be higher than 8 °C. In contrast, a value that is too small would lead to discharge rates that are too low to have a significant impact on the system.

To represent the on/off behavior of the discharging, a big-M formulation was used. In mixed-integer linear programming, multiplication of two decision variables is not allowed if the model is to remain linear. The Big-M formulation resolves this by providing a linear constraint that simultaneously enforces the on/off logic and preserves linearity[68]. The following constraint were added:

$$discharge_{i,t} \leq M \cdot on_{i,t} \tag{4.29}$$

Equation 4.29 states that if the binary decision variable is 1, i.e. discharge is allowed, the storage can discharge at most M. The value of M is set constant for each day and defined as:

$$M = load_{i,d}^{max} \tag{4.30}$$

This value was chosen to ensure the discharge limit is valid while keeping M small enough for the solver to work efficiently. However, it can be noted that from Equation 4.26, the binary variable is already indirectly linked to discharge through the flow fraction. If $on_{i,t} = 0$, then $w_{i,t}$= 0 and consequently $discharge_{i,t}$= 0. Equation 4.29 is therefore not strictly necessary but were introduced to strengthen the model, improving robustness and providing a direct and explicit connection between the binary on/off variable and the discharge variable.

A final constraint relating the binary decision variable to the discharge variable were added:

$$discharge_{i,t} \geq \epsilon \cdot on_{i,t} \tag{4.31}$$

Equation 4.31 ensures that the binary variable is only set to 1 when the storage actually discharges, avoiding the case where $on_{i,t} = 1$ but $discharge_{i,t} = 0$. The value of ϵ was chosen to be small enough to allow minimal discharges, and was therefore set to be 0.001.

Similar to the model constructed for configuration 1, the maximum outlet temperatures of the water leaving the storage after charging and discharging remain the same, as described in Equation 4.19 and Equation 4.20. The charging behavior stated in Equation 4.22 is also identical, since it is connected in the same way. However, a modification was made to Equation 4.23. Since the LTES in this configuration only takes a fraction of the flow when discharging, the discharging constraint was modified to:

$$\text{discharge}_{i,t} = \begin{cases} \text{discharge}_{i,t} \leq \dot{m}_{i,t} \cdot w_{i,t} \cdot c_p \cdot (T_{i,t}^{ret,s} - T_{discharge}^{LTES}) & if \ T_{i,t}^{ret,s} \geq T_{discharge}^{LTES} \\ 0 & if \ T_{i,t}^{ret,s} < T_{discharge}^{LTES} \end{cases} \tag{4.32}$$

This states that if discharging is allowed, the amount of discharge in this configuration is dependent on the amount of water going into the LTES. Furthermore, in this model, it is assumed that the water leaving the storage always reaches the fixed temperature $T_{discharge}^{LTES}$, and the discharge is controlled by varying the low rate into the storage.

This configuration builds on the idea that the customer can be flexible with their supply temperature. The outlet water temperature from the LTES will be higher than the desired temperature of 8 °C, and then mixed with the fully cooled water from the HX. As a result, the supply water will be slightly warmer compared to the case without installed storage. Furthermore, an increase in supply temperature on the secondary side reduces the temperature difference between supply and return.

In order to maintain the same cooling demand, the flow rate on the secondary side must therefore be increased. The required flow rate on the secondary side can be calculated by the following expression:

$$\dot{m}_{i,t}^{new,s} = \frac{load_{i,t} - discharge_{i,t}}{c_p \cdot (T_{i,t}^{ret,s} - T_{i,t}^{sup,s})} \tag{4.33}$$

The mixed water temperature is then calculated as follows:

$$T_{i,t}^{mixed,s} = \frac{\dot{m}_{i,t}^{new,s} \cdot T_{i,t}^{sup,s} + \dot{m}_{i,t}^{LTES} \cdot T_{discharge}^{LTES}}{\dot{m}_{i,t}^{new,s} + \dot{m}_{i,t}^{LTES}} \tag{4.34}$$

Since $\dot{m}_{i,t}^{new,s}$ is smaller than $\dot{m}_{i,t}$, this results in a smaller amount of water needing to be cooled in the HX, thereby reducing the load while maintaining the original ΔT. Consequently, the producer can reduce the mass rate and thereby decrease their cooling production.

4.4 Optimized Almedal Area

A theoretically ideal Almedal area was constructed based on the load profile for the entire area over the considered period. This allows for a more representative assessment of LTES performance under ideal conditions. Since some customers might experience low ΔT, the system may deviate from its designed operating conditions. This affects both flow rates and the availability of the LTES for effective utilization, as the temperature ranges are already small. Therefore, to construct an ideal system, the temperature difference was assumed to be constant at 10 °C, from which the corresponding flow rate was calculated.

The optimized Almedal area will be compared with the original data, and any differences will be evaluated in terms of the effectiveness of the LTES in improving system performance, particularly with respect to flow conditions and energy utilization. Furthermore, any benefits for the producer will be assessed using the optimized area to evaluate the theoretical potential of implementing LTES in the system.

The optimized Almedal area will be used to evaluate the implementation of between 1 and 100 LTES units, in order to assess how system performance and benefits evolve as the storage capacity increases. This makes it possible to see how the benefits change when the number of units increases. Since the area contains hourly load values way higher compared to a single customer, the α value stated in Equation 4.11 was changed to 0.0001 to ensure the model chooses to charge during nighttime. Furthermore, $\dot{m}_{charge}$ from Equation 4.5 was set to $0.5 \cdot N_{unit}$. Since the optimized system always provide a ΔT of 2 °C between the supply water on the primary side and the outlet of the LTES during charging, no marginal was needed to ensure a fully charged storage during nighttime.

4.5 Economic Assessment Method

To evaluate whether it is of benefit to install a LTES in the DC network, an economic assessment was conducted. Firstly, calculations regarding the savings for the individual customers was made. Secondly, an economic assessment from the producer's perspective was calculated.

4.5.1 Economical Assessment for Customers

Any potential savings for the customer will depend on the three economical components energy, power and flow, as stated in subsection 3.2.5. The change in total cost was be calculated as follows:

$$\Delta c_i^{tot} = \Delta c_i^{energy} + \Delta c_i^{capacity} + \Delta c_i^{flow} \tag{4.35}$$

where Δ is:

$$\Delta = \text{old cost } - \text{ new cost} \tag{4.36}$$

In terms of the investment cost of a storage, 1 m^3 of FlatICE PCM corresponds to a cost of € 3 000, which equals to 33 000 SEK if taking the average currency change from 2025[69]. The cost for the PCM material per kWh was therefore calculated as follows:

$$\frac{33\ 000\ [SEK]}{44\ [kWh]} = 750\ [SEK/kWh] \tag{4.37}$$

The investment cost of the PCM material for each LTES unit for each customer is given by:

$$c_i^{PCM} = 750 \cdot CAP_i \tag{4.38}$$

CAP_i is determined from the evaluation of the most suitable storage size for each individual customer.

However, the cost of the PCM material represents only a fraction of the total investment cost of the installation. According to the IEA-ECES Annex 30 report (2018) [70], only one LTES study presented provided data relating the material cost to the total investment cost. In that particular case, the storage material accounted for 19.2% of the total CAPEX and the cost of capacity equaled 103 €/kWh. The installation cost covered a plate-based LTES system installation to a cogeneration plant of heating. At Chalmers University of Technology, a DC tank design was constructed and conducted where the PCM equaled 50.6 % of the total investment costs, which included shipping, installment, HX and tank[71]. The total cost of the capacity equaled 2793 SEK/kWh. Thus, to estimate the cost of an installed LTES to an already existing substation, the percentage cost of the PCM was estimated as an average of the two. This accounts for a percentage of 34.9%. Consequentially, the total investment cost for each LTES system and customer is:

$$c_i^{inv} = \frac{c_i^{PCM}}{0.349} = 2\ 149\ \ [SEK/kWh] \tag{4.39}$$

The payback period for each customer will thus be:

$$PBP_i = \frac{c_i^{inv}}{\Delta c_i^{tot}} \tag{4.40}$$

To evaluate the profitability of implementing LTES, the Net Present Value (NPV) was used. The NPV of the installed storage will be given by the following equation:

$$NPV_i^{cust} = -c_i^{inv} + \Delta c_i^{tot} \cdot \frac{1-(1+r)^{-t}}{r} \tag{4.41}$$

r equals the discount rate and t equals the number of years of the project period. In this thesis, a project period of 10 years was chosen as it was considered a reasonable payback period[2]. As for the discount rate, this value was harder to determine. For private investors in energy utilities, the discount rate often ranges between 7–9% [72]. Furthermore, the Swedish authority Trafikverket uses a social discount rate of 3.5%, which accounts for an expected annual growth of 1.8% [73]. According to Energimyndigheten, this is comparable to a private discount rate of approximately 5%, which is the value of interest since the customers are assumed to be private companies. Continuing, the mortgage interest rate in Sweden is currently around 3%, which reflects a realistic cost of capital in the market and might be used as a proxy for the discount rate[74]. Therefore, four different discount rates was evaluated and compared.

Table 4.2: Discount rates used for economic evaluation for customers.

Discount rate
r = 3%
r = 5%
r = 7%
r = 9%

4.5.2 Economic Assessment for Producer

The economic assessment for the producer was based on the optimal Almedal area, since the evaluation concerned the theoretical potential for implementing LTES. For the producer, the savings in cooling production costs was evaluated in terms of reduced compression usage and total electricity consumption. Compression-based cooling is of particular relevance as absorption chillers utilize excess heat and require significantly less electricity, and was therefore considered the preferred production technology. In addition, additional revenue is generated from potential new customers who can be connected due to the capacity freed up by the LTES. The potential additional income from new customers was calculated as follows:

$$FLH = 1000 \quad [h] \tag{4.42}$$

$$c^{avg\ inc} = 1.273 \ \ [SEK/kWh] \tag{4.43}$$

$$c^{loss} = 754 \ \cdot \Delta load \tag{4.44}$$

$$c^{inc} = (\Delta load \cdot FLH \cdot c^{avg\ inc}) - c^{loss} \ \ [SEK/year] \tag{4.45}$$

Equation 4.42 represents the full load hours (FLH) used by new customers and Equation 4.43 represents the average income from new customers which was provided by Göteborg Energi[2]. Equation 4.44 represent the average loss of income from customers since a reduction in peak load decreases the yearly revenue from the capacity cost. Equation 4.45 represents the yearly total income, which is the combination of additional revenue generated by new customers and a loss of income from old customers[2]. Δload represents the amount of load reduced by the LTES, which can be used by potential new customers.

When a new customer is connected to the DC network, the producer must pay a connection cost. This cost is highly variable and depends on factors such as the size and type of customer. However, based on previous installations, it is typically around 2–3 $MSEK/MW$. In addition, the customer pays an access fee to the producer for connecting to the DC network, amounting to approximately 0.8 $MSEK/MW$. Based on these values, this thesis assumed a connection cost of 2.8 $MSEK/MW$[2]. After subtracting the access fee paid by the customer, the net cost of connecting a new customer is:

$$c^{connect} = \Delta load \ \cdot \ 2000 \ \ [SEK/kW] \tag{4.46}$$

Similar to the economic assessment for the customers, the NPV was used to determine whether the cost of LTES will be profitable for the producer. Since the income will here instead depend on the amount of freed up load in the system, the NPV was calculated as follows:

$$NPV^{prod} = -(c^{inv} + c^{connect}) + c^{inc} \cdot \frac{1-(1+r)^{-t}}{r} \tag{4.47}$$

Similar to the economic assessment for customers, four different discount rates was investigated. These can again be found in Table 4.2.

4.6 Model validation

This section presents the assumptions and limitations of the model as well as the method and results of the validation process that examined the behavior of the model. This is done for both configurations, and the results are briefly discussed to ensure rationality.

4.6.1 Model assumptions and limitations

The aim of the constructed models was to investigate the theoretical potential of implementing LTES. As such, no explicit constraints on maximum flow rates within the storage system were included. Instead, simplified assumptions were made regarding the interaction between the storage and the flow rates. Specifically, for configuration 1, it was assumed that the storage could utilize the full available mass flow from the customer at any given time. For configuration 2, the storage was limited to utilizing up to 30% of the customer-side mass flow at each time step. These assumptions neglect potential hydraulic and technical limitations of the storage system.

The models did not account for the specific characteristics of the PCM itself. Since the LTES relies on latent heat, which behaves differently from sensible heat, the melting and solidification processes are not uniform and depend on the fraction of solid and liquid phases within each container. Furthermore, the models assumed that the energy absorbed or released by the storage was solely determined by the sensible heat exchange of the water flow rate passing through the LTES, without considering the actual thermal behavior of the PCM. In configuration 1, the discharge was assumed to be determined by the temperature difference of the water mass flow. In contrast, in configuration 2, it was assumed to depend on the amount of water passing through, with the additional assumption that the water always exited the PCM at a temperature of 12 °C. This do not reflect reality, as the PCM can absorb or release energy at varying rates depending on the solid–liquid fraction, as well as the flow rate over the PCM and the inlet temperature of the water. Furthermore, cycling performance was neglected, and it was assumed that the storage could be used whenever it was possible to reduce the peak load of each day. To more accurately evaluate system performance, experimental studies or detailed simulations would have been required to capture the behavior of PCM materials under these operating conditions and configurations.

As stated in section 4.3, no data were available regarding the mass flow rates or temperatures on the secondary side. Therefore, the mass flow rate was assumed to be equal on both the primary and secondary sides, and the secondary side temperatures were assumed to be consistently 2 °C higher than those on the primary side. However, this do not reflect actual operating conditions. Additionally, due to the complexity of HXs and the interdependence between mass flow rates, pressure, and temperatures, it was assumed in configuration 2 that any reduction in mass flow rate on the secondary side would be mirrored on the primary side, while maintaining a constant temperature difference ΔT. The pressure difference of the supply and return temperatures caused by the HX was also neglected. Furthermore, the pressure difference on the secondary side would realistically most likely be lower and regulated with pumping. However, this was not considered when modeling the implementation of the storage units.

In addition, no data regarding electricity usage for pumps in the network were obtained. Therefore, exact calculations and comparisons of the network SEER could not be performed. The analysis was instead based on the potential change in compression chiller usage as an indicator of network SEER performance, since a lower compression chiller usage would result in a lower electricity consumption.

The models only optimized the maximum peak of the day, which meant that if discharging was constrained during the peak hour by flow or temperature differences, the storage did not discharge during other hours even if the total load could theoretically have been decreased. This caused a limitation in how the storage was utilized, and the maximum capacity available was not always used.

The model did not perform any changes to the production itself, but instead assumed that cooling capacity was available. If the compressors were being used during a certain hour, it was assumed that the absorption machines were operating at their maximum capacity. Therefore, if production needed to be increased, the cooling was assumed to be produced using additional compressor usage. In contrast, if the compressors were inactive, the models assumed that additional absorption capacity was available. In this case, the compressor cooling remained at zero, and the absorption machines were assumed to meet the required cooling demand. Further, even if the flow was increased, the supply temperature from the producer did not change, which is a simplification of reality.

4.6.2 Validation Methodology

To verify that the implemented model behaved as intended, a simplified dataset was created. The model operates on a daily basis and normally uses input data covering several months. Therefore, the simplified dataset consisted of four days only. The variables in the dataset were deliberately set to examine the model behavior during different operating conditions such as peaks, low load, constant load and no load. The outputs were then checked for inconsistencies or potential implementation errors. This method made it possible to closely observe how the model processes the inputs. The load input variable were the main variable of interest and was therefore chosen, while the mass flow adjusted accordingly, as well as the temperature difference. Both configurations of the model was evaluated and are presented below, where some different functionalities of each configuration are highlighted.

Furthermore, manual calculations were carried out with regards to the constraints defined in the model. The output variables where calculated step by step using the same input parameters as in the simplified dataset and then compared to the results generated by the model. The agreement of the manual calculations and the model outputs provided additional confidence in the correctness of the model implementation.

4.6.3 Validation Results for Configuration 1 - Serial

The load and flow results for the four days can be found in Appendix C. During nighttime, when demand is low or zero, the model utilizes the available capacity to charge the LTES, resulting in a slight increase in load. The results also show that the model charges the LTES during the available charging window, when the load is at its lowest. The charging does not affect the daily peak.

During the first 24-hour window, a peak occurs where the load increases from 5 to 100 kW. The model chooses to discharge at 11:00 during this peak, thereby reducing the maximum load. Since the flow rate through the LTES is higher on the secondary side, the energy stored during charging is discharged within one hour, reducing the peak to 44 kW. During nighttime, charging occurs with a rate of 8.37 kW due to the flow constraint being set to 1 kg/s. Since more flow can be used for discharging, all of the stored energy can be utilized within one hour during discharging.

During the second 24-hour window, the load remains consistently high, with an additional small peak occurring for one hour. Once again, the LTES charges fully during the night and then operates to level the load. It discharges more evenly, ensuring that not only the peak is reduced as much as possible, but also that the overall maximum load of the system is lowered. This approach prevents the creation of new peaks.

During the third 24-hour window, the load starts at 50 kW and increases to 100 kW during the day. Here, the LTES fully focuses on lowering the larger load, which would bring down the maximal peak load of the day. The SOC during this day shows an even discharge at a reasonably fast pace.

During the last 24-hour window, the load is constantly low with values of 5 and 10 kW respectively. Here, one can see that the storage charges at a lower rate to prevent the creation of new peaks.

As for the flow, the results show that the peak flow is increased during nighttime, almost to the extent of creating new peaks when the LTES is being charged. This indicates that the model does not care about the flow peaks in the same way as the load. The total volume flow during the period is increased from 197 m^3 to 261 m^3. This is expected, as more flow is required during charging compared to discharging due to a lower ΔT when charging.

4.6.4 Validation Results for Configuration 2 - Parallel

Similar to the validation for configuration 1, the results of the load and flow curves for validation of configuration 2 can be found in Appendix C. During the first 24-hour window, the model is only able to reduce the peak to 82 kW, significantly less compared to configuration 1. This is due to the discharging being constrained by the flow fraction on the secondary side. It discharges at maximum capacity for one hour during the day, and does therefore not find value in storing more cooling than the 18 kW during the night. For peak loads like this one, the flow faction is what mainly affects the possibility to discharge for the configurations.

The model only charges fully during the third 24-hour window. For the other 24 hour windows, it only charges the amount that can be used for discharging during the following day. As for the discharging, it behaves similarly as for configuration 1, with the exception of the flow fraction constraint stated above.

The last 24-hour window has a very small peak, and the model acts in a similar way as for the first day, with the flow fraction reducing the ability to discharge. Due to this, the maximal discharge is 1.8 kW. Since the peak is 5 kW higher compared to the rest of the load during that day, the model does not find value in reducing the load further.

Similar to configuration 1, the results show that the peak flow is increased during the night. This behavior is expected since they both operate with the same temporal constraints. It can be seen that the flow increases during nighttime due to charging of the LTES, while decreasing during peak demand periods as the storage is discharged. This confirms that the model utilizes low-demand periods to charge and discharges during high-demand hours. The total volume flow is increased from 197 m^3 to 232 m^3. However, comparing the results with configuration 1, the peak flow is decreased which also is expected.

4.7 Sensitivity Analysis

To evaluate the system response, sensitivity analyses was performed. In this section, the methodology behind the sensitivity analyses are described. The result of these are later presented in section 6.1.

4.7.1 Loss factor

First, a loss factor for the PCM was introduced. Due to the lack of commercialized, installed and active LTES systems, no further system efficiency was assumed beyond the capacity provided by the company producing the PCM containers. It was therefore beneficial to assume a loss factor of the system, to account for potential unknown efficiency fluctuations in the performance of the PCM that the model could not predict. Alam et al. [34] stated that using a loss factor was essential since the PCM was not fully solidified nor fully melted, limiting the extent to which the stated storage capacity could be fully utilized. The findings of the article connects a higher loss factor to a smaller temperature gap between the melting and solidifying temperature and the feed water. Since the DC network in Gothenburg has to utilize a rather small temperature range from the solidifying/melting temperature, the loss factor could act as a precaution of the uncertainty of the capacity of the storage. This thesis investigated three different loss factors, stated in Table 4.3. These was investigated through reducing the storage capacity.

Table 4.3: Loss factors tested.

Test no.	**Loss factor** [%]
1	10
2	20
3	30

4.7.2 Flow fraction for discharging

The second sensitivity analysis concerns the fraction of the mass flow rate used for discharging in configuration 2. In the current model, up to 30% of the mass flow on the secondary side can be redirected to the LTES. Increasing this value allows a larger fraction of the return water to be cooled by the storage. However, such an increase would also result in a higher supply temperature to the customer. It was therefore valuable to investigate the effects of this parameter in order to evaluate its impact on these two factors. The analysis included two different fractions, presented in Table 4.4.

Table 4.4: Flow fractions for discharging tested.

Test no.	w^{max} **value** [%]
1	20
2	50
Base Case	30

4.7.3 Investment Costs

The investment cost is calculated from two installations of LTES. However, due to it being estimated with few sources due to the technology not being commercialized in networks, this number is highly uncertain. Therefore, a sensitivity analysis was carried out, which allowed for an assessment of how sensitive the profitability is to these assumptions.

This sensitivity analysis affect customers as well as producers, therefore both will be investigated. The different investment costs that was investigated are presented in Table 4.5.

Table 4.5: Investment costs tested.

Test no.	**Investment costs** $[SEK/kWh]$	**PCM Share** [%]	**Percentage Change** [%]
1	1 719	43.6%	80%
2	2 579	29.1%	120%
3	3 223	23.3%	150%
Base Case	2 149	34.9%	100%

5 Results and Analysis

This chapter presents findings from literature, followed by the modeling results, which includes the two modeled configurations as well as the optimized Almedal area. Lastly an economic assessment is presented.

5.1 Theoretical Results

To answer research question 1, key factors influencing latent energy storage systems and the considerations required for their implementation are presented in this section. Although this report does not include the design of a specific LTES, understanding these factors is essential for assessing the feasibility of implementation.

5.1.1 Findings of Literature Review

An examination of different storage types indicated that LTES are suited for applications involving low temperatures, limited installation space, and small temperature differences. This since the energy is stored or released in the phase change process which occurs around a single temperature. LTES also often offers higher energy density, thanks to the large amount of energy stored or released in the phase change, allowing for more compact installations compared to most TES systems. Previous research also suggests that LTES can outperform chilled water STES, primarily by providing longer periods of stable cooling at smaller scale. At present, STES is predominantly used in large-scale energy storage systems, whereas LTES is better suited for control-oriented strategies and small-scale applications. Thermochemical storage is another potential option, however its application is challenging as it has primarily been tested at temperatures above 50 °C.

The suitability of PCM depends on its classification, as different types offer different advantages. In practice, PCMs are often modified or combined to meet specific application requirements. Melting temperature ranges compatible with the Gothenburg DC system are available and considered feasible, however the choice of PCM type is a critical consideration. Key properties influencing performance include the heat of fusion $[kJ/kg]$, which determines how much energy can be stored, and thermal conductivity $[W/(m \cdot K)]$, which determine both the duration and energy requirement of the phase change.

Organic PCMs are stable, do not undergo phase separation, and exhibit a consistent heat of fusion over time. They are also less prone to supercooling, which is highly beneficial in systems with a narrow operating temperature range as a majority of thermal energy is stored and released during the phase change process. However, supercooling may occur when using the material in small encapsulations. Their flammability is a factor that must be considered in system design, but it becomes more critical in systems with higher operating temperatures. Inorganic PCMs, however, such as salt hydrates and metals, generally offer higher heat of fusion and thermal conductivity. Metallic PCMs typically have melting temperatures that are too high for DC applications and are therefore considered unsuitable in this context. In-organics are also less flammable than organic PCMs but may cause corrosion in containment materials, which reduces their lifespan. Furthermore, they are more susceptible to supercooling, which increases both the energy requirement and the effective melting range of the material.

When designing an LTES system, several factors must be considered. First, the design should avoid unutilized zones, which arise due to low thermal conductivity and short charging and discharging time frames. Typically, only a thin layer of PCM surrounding the HTF actively participates in the phase change, due to their low thermal conductivity. Therefore, the design should maximize the heat transfer area between the PCM and the HTF and ensure that the surrounding PCM layer is thin enough to complete the phase change within the specified time frame. One approach is to circulate water through tubes embedded in a PCM container. Another is to encapsulate the PCM and allow the HTF to flow around the capsules. The latter can provide a large heat transfer area and allows better utilization of the PCM volume. Common encapsulation formats include pods, balls, ice packs, and tubes. Another important consideration is the occurrence of phase separation in PCM mixtures, particularly after repeated cycling due to uneven solidification between the molecules in PCM mixtures. To mitigate this issue, the PCM either requires stirring, or the system can be designed with smaller tanks or encapsulated PCM containers. Such designs can also improve heat transfer performance by accounting for thermal conductivity of both the PCM and the HTF. Overall, the efficiency and performance of an LTES system depends strongly on the design and must therefore be adapted to the specific application, operating conditions, and desired charging and discharging behavior.

Another challenge is that the melting temperature of a PCM is better represented as a temperature range rather than a fixed value, as materials often exhibit temperature gliding during phase change. Consequently, the available latent energy is not constant within this range, and if the temperature difference between the HTF and the melting temperature of the PCM is small, the full potential energy available may not be utilized. Supercooling further broadens this range and reduces storage efficiency, and both these factors needs to be considered and evaluated when designing the storage.

5.1.2 Findings of Theoretical Framework

The DC network in Gothenburg is designed to have a supply temperature of 6 °C and a return temperature approximately 10 °C higher on the primary side. On the secondary side, the supply temperature is designed for 8 °C, with the return temperature expected to be around 10 °C higher. The primary side supply temperature and the secondary side return temperature are therefore deemed as the best alternatives for charging and discharging respectively, since these streams have the largest temperature difference and therefore the greatest potential for maximizing the utilization of the LTES. Consequently, the melting temperature of the PCM has to be within this range.

A PCM melting temperature of at least 10 °C is desired, to be able to charge the storage with the supply water on the primary side. This allows for a 4 °C temperature difference, if assuming the designed temperature of the stream. However, if accounting for factors such as gliding temperatures, supercooling effects and varying supply and return temperatures, this difference may be reduced to as little as 1 °C. This can reduce the effectiveness of charging significantly. In contrast, for the same assumed PCM melting temperature, the return water on the secondary side exhibits a higher temperature difference but also a larger seasonal variation, ranging from 8 to 30 °C over the summer period. As a result, both the design process and the determination of a suitable PCM melting temperature becomes more challenging.

This report examines two ways of connecting the LTES to the substation of the DC network. Both are constructed using the coldest and warmest temperature streams available. In addition to redirecting the flow to the storage, additional considerations may be required to prevent mixing between the two water streams. This can be achieved by using heat exchangers (HX). Based on this, four feasible HX configurations for the LTES implementation were identified. However, implementing the HXs would decrease the temperature difference between the supply/return temperatures and the storage melting/solidifying temperature. Even a reduction of only 1-2 °C could affect the storage utilization significantly, due to the DC network's already narrow temperature range. Furthermore, adding HXs to the system also increases the investment cost of LTES, which can reduce the incentive of investment. The proposed designs can be found in Appendix C. In the constructed models, no HXs are assumed.

5.2 Modeling Results of Configuration 1 (Serial)

This section presents the results of configuration 1, to answer research question 2. The results and corresponding evaluation will highlight the load and flow of the system. The results are strictly based on the provided data of Almedal from 2025. The load and flow profiles for all individual customers are found in Appendix A.

5.2.1 Load and Flow Evaluation

The peak load and peak flow reduction based on the number of LTES units for all customers are presented in Figure 5.1 and Figure 5.2. These are normalized to their original peaks, where 100% corresponds to the original peak values. In addition, the primary reason for why peak reduction stagnates for each customer is summarized in Table 5.1.

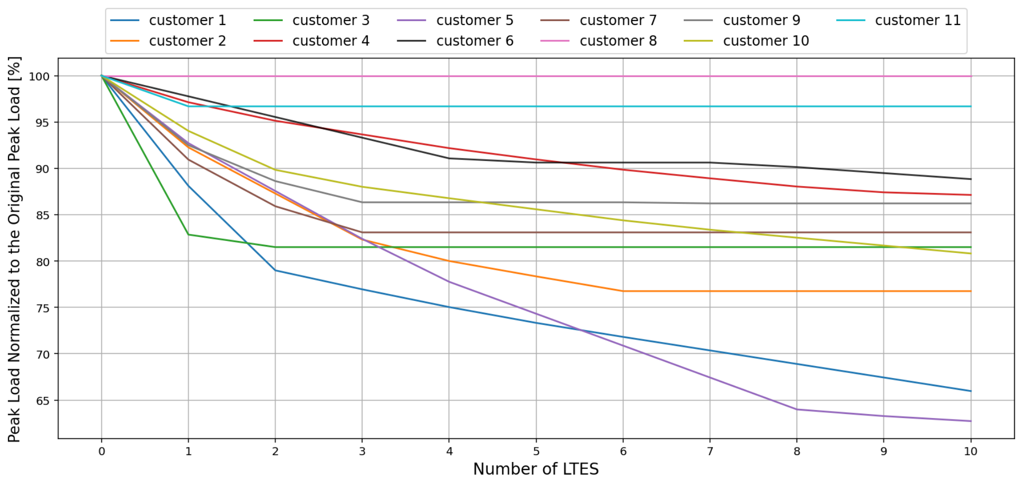

Figure 5.1: Peak load normalized to the original peak load dependent on the number of LTES units, configuration 1.

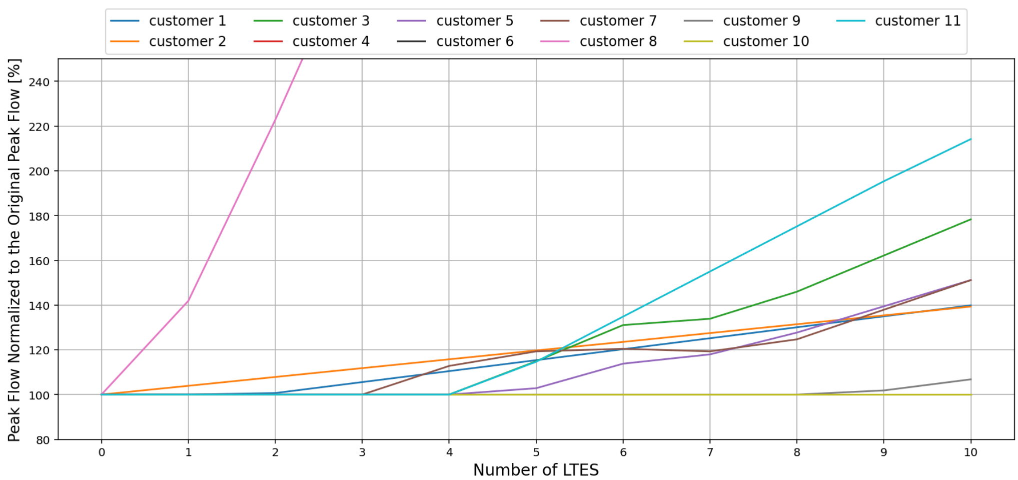

Figure 5.2: Peak flow normalized to the original peak flow dependent on the number of LTES units, configuration 1.

From the results, all customers except customer 8 achieve peak load reduction with LTES. Customer 8 shows no improvement due to the cooling being inactive during nighttime, preventing charging of the storage. For customer 6, the peak load decreases up to 5 LTES units, remains stagnant until 8 units, and then decreases again. This behavior occurs because the model prioritizes charging during periods

Table 5.1: Primary reason why peak reduction stagnates, configuration 1.

Reason	Customer
Cooling inactive	8
High supply water temperature	6
Peak outside of discharging window	11, 3, 7
Low return water temperature	2
High load during night	9
Continuous peak reduction	1, 4, 5, 10

of low load due to the charging penalty in the objective function, and the maximum charging that can be done is constrained. At low charging capacity, the LTES is charged during low-load hours at its maximum rate. As the allowed charging flow increases with the number of LTES units in the system, the charging capacity increases, enabling more charging to be shifted to low-load hours while charging during higher-load hours is reduced. This increases the charging capacity and enables more charging to be shifted to low-load hours, while charging during higher-load night hours is reduced. At 8 storage units, the charging capacity is large enough to eliminate charging during higher-load periods entirely. Further increasing charging capacity continues to reduce the daytime peak load. However, charging for customer 6 are also constrained due to the fact that the supply water temperature on the primary side frequently exceeds 8 °C during nighttime. This limits charging to the few hours when this condition is met and reduces the potential peak load reduction. As a result, the storage is only partially utilized (approximately 40–50%) regardless of the number of installed units.

Customer 11 shows no peak load reduction beyond one LTES unit. Similarly, customers 3 shows a stagnation in peak load reduction after two storage units, and customer 7 after three storage units. This is due to peak loads occurring outside of the discharging window, preventing the storage to reduce peaks further. Customer 2 shows reductions for up to six units, after which the peak reduction stagnates. This is due to the return water from the customer being below 12 °C, preventing discharging from taking place. Customer 9 experience a reduction with up to three units. No further reduction happens due to relatively high load during the night before the peak load occurs. This causes the storage to avoid further charging, as the cost of charging outweighs the potential peak load reduction benefit. Customers 1, 4, 5, and 10 continuously reduces peak load with more storage units.

Regarding peak flow, no reduction is observed. This is because the storage reduces the temperature difference and not volumetric flow when configured this way. For smaller customers (1, 2, 3, 5, 7, 8, and 11), peak flow increases with additional storage units because of low baseline flow rates, resulting in charging during nighttime introduces new peaks. Additionally, for some of the customers, temperature differences between supply and return water are small during low peak hours. This increases the flow rate beyond the design value in order to meet the load demand. Since the model only considers peak load, it prioritizes charging regardless of the flow rate. This can specifically be seen for customer 1 and 2, where the peak flow increases already after one or two storage units. For larger customers (4, 6, and 10), peak flow remains unchanged. This is because their daytime flow rates are significantly higher than their nighttime flows, meaning that charging during the night does not affect the peak flow.

Based on these results, a suitable number of LTES units for each customer is selected and summarized in Table 5.2. Red, yellow, and gray cells indicate increase, no change, and no storage implementation respectively. For customers benefiting from more storage capacity, a maximum of four LTES units is considered appropriate due to physical size constraints. At four units, the PCM material alone occupies 4 m^3 and weighs over 4 tonnes. Since the available space around substations at customer sites is often limited, four storage units were considered sufficient to achieve a significant reduction in peak demand, while still being small enough to potentially allow retrofit into existing installations without major modifications. The total system impact for the Almedal area is also presented, including aggregated peak load and peak flow changes. The load and flow difference for the total Almedal area is visualized in Figure 5.3 and Figure 5.4.

Table 5.2: Number of storage units chosen for each customer and corresponding peak load and peak flow reduction, configuration 1.

Customer no.	**Number of LTES**	**Old peak load** $[kW]$	**New peak load** $[kW]$	**Old Peak Flow** $[m^3/h]$	**New Peak Flow** $[m^3/h]$
1	2	370.0	292.3	73.7	74.2
2	4	442.4	353.9	91.5	105.9
3	1	173.0	143.3	22.3	22.3
4	4	993.0	915.3	201.0	201.0
5	3	425.0	350.2	30.8	30.8
6	4	960.0	874.3	93.2	93.2
7	3	207.0	172	27.3	27.3
8	0	25.3	25.3	3.58	3.58
9	3	586.3	506.2	51.9	51.9
10	4	738.0	640.4	89.9	89.9
11	1	151.0	146.00	17.9	17.9
Almedal	29	4201.1	3899.3	555.9	555.9

The summary of storage units results in a total of 29 LTES units, with a total capacity of 1320 kWh. If all customers were to introduce storage units, the Almedal area would achieve a load reduction of 302 kW. However, the peak flow rate would never be reduced in this configuration, since the decreased cooling demand reduces the temperature difference rather than the volumetric flow rate. The reason why peak flow rate is not increased even though two of the customers show increased peak flow values is due to the fact that each customer's peak flow does not occur at the same hour.

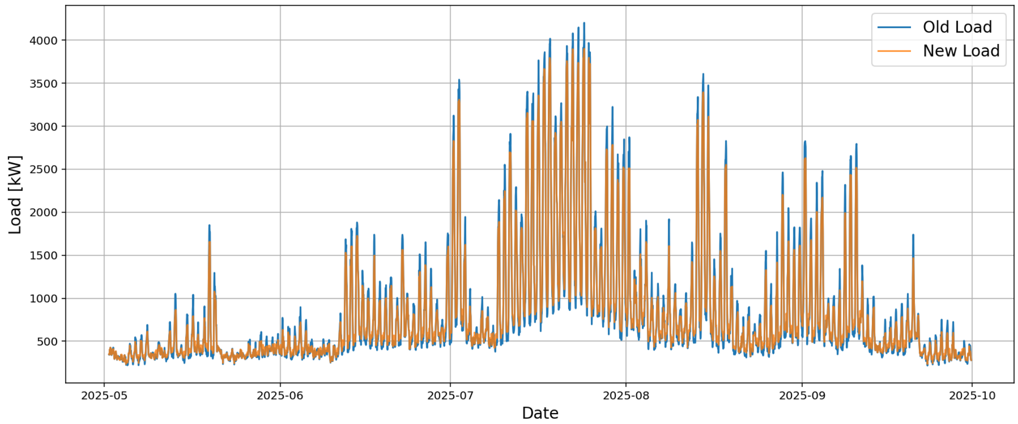

Figure 5.3: Load for Almedal area with and without implemented storage units, configuration 1.

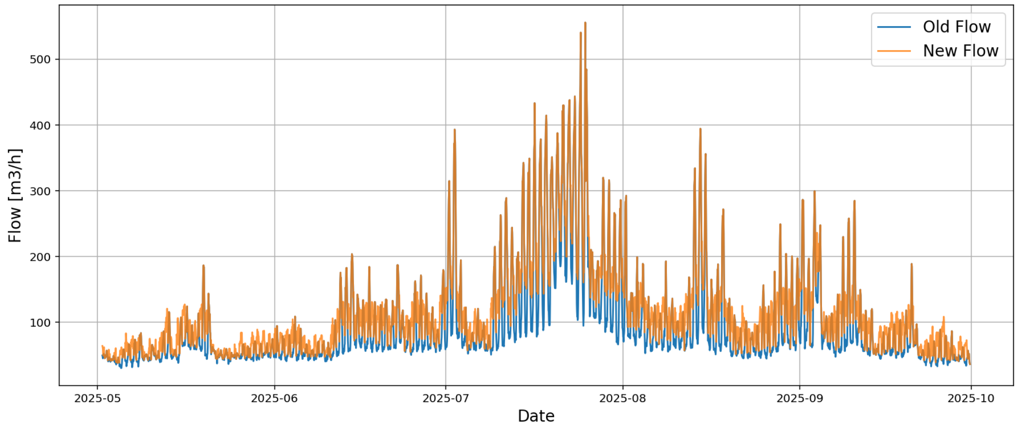

Figure 5.4: Flow for Almedal area with and without implemented storage units, configuration 1.

While implementing LTES in the system could reduce the load and therefore cooling cost for customers, the peak flow rate remains unchanged since the reduction is achieved through a lower temperature difference rather than a reduced flow rate. For this reason, the configuration is not considered a desirable way of integrating LTES into the system. It can be viewed as beneficial since customers can achieve cost savings due to reduced cooling demand, however, the unchanged volumetric flow in the pipes means that no additional customers can be connected to the pipeline. In addition, a large decrease in primary side return temperatures are not desired, since the cooling machines are designed to be provided with water of 14 °C.

For these reasons, no further analysis will be conducted using this configuration. While it offers peak shaving for customers, it does not make better use of the existing network infrastructure compared to the current system and no advantages are achieved from a producer perspective.

5.3 Modeling Results of Configuration 2 (Parallel)

This section presents the results of configuration 2, to continue answering research question 2. The results and corresponding evaluation will highlight the load and flow of the system, and are strictly based on the data from Almedal for 2025. The load and flow profiles for each individual customer can be found in Appendix B.

5.3.1 Load and Flow Evaluation

The peak load and peak flow reductions based on the number of implemented LTES for each customer are presented in Figure 5.5 and Figure 5.6. Similar to configuration 1, the graphs visualize the normalized peaks where 100% corresponds to the original peak values. The primary reason for why peak reduction stagnates are again summarized in Table 5.3.

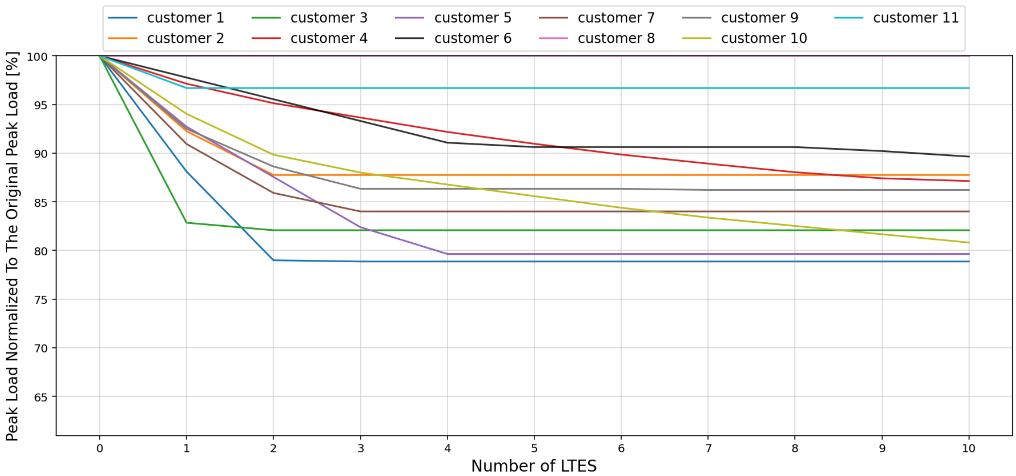

Figure 5.5: Peak load reduction depending on the number of LTES units, configuration 2.

Table 5.3: Primary reason why peak reduction stagnates, configuration 2.

Reason	Customer
Cooling inactive	8
Flow fraction constraint	1, 2, 3, 5, 7
High supply water temperature	6
Peak outside of discharging window	11
High load during night	9
Continuous peak reduction	4, 10

Similar to configuration 1, customer 8 does not reduce its peak load regardless of the number of storage units implemented. Customers 1, 2, 3, 5, and 7 are able to

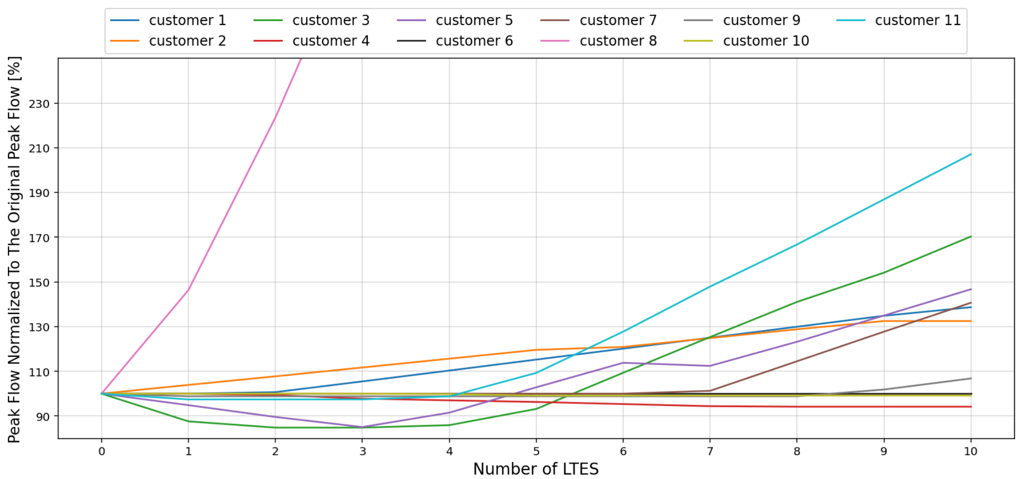

Figure 5.6: Peak flow reduction depending on the number of LTES units, configuration 2.

reduce their peak demand using between 2 and 4 LTES units, after which the peak reduction stagnates and no further decrease is observed. For these customers, this limitation is due to the flow fraction set for discharging. At this point, the available flow being redirected to the storage reaches its maximum, meaning that no additional discharging can occur during this hour. Consequently, further peak reduction is not possible, regardless of the storage capacity. As for the flow, customer 3 and 5 reduces the peak flow with up to 3 LTES, before it starts to increase again. Customer 1 and 2 continuously increase their peak flow, while customer 7 experience a stagnated peak flow up to 7 units before it increases.

Customer 4 and 10 both manage to continuously decrease their peak demand with increased storage capacity, similar to the other configuration. These customers are among the largest ones, meaning they both have a large flow rate and therefore never reaches their maximum discharge capacity during peak load hours. Both of their peak flow rates remains relatively stagnant, however customer 4 experience a small decrease as more storage units are implemented.

Customers 6, 9 and 11 stagnates for the same reasons as for configuration 1. Customer 6 has too high supply water temperatures and the model prioritizes removing charging during high-load hours, customer 9 sees charging as more costly compared to the available reduction in peak load and customer 11 has a peak outside of the discharging window.

Overall, many of the customers show similar behavior as in configuration 1, with the exception of some customers that are now constrained by the flow fraction. Regarding peak flow, some customers in configuration 2 experience a reduction in peak flow, in contrast to configuration 1. However, the behavior of increasing peak flows due to nighttime charging or low temperature differences is still present, which is why the majority of customers show an increasing peak flow with a larger number of implemented LTES units.

Based on the observations above, the number of storage units deemed most suitable for each customer is presented in Table 5.4. The total number of LTES units for the entire Almedal area, obtained by summing the LTES units across all customers, is presented at the bottom of the table. The graphs for the whole period and each customer with implemented LTES can be found in Appendix B. Similar to configuration 1, four LTES units was concluded to be the maximum suitable storage size, due to the limited space at customer sites.

Table 5.4: Number of storage units chosen for each customer and corresponding peak load and peak flow reduction, configuration 2.

Customer no.	**Number of LTES**	**Old peak load** $[kW]$	**New peak load** $[kW]$	**Old Peak Flow** $[m^3/h]$	**New Peak Flow** $[m^3/h]$
1	2	370.0	292.3	73.7	74.2
2	2	442.4	388.2	91.5	98.5
3	1	173.0	143.3	22.3	19.6
4	4	993.0	915.3	201.0	195.0
5	3	425.0	350.2	30.8	26.2
6	4	960.0	874.3	93.2	93.2
7	3	207.0	173.9	27.3	27.3
8	0	25.3	25.3	3.58	3.58
9	3	586.3	506.2	51.8	51.2
10	4	738.0	640.4	89.9	89.7
11	1	151.0	146.0	17.9	17.4
Almedal	27	4201.1	3943.9	555.9	537.9

For the total Almedal area, if the customers had implemented LTES units, the total peak demand 2025 would have been reduced by around 257 kW (6.1%), and the peak flow would have been reduced with 18 m^3/h (3.2%). The load and flow difference for the whole season are presented in Figure 5.7 and Figure 5.8.

As can be seen, the load and flow profiles of the total area show that having LTES implemented reduces both the peak load and peak flow. However, the flow reduction can be compared to what the flow reduction would be if all customers had a temperature difference of 10 °C. In that case, a load of 4200 kW would with a 10 °C difference have a flow of 362 m^3/h, which is around 200 m^3/h, or 34.9%, less compared to the measured peak flow. This indicates that the temperature difference between the supply and return water is significantly lower than the design value of 10 °C, leading to elevated flow rates to compensate for the high cooling demand. This is discussed in more detail in subsection 6.2.1. Furthermore, having supply and return water temperatures closer to the melting point of the PCM reduces the potential of full utilization of the storage, since PCM have shown to be significantly less effective as the temperature gap decreases.

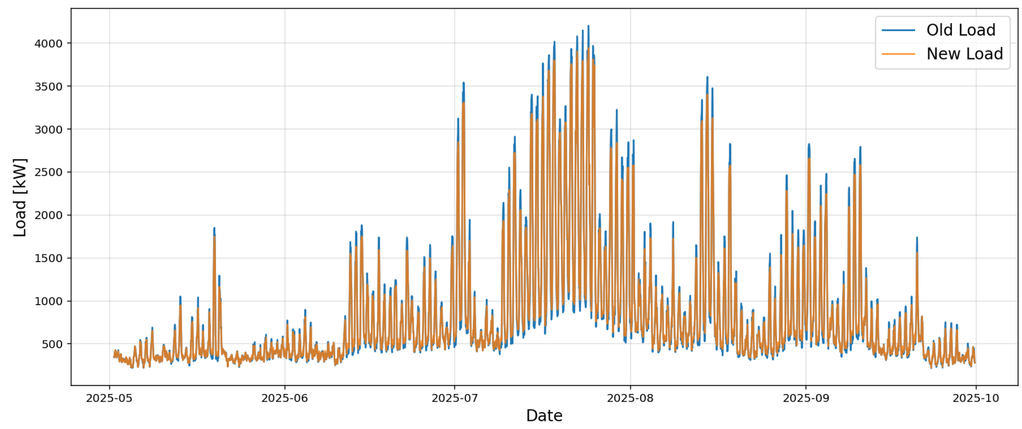

Figure 5.7: Load for Almedal area with and without implemented storage units, configuration 2.

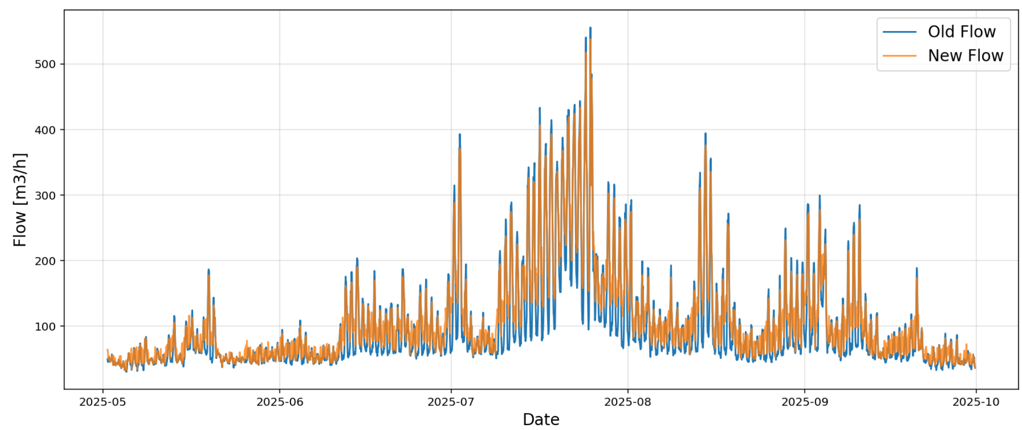

Figure 5.8: Flow for Almedal area with and without implemented storage units, configuration 2.

One customer that is highly affected by this is customer 4, where the return water temperature on the secondary side, as well as the average temperature difference, is very low. This results in a flow rate that is higher than expected to meet the cooling load, which can be seen between the load and flow difference presented in Figure 5.9. The peak flow is significantly higher than what would be expected for the experienced peak load, with a value around 201 m^3/h. During this hour, the load is 780 kW and the temperature difference is 3.3 °C. Increasing this difference by only 2 °C would result in a flow decrease of 74 m^3/h, which is significantly higher than what the LTES can achieve. The low return water temperature would also theoretically be a constraint on utilization availability. However, since the flow rate is high, the low temperature does not constrain the availability of discharging, as the available flow fraction is sufficient. If this was not the case, the low return temperature could become a significant constraint on the system.

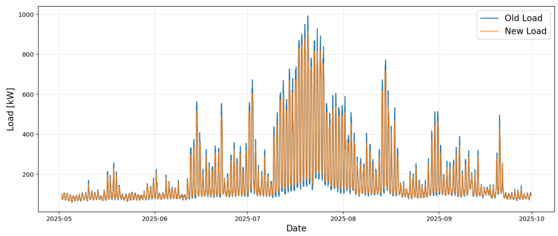

(a) Load for customer 4.

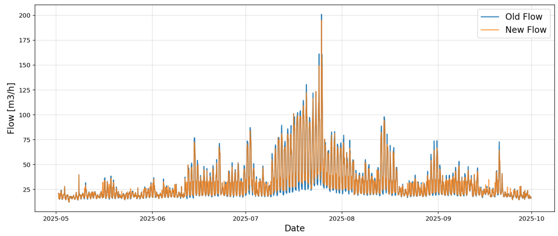

(b) Flow for customer 4.

Figure 5.9: Load and flow profile for customer 4.

In addition to load and flow reductions, the compression usage also decreases. The compression usage over the period are presented in Figure 5.10.

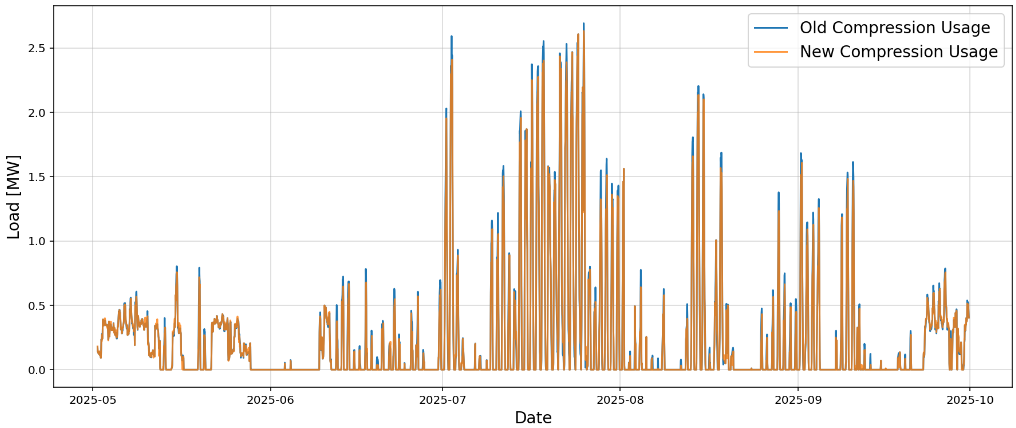

Figure 5.10: Cooling from compression for Almedal area.

With 27 LTES units implemented, the total compressor usage is reduced by approximately 46 MWh, which in turn lowers the electricity consumption. These results indicate that when storage units are added, less compression is required, as it is replaced by absorption chillers when charging the LTES during low-load hours. Furthermore, a decrease in compression usage would potentially increase the network SEER, since less electricity is used to provide the amount of cooling needed over the period. However, as stated in subsection 4.6.1, no data regarding the electricity requirement or consumption of pumps were obtained and therefore no exact calculation of the network SEER can be evaluated.

5.4 Modeling Results of Optimized Almedal Area

To answer research question 3, an optimized Almedal area is considered and evaluated in this section. See method section 4.4 for further explanation and assumptions. For the optimized area, configuration 2 is used.

5.4.1 Load and Flow Evaluation

As stated in subsection 5.3.1, the flow rate exceeds the expected value with over 200 m^3/h in the actual Almedal area. This is because the supply water temperature from producer is higher while the return water temperature from customers is lower during many hours of the period. Furthermore, having deviating temperatures at customer sites reduces the potential availability of having LTES, since the storage is sensitive to narrow temperature ranges. The optimized Almedal area is therefore used to draw general conclusions regarding the potential of LTES, since the results are derived from an ideal system configuration.

Based on this, an evaluation of the reduction of peak load and peak flow in relation to the number of implemented LTES units is conducted. The results are shown in Figure 5.11 and Figure 5.12. The red markers indicate the number of LTES required to achieve the same reduction in peak load and peak flow as for the actual Almedal area, while the green markers indicate the reduction achieved with the same number of LTES as in the actual Almedal area. In Figure 5.11, the two dashed lines indicates the amount of peak load reduced per installed kWh of LTES.

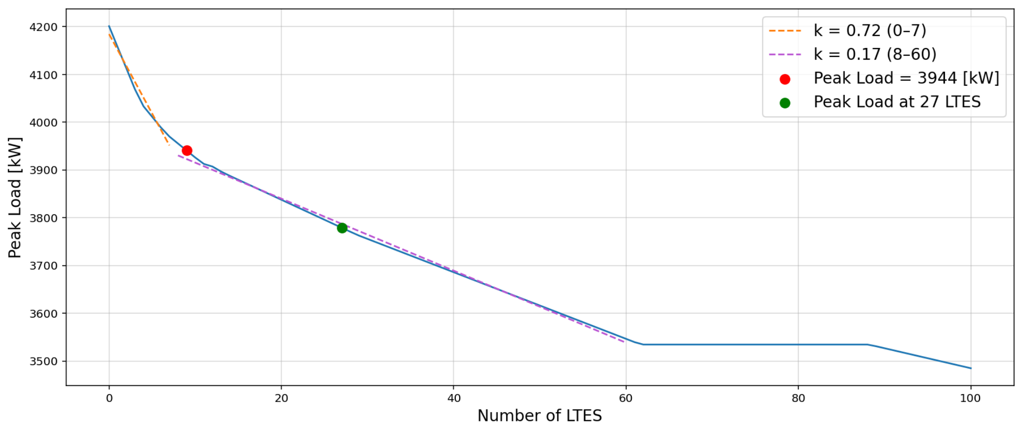

Figure 5.11: Peak load based on the number of LTES.

Both peak load and peak flow decrease as the LTES capacity increases. As shown in Figure 5.11, the reduction is more significant at low numbers of installed storage units, with an average peak reduction of 0.72 kW/kWh of installed storage capacity. Between 7 and 60 LTES units, the reduction is decreased down to 0.17 kW/kWh. This is because the highest peaks are reduced first, which represent a smaller and more concentrated load. Once these are mitigated, further reductions target a broader load profile, requiring more storage capacity and resulting in a lower marginal peak reduction. At around 60 LTES units, the peak remain constant up to approximately 90 LTES units, after which they start to decrease again. This behavior is caused due to the same constraint as for customer 6 in configuration 1. The model shifts charging to low-load hours, and when the hours with higher load are removed, peak reduction continues again.

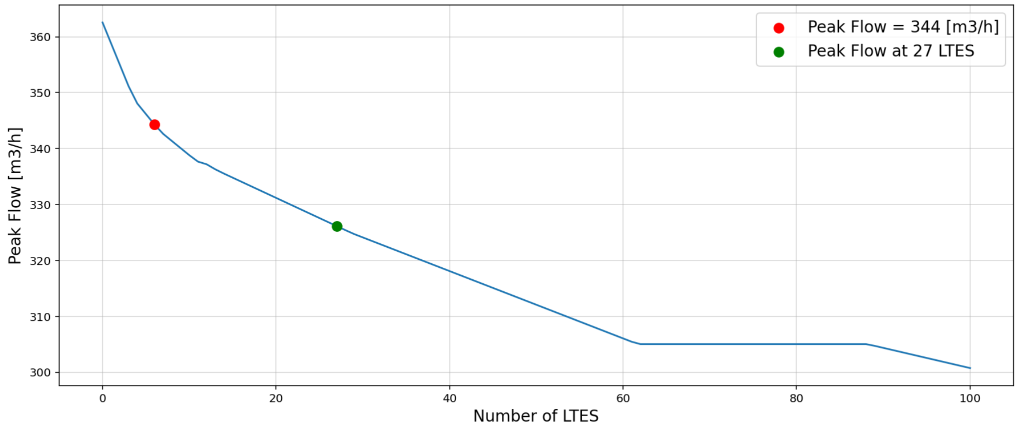

Figure 5.12: Peak flow based on the number of LTES.

Looking at the red markers in the figures above, matching the same level of reduction in the actual Almedal area would require 9 LTES for peak load and 6 units for peak flow. These values are significantly lower compared to the 27 units required in the actual Almedal area. Considering the green markers, corresponding to the load and flow reduction with 27 LTES units, the peak load is reduced to 3 779 kW, resulting in additional decrease of 165 kW compared to the actual area. The total decrease in peak load equals 421 kW, which corresponds to 10.0%. The new peak flow equals 362 m^3/h. The reduction of the new peak is 36 m^3/h, corresponding to a reduction of 10.0%, approximately twice that of the actual system. These results indicate that when the system is optimized, the storage units operate more effectively. To further compare the actual and optimized systems, the load and flow profiles for the optimized Almedal area with 27 LTES units are presented in Figure 5.13 and Figure 5.14.

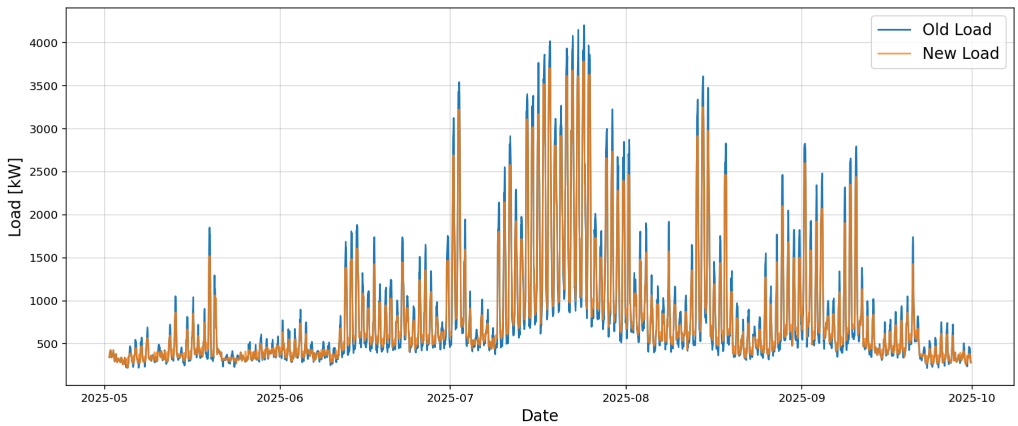

Figure 5.13: Load profile of an optimized Almedal area (27 LTES).

While the load profile appears nearly identical, except for a greater load reduction, the flow profile is significantly lower. Furthermore, in the optimized area, the flow profile is proportional to the load profile due to the constant temperature difference. These figures clearly show that the flow in the actual area deviates significantly from

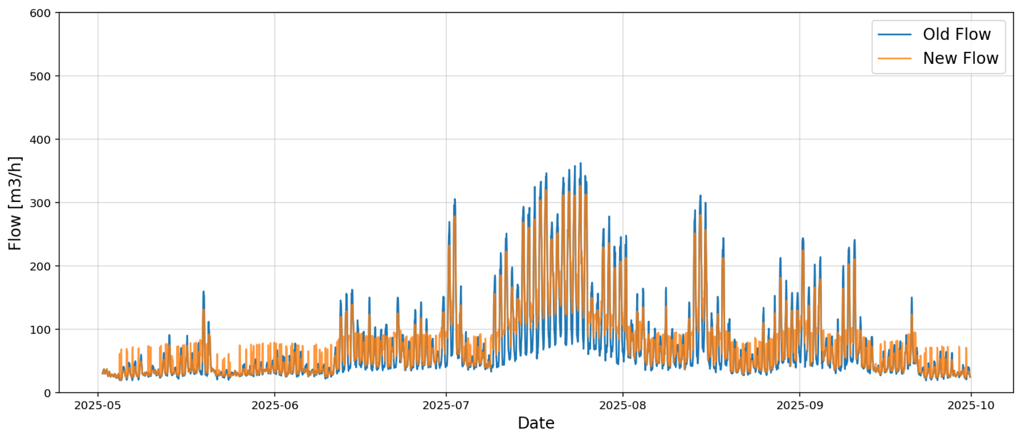

Figure 5.14: Flow profile of an optimized Almedal area (27 LTES).

the designed conditions, and that simply increasing the temperature difference can reduce the flow to a much greater extent than implementing LTES alone can achieve.

Furthermore, with increasing number of LTES in the system, the compression usage reduces. The cooling delivered from compression chillers based on the number of LTES is presented in Figure 5.15.

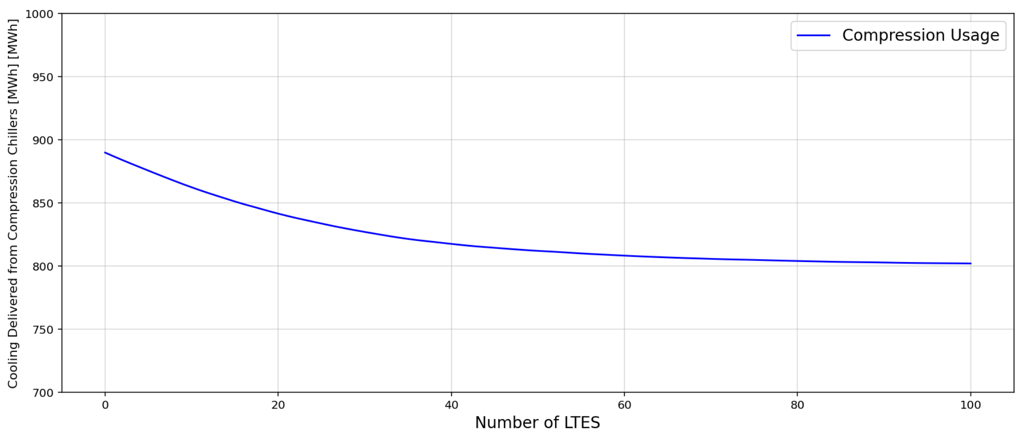

Figure 5.15: Cooling delivered from compression chillers based on the number of LTES.

As shown, the cooling from compression shows a decreasing trend as more storage units are added to the system. With 27 units implemented, the compressor usage decreases by 59 MWh, indicating that an optimized system achieves greater reductions with the same amount of LTES. Furthermore, a larger decrease in usage of compression chillers would result in even less electricity needed to provide the cooling, meaning that an optimized system has the potential to increase the network SEER even more compared to the measured case.

5.5 Economic Assessment

This section presents the economic assessment of LTES from the customer perspective, the producer perspective, and a shared economic perspective. It is worth noting that these evaluations are based on configuration 2 and continue answering research question 2 and 3.

5.5.1 Customer Perspective

The implementation of LTES in the DC network results in both peak load and peak flow reduction, leading to reduced capacity costs for the customers. The total yearly savings, the investment cost based on the chosen number of LTES for each customer and the corresponding PBP are presented in Table 5.5. Positive values indicate a reduction in cost compared to the case without storage, while negative values indicate an increase in cost. The NPV is calculated assuming the customer pays the full cost of the investment. For the total savings based on the number of implemented LTES for each customer, see Appendix C.

Table 5.5: Yearly savings, investment cost and PBP, configuration 2.

Customer no.	**Energy savings** [SEK]	**Peak savings** [SEK]	**Flow savings** [SEK]	**Total savings** [SEK]	c^{inv} [SEK]	PBP [years]
1	0	54 022	-8 523	45 499	189 112	4.16
2	0	37 649	-2 646	35 002	189 112	5.40
3	0	25 335	-3 342	21 993	94 556	4.30
4	0	47 765	-5 303	42 462	378 223	8.91
5	0	52 010	-10 295	41 716	283 668	6.80
6	0	52 698	-6 754	45 945	378 223	8.23
7	0	28 266	-2 150	26 116	283 668	10.86
8	0	0	0	0	-	-
9	0	49 262	-4 492	44 769	283 668	6.34
10	0	60 024	-9 601	50 423	378 223	7.50
11	0	4 270	-1 935	2 335	94 556	40.50

As observed, peak cost savings are the main contributor to the total cost reductions of implementing LTES. In contrast, flow costs increase, as charging requires a higher mass flow than what is reduced during discharging. This effect is strongly influenced by storage utilization and supply temperature. For example, customers 5 and 9 have the same number of storage units, yet their flow costs differ significantly while their peak cost savings are similar. This is because customer 5 has higher supply water temperatures during charging, increasing the required flow. In addition, customer 5 charges more in total due to several smaller peaks outside high-demand hours, further increasing total charging over the period. A similar pattern is observed for customers 1 and 10, explaining their comparatively higher flow costs. As for the PBP, only two customers show values above 10 years, and customer 11 exhibits savings that are too small to justify LTES as a viable option.

The NPV of each customer, based on investment costs and yearly savings, is shown in Figure 5.16 for a 10-year project period with different discount rates. Customers 8 and 11 are excluded from the analysis, as either no storage is implemented or the resulting savings are insufficient to justify LTES implementation.

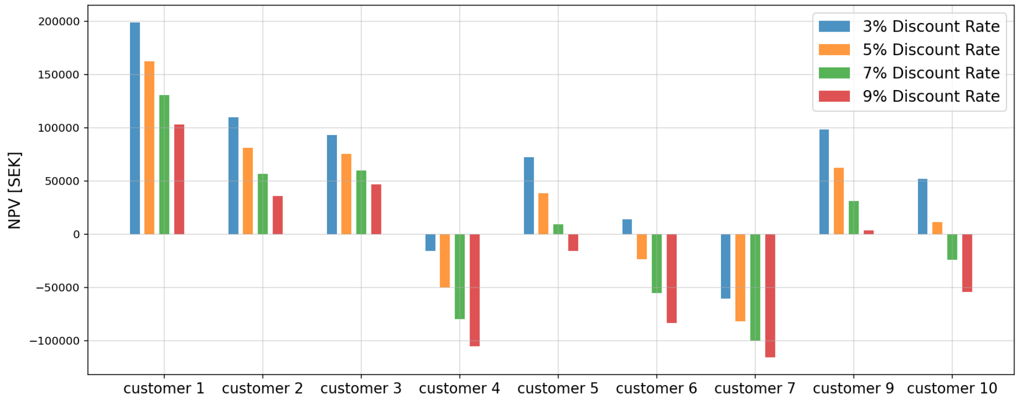

Figure 5.16: NPV of different discount rates with a 10 year project period, configuration 2.

Four of the customers show a profitable project independent of the discount rate, while two never obtain a positive value. These customers, 4 and 7, also exhibit the longest PBP out of the customers in the analysis. Comparing the discount rates, the majority of customers achieve a profitable project both at a discount rate of 3% and 5%, while approximately half of them show profit at 7%. This indicates that LTES is generally profitable for most customers, although the level of profitability depends on the chosen discount rate.

5.5.2 Producer Perspective

As stated in subsection 4.5.2, the economic assessment for the producer is based on an optimized system to represent the theoretical potential for utilizing the LTES. In this following analysis, it is also assumed that the producer pays the full investment cost of the storage units.

In terms of electricity costs, implementing 27 LTES units in an optimized system would result in savings of 6 345 SEK/year. Compared to the other costs associated with implementing the storage system, this saving is relatively insignificant and therefore has little to no impact on the economic assessment. Consequently, it has not been included in the following calculations.

The NPV includes investment and connection costs, revenue generated from new customers and the loss of revenue due to reduced income from capacity charges. The savings in electricity costs are considered too small to have a meaningful impact, and are therefore excluded in the analysis. The results are presented in Figure 5.17, which illustrates the NPV across four different discount rates.

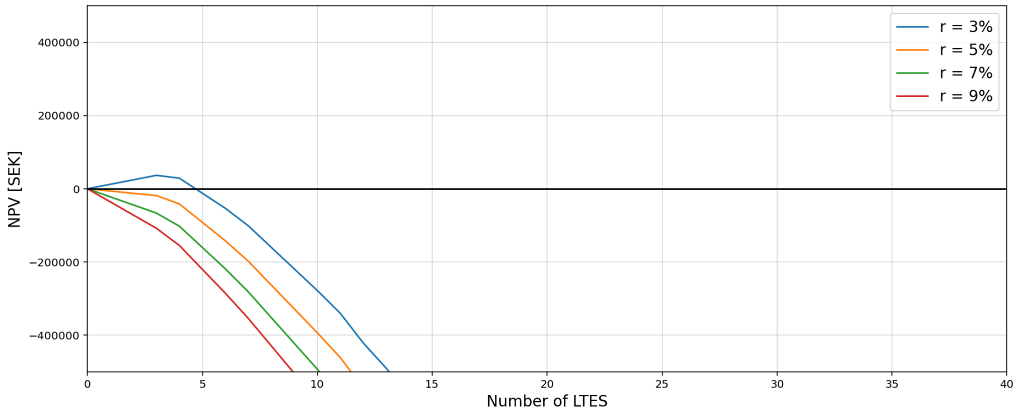

Figure 5.17: NPV of different discount rates with a 10 year project period, optimized Almedal area.

Implementing LTES in the system appears to be almost non-profitable for the producer. A discount rate higher than 3% will result in a non-profitable investment independently of the number of LTES implemented. At a discount rate of 3%, the NPV shows to be profitable for up to 4 storage units, before turning negative for further implementations. This indicates that the loss of revenue combined with the investment and connection costs appears to outweigh the additional income from new customers. Additionally, the assessment assumes an optimized system, i.e. with a ΔT of 10 °C, which differs notably from the actual system today.

Overall, if the producer were to invest in LTES storage, the load and flow in the system, as well as compressor usage, would be reduced. This would, in turn, lead to savings in electricity consumption and a potential increase in the overall network SEER during the period. However, the savings and additional income generated would not be sufficient to cover the investment costs, meaning that, from the perspective of the producer, the investment would not be profitable.

5.5.3 Shared Investment Assessment

The previous results are based on the assumption that either the customer or the producer bears the full investment cost of the storage. From the NPV evaluation for both parties, the incentives for investing in LTES is stronger for customers rather than the producer, therefore customers are more likely to invest in storage. However, LTES still reduce both load and flow in the area, and enabling more customers to connect creates opportunities for network expansion, thereby also providing benefits in favor of the producer. Since both parties benefit from LTES implementation, a cost-sharing approach could be considered to reduce the economic burden for both parties. Note that this analysis is based on the optimized system for an average comfort customer. The full calculations are provided in Appendix C.

The cost that the producer and customer are willing to pay per installed kWh of LTES is presented in Figure 5.18, based on a discount rate of 9% and a project period of 10 years. The lines indicate the producer, customer, and combined investment, while the markers indicate the break-even points, i.e. where the NPV is zero. Furthermore, this is based on the assumption that if implementing a LTES unit, the peak load can be reduced by 0.72 kW per installed kWh of LTES, as shown in Figure 5.11. Furthermore, for additional discount rates, the willingness to pay for both producer, customer and them combined are presented in Table 5.6.

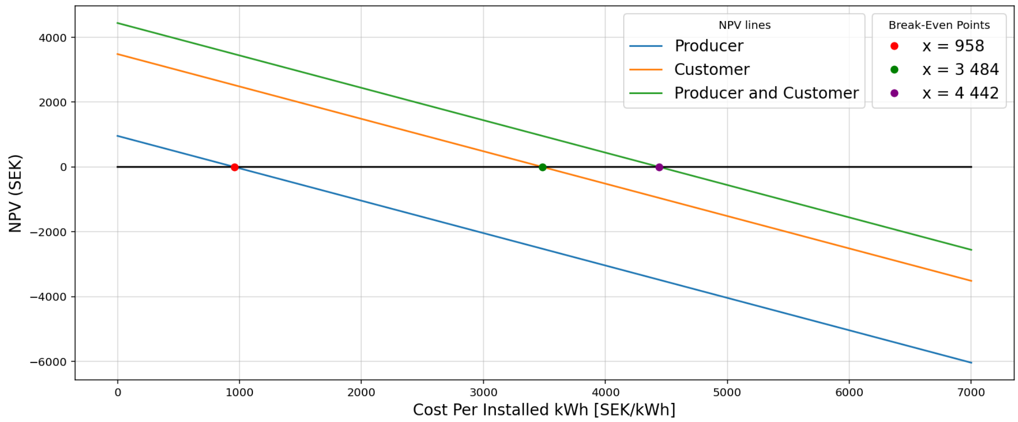

Figure 5.18: Break-even willingness to pay (r = 9%) per installed kWh of LTES for the producer, customer, and combined case.

Table 5.6: Willingness to pay for producer, customer and combined for different discount rates and a load reduction of 0.72 kW/kWh.

Discount rate [%]	**Producer** [SEK/kWh]	**Customer** [SEK/kWh]	**Producer & Customer** [SEK/kWh]
3	1 748	4 631	6 378
5	1 445	4 192	5 637
7	1 185	3 813	4 998
9	958	3 484	4 442

From the perspective of the producer, the cost includes the connection cost, loss of revenue and additional income from new customers. From the perspective of the customer, there is no additional costs other than the investment of the LTES. The results show that depending on the discount rate, the producer is willing to pay between 958 - 1 748 SEK/kWh of installed LTES. Comparing with the customer, the willingness to pay range between 3 484 - 4 631 SEK/kWh. This aligns with previous findings, indicating that customers benefit more from storage and are therefore willing to pay more. For the combined case, the break-even investment cost is between 4 442 - 6 378 SEK/kWh, at which NPV equals zero. This represents the maximum cost at which the investment remains economically viable for both parties, if they both are willing to pay their maximum amount.

If both parties share the investment, the producer can pay between 21–27% of the total investment while still remaining profitable. However, this represents the theoretical maximum at which both parties remain profitable, and the cost-sharing distribution may vary depending on the investment cost of the storage system. When compared with the calculated investment cost of the LTES (2 149 SEK/kWh), the customer would be able to cover the full cost independently of the discount rate and still obtain a profit. In contrast, the producer would not be able to independently cover the full investment cost while maintaining profitability regardless of the discount rate, but could contribute between 45–81% of the investment while still maintaining an NPV above zero.

Looking at Figure 5.11, after approximately seven installed storage units, the peak load reduction achieved by additional units decreases significantly. Between 8–60 LTES units, the average reduction is 0.17 kW/kWh, which corresponds to approximately a 76% lower reduction compared to the first seven units. As a result, if further investments in storage were to be made, the willingness to pay would decrease to between 226–413 SEK/kWh for the producer and between 822–1,093 SEK/kWh for the customer. Consequently, at the calculated investment cost and independently of discount rate, such a small reduction would mean that no party, whether investing individually or together, would obtain a profit from installing additional storage units.

The results obtained above indicate that both the willingness to pay and the profitability of the parties depend strongly on the reduction achieved by the storage units. Therefore, it is of interest to investigate which reduction rates are required for the parties to obtain a profit. The required reduction rates, for each discount rate and based on the calculated investment cost (2 149 SEK/kWh), are presented in Table 5.7. The reduction rate is based on the combined case.

Table 5.7: Required reduction rates for both parties to remain profitable, combined case.

Discount rate [%]	**Required reduction** [kW/kWh]
3	0.24
5	0.27
7	0.31
9	0.35

Looking at the table, a reduction of 0.35 kW/kWh is required for the LTES to be profitable for both parties, independently of the discount rate. Given the higher average reduction of 0.72 kW/kWh for the first 7 units and 0.17 kW/kWh for units 8–60, approximately 21 LTES units are required for the overall average reduction to reach 0.35 kW/kWh. If taking a value of 0.24 kW/kWh, the system could have approximately 55 LTES units in total to reach this average reduction. Therefore, the maximum number of LTES that can be implemented to still result in profit for the parties depends on what discount rate is applied.

Worth noting is that these results are based on the Almedal area being represented as one aggregated customer, meaning that the actual peak load reduction may vary in a real implementation where LTES are installed at individual customer sites. As shown in previous results, different customers experience different levels of peak reduction, which further increases the uncertainty in system-level performance and profitability.

Overall, the results imply that customers gain greater economic benefits from LTES compared to the producer. However, the feasibility of a cost-sharing approach depends strongly on the achieved marginal reduction of additional storage units. While early installations provide high reductions, the performance decreases significantly as more units are added to the system. This implies that profitability is not only dependent on the investment cost and discount rate, but also on how effectively additional LTES units contribute to peak reduction. In the studied case, the number of units that can be justified before the average performance drops below the profitability threshold is limited, and depends greatly on the discount rate used in the calculations. Finally, these results highlight that the cost-sharing and investment incentives are highly sensitive to system performance assumptions. Changes in reduction efficiency or economic parameters may therefore change both the optimal number of LTES units and the resulting economic distribution between producer and customer.

5.5.4 Arena Area

The implementation of LTES in the DC system could potentially reduce the flow to an extent that the pipelines for the proposed Arena area could be reduced. If a reduction in pipe dimension would be possible, the total savings would be:

$$\Delta c^{pipe} = (21\ 735 - 20\ 261)\ \cdot 250\ +\ (82\ 426 - 74\ 793) = 376\ 133\ SEK \qquad (5.1)$$

The Almedal area experienced a similar peak load during 2025 as what is expected for the new Arena area, and can therefore be used to evaluate whether LTES could help sizing down in pipe dimension. In the optimal system configuration, the peak flow rate for a load of 4.2 MW would be 362 m^3/h. In that case, the LTES would therefore have to decrease the flow by 62 m^3/h to meet the requirement for smaller pipes.

However, as shown in Figure 5.12, approximately 100 LTES units would be required to reduce the peak flow to around 300 m^3/h. This corresponds to approximately 100 m^3 of PCM material, and the associated investment cost would exceed 9 MSEK. Comparing this with the saved cost from sizing down one pipe dimension, the investment cost is approximately 24 times higher. From this perspective, it can be concluded that implementing LTES is not economically viable if the producer were to invest in the storage. If, instead, the customers were to invest in the storage, the total savings, based on a break-even approach, a project period of 10 years, and independent of discount rate, would need to exceed 1.1 MSEK yearly for the investment to be profitable. This level of savings would not be achieved through peak reduction, and it can therefore also be concluded that having customers bear the investment is economically unfeasible.

Furthermore, these results are based on an optimal system perspective and do not account for fluctuations or deviations in temperatures or flow rates. If LTES were to be implemented for this purpose, it would require idealized operation during high-load hours, since any deviations could result in the maximum pipe flow rate being exceeded. In addition, reducing the pipe dimension would constrain the system's ability to connect new customers, as the LTES in this configuration would already fully utilize the available pipe capacity for the included customers. Consequently, if LTES were implemented, the producer would not gain additional benefits beyond the savings from downsizing the pipe dimension, while also potentially losing revenue from customers due to the peak cost savings enabled by LTES. Therefore, it can be concluded that implementing LTES in this configuration is not economically viable for either party within the studied context.

6

Further Analysis and Discussion

In this chapter, further analyses of the results are presented alongside a discussion of the findings. First, the sensitivity analyses performed are covered.

6.1 Sensitivity Analysis

This section covers the sensitivity analyses preformed. These are all evaluated using configuration 2.

6.1.1 Loss Factor

An analysis of customer peak reductions with a loss factor of 10%, 20% and 30% was performed. The results can be found in Appendix C. Worth noting is that customer 8 is not included in the graphs since no storage unit is installed. The percentage of peak reduction for different loss factors with 27 LTES implemented for the actual Almedal area are presented in Table 6.1. The results indicate that a low loss factor consistently leads to greater peak shaving, while higher ones reduces the amount of peak reduction.

Table 6.1: Peak shaving at different efficiency levels for the total Almedal area.

Loss Factor	**0%**	**10%**	**20%**	**30%**
Peak Reduction	6.12%	5.89%	5.61%	5.27%

If accounting for a loss factor, the amount of energy that can be used for each implemented LTES reduces, resulting in a lower reduction per installed kWh of storage. This leads to a higher cost per reduced kW in the system. If implementing the different loss factors to the optimized system, the reduction for implementing between 0-7 LTES units is 0.72, 0.68 and 0.63 kW/kWh respectively. For further implementation, the reduction is 0.17, 0.15 and 0.14 kW/kWh. This indicates that as the loss factor increases, the reduction decreases and consequently the willingness to pay. If taking the largest loss factor analyzed, i.e. 30%, the willingness to pay for both parties is combined 3 887 SEK/kWh of installed LTES, which still is significantly higher compared to the estimated investment cost of the storage. However, if aiming for the same reduction in the system, a larger amount of LTES would be required in order to achieve the same reduction.

6.1.2 Flow Fraction When Discharging

The amount of flow that can be redirected into the LTES determines how much discharging can occur each hour. However, it also influences the increase in supply water temperature on the secondary side. The average temperature increase during discharging, for different maximum flow fractions, is presented in Figure 6.1. The average is calculated only for hours during which discharging occurs, in order to provide a representative measure of the temperature increase caused by the LTES. The results show that, regardless of the maximum flow fraction, the temperature increase never exceeds 1 °C. This indicates that if the LTES can maintain an outlet temperature of 12 °C, customers will not experience any significant increase in temperature.

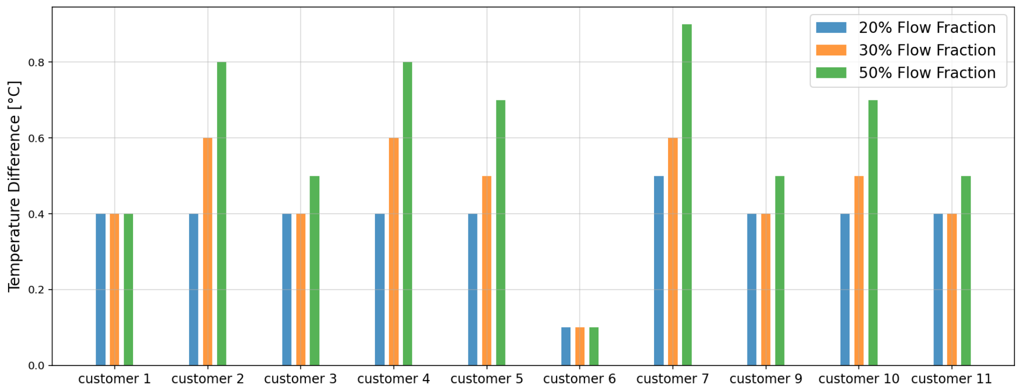

Figure 6.1: Average increase of supply water temperature on secondary side during discharging for different maximum flow fractions.

A visualization of the peak load and peak flow reductions for the different examined flow fractions can be found in Appendix C. When reducing the flow fraction to 0.2, seven out of eleven customers experience a decrease in peak load reduction. This indicates that a lower flow fraction imposes stronger operational constraints, limiting the available discharge capacity for more customers. For flow, the change is minor, with only two customers showing a slight decrease in peak flow reduction due to limited discharge availability. When increasing the flow fraction to 0.5, only three customers achieve further noticeable reductions in peak load. This is because other constraints, such as peaks occurring outside the discharging window, become the governing limitation. Regarding flow, three customers achieve increased reductions. However, at higher numbers of implemented LTES, the increased discharge capacity leads to more charging, and thus a higher increase in peak flows.

For an optimized system, when reducing the flow fraction to 0.2, the decrease in peak load between 0-7 installed LTES remains the same with a value of 0.72 kW/kWh. Further reductions occur up to 40 units at a rate of 0.18 kW/kWh. After 40 units, no further reduction is seen in the system. If instead increasing the flow fraction to 0.5, the reductions are the same as for the original case, but continues up to around 65 units. The flow fraction therefore has no significant effect on the amount of load that is reduced, but rather on when peak reduction stagnates. This indicates that the peaks are not governed by the flow fraction constraint, which is due to the same reasoning as for the larger customers. That is, the flow provided to the system each hour is sufficiently large that the system does not reach its maximum possible discharge flow. Furthermore, this also indicates that the flow fraction does not have a significant impact on the cost per reduced kW of peak, and that the willingness to pay for LTES remains unchanged.

Overall, the results show that the system is more sensitive to decreases in flow fraction than to increases. Lower values significantly restrict discharging capabilities, while higher values provide small returns due to other operational constraints becoming dominant. Variations in flow fraction do not significantly affect the resulting temperature increase on the supply side if assuming a constant LTES outlet temperature of 12 °C. For an optimized system, the flow fraction have no large impact on the willingness to pay, but rather affect after how many LTES units the peak reduction stagnates.

6.1.3 Investment Cost

The investment cost, as mentioned in section 4.7, is estimated with few sources and is therefore an uncertain parameter. Since it highly affected the profitability of implementation, alongside with the incentive to invest in LTES, its impact on these factors are investigated.

The different investment costs investigated with each discount rate are visualized in Figure 6.2. Looking at the graphs, the expected outcome of decreasing profitability with decreasing discount rates is evident and similar to the model results. What is also apparent is that even fewer customers reaches a profitable investment with the increased investment cost.

(a) Discount rate = 3%.

(b) Discount rate = 5%.

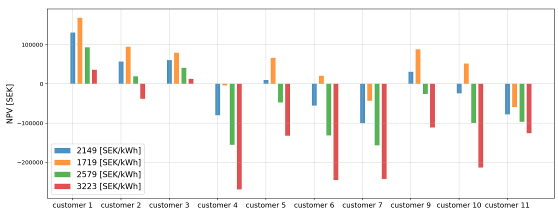

(c) Discount rate = 7%.

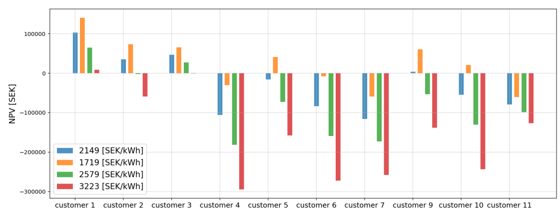

(d) Discount rate = 9%.

Figure 6.2: NPV of different investment costs for customers.

At a 3% discount rate, the majority of customers achieve a positive NPV at the lowest investment cost (1 719 SEK/kWh), with six customers remaining profitable. However, as the investment cost increases, profitability declines. At the highest cost level (3 223 SEK/kWh), only customer 1 and customer 3 remain profitable. Customer 2 is only profitable at low discount rates or investment costs, and become unprofitable as they increases. Customers 7 and 11 exhibit negative NPVs across all scenarios, indicating that LTES is not economically viable for these cases.

Furthermore, at an investment cost of 2 579 SEK/kWh, five of the customers are profitable at a discount rate of 3%, indicating that an investment cost of this value still show incentive to invest in LTES. At a 5% discount rate, only four customers show positive values, comparing to six being profitable for the base case. Similarly, at a 7% discount rate, only three compared to five show positive NPVs. This suggests that a 20% increase in investment cost affects more customers as the discount rate increases.

The analysis also highlights the sensitivity of different customers to cost assumptions. For example, as stated above, customer 1 remains profitable independently of investment cost and discount rate, indicating a strong incentive to invest in LTES. In contrast, customer 5 shows large variations in NPV depending on both discount rate and investment cost, suggesting a high sensitivity and uncertainty regarding the incentive. The profitability changes significantly both in terms of investment cost and discount rate, and each customer is affected differently. This concludes that some customers are more sensitive than others, and that the investment cost and discount rate being two almost equally important factors in terms of how it affects the customers incentive to implement LTES.

These results also show how the customers deviate from the optimized system analysis. From subsection 5.5.3, it was found that, for implementing up to seven LTES units, the reduction has an average value of 0.72 kW/kWh. For that case, customers could, independently of the discount rate, bear an investment cost between 3 484–4 631 SEK/kWh and still remain profitable. The costs investigated in this analysis all lie below this range, and each customer have less than seven LTES implemented, but still the majority of customers show negative NPVs. This indicates that the customers have a reduction per installed kWh of LTES way below what the optimized system achieved. From the perspective of the producer, if they were to invest in the entire storage system, the only scenario in which the NPV is non-negative is with a discount rate of 3% and an investment cost at 80% of the calculated value. Otherwise, the producer obtains negative returns.

For the investment to be profitable, customers must contribute to the upfront cost. At an investment cost of 1 719 SEK/kWh, a high peak reduction increases the overall incentive, allowing the producer to cover a larger share of the investment. However, if the peak reduction per installed kWh of LTES decreases significantly, even the combined investment case is insufficient to achieve profitability, including at the lowest investment cost. This highlights the importance of carefully evaluating the reduction potential for each individual customer before drawing conclusions regarding investment costs and economic incentives.

6.2 Further Analysis

From the results, it is found that there are several factors affecting the utilization of the LTES. This section evaluates some of the key factors.

6.2.1 Low Delta-T

In Figure 6.3, a correlation between profitability and the average temperature difference of each customer is presented. The NPV is calculated using a discount rate of 3% and the analysis is based on configuration 2. The results indicate that improving the temperature differences is not only beneficial for the initial reduction of load and flow, but also enhances the effectiveness of peak reduction when storage is implemented. This is further supported by comparing the total reduction of the Almedal area under realistic temperature differences and the theoretically ideal case.

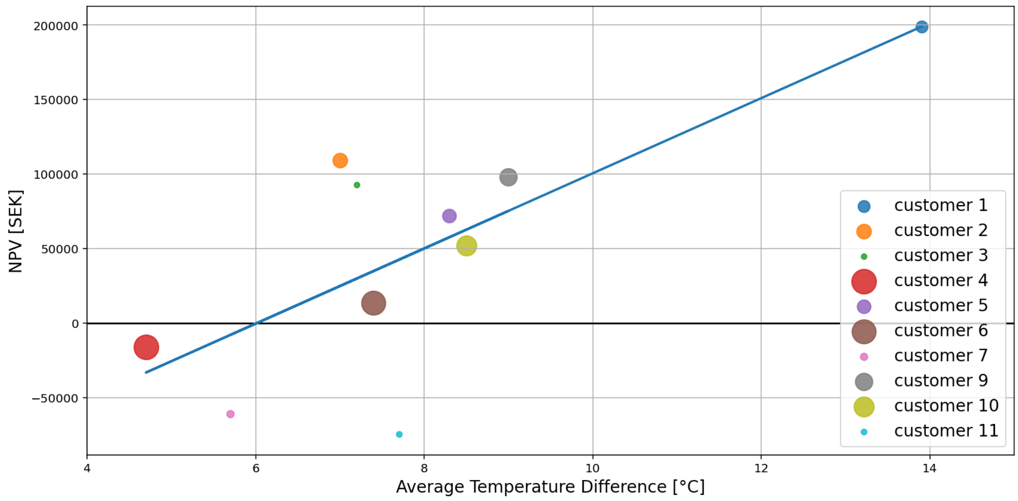

Figure 6.3: NPV (r = 3%) of each customer and average temperature difference of the supply temperature on the primary side. Size of circles indicates size of maximal peak of the customer [kWh/year]. Notation: The x-axis starts at 4 °C.

It is of importance to consider that if LTES were to be implemented, the customers have to maintain a good regulation of their temperatures to effectively be able to use the storage units. There are two main ways of achieving this. Either Göteborg Energi could decrease its cooling supply temperature, thereby increasing the temperature range on the charging side, which would ensure improved operation of the storage. This could also enhance efficiency of the storage units, as performance may improve with respect to supercooling. The other alternative is that customers ensure high return temperatures to the HX and to the LTES, which would both decrease excessive flow rates and ensure that discharging of the storage can occur properly. This means that an improved substation, preferably together with demand-side management, would increase the value of the LTES significantly, and should be considered.

6.2.2 Lowered Primary Side Return Temperature

During charging of the storage units, the return temperature on the primary side will be lower. This is due to the charging outlet temperature being set to 8 °C, resulting in a decreased return temperature. The model charges with additional flow and can result in a significant flow increase since many of the customers experience low flow rates during nighttime. To evaluate the impact, a mixed temperature was calculated the same way as in configuration 2's Equation 4.33. The results are presented in Table 6.2. $T^{ret,old}_{charge}$ and $T^{ret,new}_{charge}$ is the old and new average return temperature during charging hours on the primary side. $T^{ret,old}$ and $T^{ret,new}$ is the old and new average return temperature for all hours on the primary side. Lastly, a new average temperature difference between supply and return is included.

Table 6.2: Comparison of average return temperatures before and after charging, and total charging hours for all customers.

Customer no.	$T^{ret,old}_{charge}$ $[°C]$	$T^{ret,new}_{charge}$ $[°C]$	$T^{ret,old}$ $[°C]$	$T^{ret,new}$ $[°C]$	New ΔT $[°C]$	Charging Hours
1	21.19	11.54	20.97	18.30	11.2	1009
2	12.70	9.21	13.47	13.07	6.6	421
3	14.40	10.17	14.28	13.26	6.2	881
4	10.60	9.68	11.02	10.91	4.6	455
5	15.20	9.16	15.55	14.17	7.0	833
6	15.30	11.73	15.35	14.99	7.0	366
7	12.70	9.21	12.10	11.84	5.4	269
9	15.71	11.63	15.83	15.40	8.1	388
10	14.67	10.68	14.92	14.17	7.8	686
11	12.17	9.04	15.81	15.40	3.5	478

The table shows that the difference in temperature varies between customers. Looking at the average temperatures during charging hours, there is a clear difference between scenarios with no charging and extensive charging. Customer 1 exhibits a lower return temperature during charging because of the flow to the HX being smaller than the flow to the LTES. The other customers show smaller ranges with customer 4 having the smallest difference of less than 1 °C.

Considering the total return temperature difference, the impact is less pronounced where most customers have differences below 2 °C. Customer 1 again exhibits the largest difference, with a new return temperature of 2.7 °C lower than without charging. This is due to the high number of charging hours and the big temperature difference of the charging hours. As shown in Table 6.2, no other customer charges as frequently.

6.2.3 Lower Load Limit for Storage Implementation

From the results, it was found that customer 8 is not suitable for an LTES due to cooling being turned off during nighttime. It is the smallest customer in the area, with a peak load of 25.3 kW, a peak load significantly smaller compared to the rest of the customers and also smaller than the capacity of a storage unit itself. Implementing storage for a customer of this size could therefore potentially increase the cooling requirement to such an extent that the load would increase excessively. Therefore, its peak can be considered to have little to no effect on the overall system, and the customer is deemed too small for the installation of an LTES.

Analyses of the flow profiles shows that, for smaller customers, charging the storage during nighttime can create new peak flows. Since reducing flow peaks is also wanted, this is an undesirable effect of LTES implementation. In the current setup, the maximum charging flow rate was defined to ensure full charging during nighttime assuming a temperature difference of 1 °C. However, if the producer can ensure a supply temperature of 6 °C or lower, the required flow rate could potentially be reduced, thereby mitigating this issue to some extent. Nonetheless, if peak flows were to be increased when implementing LTES, these customers could also be considered having too small flow profiles to benefit from LTES from a system perspective.

It is, however, difficult to define a clear threshold for how small a customer can be for LTES to remain beneficial. This must instead be evaluated from a system perspective, considering how individual customers peaks influence the overall network. Even though a few customers might experience higher peak flows, if these do not coincide, then the system might not see as much of negative effects. Additionally, the customer must experience meaningful benefits. For smaller customers, whose costs are already relatively low, the incentive to invest in LTES may be smaller. Therefore, it is essential to assess each customer individually, taking into account their size, load profile, and flow characteristics. The storage system must be appropriately sized, so that it does not require excessive cooling capacity relative to the customer's demand and does not introduce unfavorable operational effects.

6.3 Discussion

Looking at the results obtained from both model configurations, customers have several variables that can be adjusted to achieve reductions in both flow and load, in addition to the implementation of a storage. In subsection 5.5.4, the results indicate that LTES is not a solution to reducing the network dimensions. Instead, it could be used as a solution for mitigating peak load and flow variations. To reduce the base load of cooling in the Arena area, the storage system would have to be scaled up to 100 LTES, demanding significantly large storage capacity.

Furthermore, customers 8 and 11 were chosen not to be included in the majority of the calculations. This is due to customer 8 generating a negative economic outcome from installing LTES, and customer 11 experiencing an unrealistic payback period.

The two customers are the smallest in the system, with customer 8 having a peak load of 25.3 kW, which is significantly smaller compared to the rest. As stated above, implementing storage for a customer of that size is considered unrealistic, due to the storage requiring more cooling capacity than the customer itself. Customer 11 is second to customer 8 and has a larger peak load of 151 kW. However, while customer 11 is deemed unprofitable, customer 3 is evaluated as suitable for a storage unit, even though both its peak load and ΔT are similar to those of customer 11. This is because customer 11 has peak demand occurring outside of the discharging window, and its cooling is turned off some of the time. Therefore, customer 11 may be suitable for storage if its cooling demand were continuously active and if the charging and discharging windows were adjusted to match its load profile. The charging and discharging windows were initially set to match the majority of customers, however, customer 11 demonstrates that it is important to define these individually with respect to each customer's load pattern.

The return temperatures of LTES charging indicated that charging leads to lower primary side return temperatures. After charging, the flow is assumed to return to the producer, and the lowered ΔT caused by the charging becomes an undesirable consequence. One approach to mitigate this and achieve higher return temperatures during charging, the supply water to the LTES during charging could potentially be utilized twice. The water would first be used to charge the LTES, then pass through the HX to cool the secondary side return water. This could further reduce cooling production, help mitigate excessive flow rates during nighttime and as a result lower increased flow costs for customers. However, this approach would require greater flexibility at customer sites, as slightly higher nighttime supply temperatures would need to be acceptable. The producers would also lose revenue of increased flow costs from customers.

Even though the implementation of LTES has been shown to reduce both peak load and peak flow, it is important to highlight the assumptions made in this analysis. The model assumes that the PCM can sufficiently solidify and melt using the supply water on the primary side and the return water on the secondary side. In reality, achieving a complete phase change when the heat-transfer medium is close to the melting temperature is often difficult, due to gliding temperatures and supercooling. These constraints are not included in the model and may affect the performance of the LTES. Furthermore, the model assumes that the storage system has the same charging and discharging capacity regardless of flow rates and temperatures, which may also influence actual performance. In addition, cycling performance is neglected. Because there are few existing installations using PCM for cooling storage, especially in DC systems, it is difficult to define accurate constraints. Further simulations and experimental testing of the material are therefore needed to properly evaluate performance and feasibility of LTES in these systems.

7
Conclusions

This thesis has investigated the suitability of LTES as an energy storage solution in DC networks.

The use of LTES in the DC network is considered feasible. Several important and complex design aspects have been identified, including gliding temperatures, low thermal conductivity and phase separation. A PCM with melting temperature of around 10 °C is available and suited for the Gothenburg DC network. Furthermore, storage capacities of 44, 88, 132 or 176 kWh are deemed reasonable for typical substations depending on customer size, behavior and space availability.

It was found that an LTES configured to pre-cool the flow before the HX (configuration 1) reduces customer costs by lowering the required cooling load. However, the volumetric flow rate on the primary side is not reduced with this configuration. The decrease in cooling load is a consequence of a smaller temperature difference over the HX, leading to a lower return temperature to the producer. Therefore, this configuration is not desirable from a system perspective. By instead allowing the LTES to cool a fraction of the flow and subsequently mix it with the HX outlet (configuration 2), both peak load and peak flow can be reduced. This is with the assumption that customers can receive a more flexible supply temperature. Although, it is shown that if the storage units are able to deliver a return temperature of 12 °C, the resulting increase in supply temperature on the secondary side remains below 1 °C. Nevertheless, the effectiveness of the storage is strongly influenced by parameters such as the flow fraction, temperature levels, and the timing of peak load occurrence. The charging and discharging windows also affect the peak load reduction, and needs to be set individually for optimal performance.

Modeling the integration of LTES in the Almedal area demonstrated potential peak load and peak flow reductions. In 2025, the area reached a peak load of 4.2 MW, which could have been reduced by approximately 257 kW (6.1%) with 27 LTES units. Similarly, the peak flow of 556 m^3/h could have been reduced by 18 m^3/h (3.2%). Further, the compression usage could decrease by 46 MWh, potentially improving the network SEER.

In the optimized scenario without storage implementation, improved substation performance ($\Delta T = 10$) reduced the peak flow to 362 m^3/h, corresponding to a reduction of 34.9%. This indicates that substation performance optimization has a greater impact on flow reduction than storage implementation alone. If storage is combined with optimized operating conditions and the same number of LTES units is implemented, the peak flow could further be reduced to 326 m^3/h (10.0%), and the peak load reduced by 421 kW (10.0%). This indicates that an optimized system scenario enhances the effectiveness of the LTES units. In addition, it was shown that the compression usage could be further decreased with 13 MWh in the optimized system.

From an economic perspective, the results and sensitivity analysis of investment cost showed that profitability is highly case-dependent. While some customers achieve a stable positive NPV across several discount rates, others are highly sensitive to small changes in operating conditions and storage size. Overall, LTES provides greater economic benefits for customers than the producer. In the optimized system, with a reduction of 0.72 kW/kWh of installed LTES, a cost-sharing scenario would allow the producer to bear approximately 45-81% of the calculated investment cost depending on the discount rate, while the customer could cover the full investment cost in all cases and still remain profitable. However, profitability is strongly driven by the achieved peak reduction. For a shared investment to remain viable for both parties, the required reduction lies between 0.24–0.35 kW/kWh of installed LTES depending on the discount rate.

The sensitivity analysis showed that when accounting for a higher loss factor, some customers may require a larger storage capacity to achieve the desired reduction. Therefore, testing should be conducted prior to implementation. The flow fraction used for discharging indicates that the system is more sensitive to reductions in this parameter than to increases. This is due to other factors, such as the available charging and discharging windows becoming the new governing constraints. This parameter also did not show any significant impact on profitability for either the customer or the producer.

Future research is recommended to include pilot testing of an LTES system integrated with a substation operated by Göteborg Energi. Such a pilot would need to evaluate feasible temperature ranges, selection and performance of the PCM, as well as system integration and control strategies, all of which are critical considerations prior to commercial deployment at customer sites. Furthermore, as previously noted, each customer must be individually assessed and paired with appropriate charging and discharging windows, as well as a suitable PCM melting temperature, to ensure optimal system performance. The control strategy for the storage system also requires further investigation, particularly regarding the effectiveness of a daily operating cycle.

Bibliography

[1] Maria Jangsten. *THESIS FOR THE DEGREE OF DOCTOR OF PHILOSOPHY District Cooling-Towards Improved Substation Performance.* Department of Architecture and Civil Engineering, Gothenburg, 2022.

[2] Rikard Edland. Correspondence with Supervisor. *Process Engineer at Göteborg Energi AB*, 2026.

[3] Göteborg Energi AB. Preliminara Miljovarden Fjarrkyla Platsbaserade 2025. 1 2026.

[4] Göteborg Energi AB. Miljovarden fjarrkyla centrala natet 2024 slutliga. 6 2025.

[5] Yihuan Zhou, Haijing Huang, Jinhui Ma, Qiuping Liu, and Yapeng Guo. Complex spatiotemporal thermal effects caused by urban densification: Patterns, characteristics, mechanisms and strategies. *Building and Environment*, 288:114008, 1 2026.

[6] European Environment Agency (EEA). Global and European temperatures, 6 2025.

[7] Poul Alberg Østergaard, Sven Werner, Anders Dyrelund, Henrik Lund, Ahmad Arabkoohsar, Peter Sorknæs, Oddgeir Gudmundsson, Jan Eric Thorsen, and Brian Vad Mathiesen. The four generations of district cooling - A categorization of the development in district cooling from origin to future prospect. *Energy*, 253, 8 2022.

[8] Valerie Eveloy and Dereje S. Ayou. Sustainable district cooling systems: Status, challenges, and future opportunities, with emphasis on cooling-dominated regions. *Energies*, 12(2), 1 2019.

[9] Afshin J Ghajar, Patrick H Oosthuizen, and William E Carscallen. DISTRICT COOLING Theory and Practice HEAT TRANSFER A Series of Reference Books and Textbooks Series editor. Technical report.

[10] Göteborg Energi AB. Miljövärden Återvunnen och fossilfri fjärrkyla.

[11] Göteborg Energi AB. Återvunnen och fossilfri fjärrkyla.

[12] Stephen Bourne and Atila Novoselac. Compact PCM-based thermal stores for shifting peak cooling loads. *Building Simulation*, 8(6):673–688, 12 2015.

[13] Göteborgs Stad. Evenemangsområdet.

[14] Elisa Guelpa and Vittorio Verda. Thermal energy storage in district heating and cooling systems: A review. *Applied Energy*, 252:113474, 10 2019.

[15] Yusra Tahir, Junjie Liu, and Lizhi Jia. State-of-the-art low temperature phase change material (PCM) for air conditioning system. *Energy and Buildings*, 350, 1 2026.

[16] Pepe Tan. *Thesis for the degree of Doctor of Philosophy Design of Thermal Energy Storage with Phase Change Materials Investigations within Material,*

Device and System Scale. Department of Architecture and Civil Engineering, Gothenburg, 2020.

[17] Yilin Fan and Lingai Luo. Energy storage by sensible heat for buildings. *Handbook of Energy Systems in Green Buildings*, pages 953–993, 5 2018.

[18] Aditya Chauhan, V. V. Tyagi, Sanjeev Anand, A. K. Pandey, Ahmet Sari, and F. A. Al-Sulaiman. Energy storage by PCM for building applications. In *Handbook of Energy Systems in Green Buildings*, pages 995–1023. Springer Berlin Heidelberg, 5 2018.

[19] Stefano Mazzoni, Jia Yin Sze, Benedetto Nastasi, Sean Ooi, Umberto Desideri, and Alessandro Romagnoli. A techno-economic assessment on the adoption of latent heat thermal energy storage systems for district cooling optimal dispatch & operations. *Applied Energy*, 289:116646, 5 2021.

[20] Gang Li. Sensible heat thermal storage energy and exergy performance evaluations. *Renewable and Sustainable Energy Reviews*, 53:897–923, 1 2016.

[21] Yuhao Lan, Yingxin Wu, Zhengguo Zhang, Xiaoming Fang, and Ziye Ling. Thermochemical cooling for high-power chip using sodium acetate trihydrate/-expanded graphite: A new strategy and model. *Applied Thermal Engineering*, 253:123750, 9 2024.

[22] Huashan Bao and Zhiwei Ma. Thermochemical energy storage. *Storing Energy: with Special Reference to Renewable Energy Sources*, pages 651–683, 1 2022.

[23] Atul Sharma, V. V. Tyagi, C. R. Chen, and D. Buddhi. Review on thermal energy storage with phase change materials and applications, 2 2009.

[24] Farah Souayfane, Farouk Fardoun, and Pascal Henry Biwole. Phase change materials (PCM) for cooling applications in buildings: A review, 10 2016.

[25] Hyungil Jang, Youngho Han, Junyeong Jeong, Byungwook Youn, and Doojin Lee. Fire-retardant phase-change material composites: A review of organic and inorganic systems for thermal safety. *Composites Part B: Engineering*, 314:113448, 4 2026.

[26] Shamseldin A. Mohamed, Fahad A. Al-Sulaiman, Nasiru I. Ibrahim, Md Hasan Zahir, Amir Al-Ahmed, R. Saidur, B. S. Yılbaş, and A. Z. Sahin. A review on current status and challenges of inorganic phase change materials for thermal energy storage systems, 2017.

[27] Bilal Lamrani, Rubayyi T. Alqahtani, Abdelhamid Ajbar, and Mouhcine Benaicha. Dynamic performance analysis of sensible and latent cold thermal energy storage systems for building cooling networks. *Case Studies in Thermal Engineering*, 71, 7 2025.

[28] Y. L. Shao, K. Y. Soh, M. R. Islam, and K. J. Chua. Thermal, exergy and economic analysis of a cascaded packed-bed tank with multiple phase change materials for district cooling system. *Energy*, 268, 4 2023.

[29] Michael Jokiel. Development and performance analysis of an object-oriented model for phase change material thermal storage. Technical report, 2016.

[30] Xiwen Cheng and Xiaoqiang Zhai. Thermal performance analysis and optimization of a cascaded packed bed cool thermal energy storage unit using multiple phase change materials. *Applied Energy*, 215:566–576, 4 2018.

[31] Morshed Alam, Patrick X.W. Zou, Jay Sanjayan, and Sayanthan Ramakrishnan. Energy saving performance assessment and lessons learned from the op-

eration of an active phase change materials system in a multi-storey building in Melbourne. *Applied Energy*, 238:1582–1595, 3 2019.

[32] Emilia Pisani. Optimizing Homes with Modular TES, 4 2025.

[33] Gustafsson Ola. Correspondence with Professional. *Project Leader at RISE Research Institute of Sweden.*

[34] Morshed Alam, Shyan Devapriya, and Jay Sanjayan. Experimental investigation of the impact of design and control parameters of water-based active phase change materials system on thermal energy storage. *Energy and Buildings*, 268, 8 2022.

[35] Lokesh Kalapala and Jaya Krishna Devanuri. Influence of operational and design parameters on the performance of a PCM based heat exchanger for thermal energy storage – A review. *Journal of Energy Storage*, 20:497–519, 12 2018.

[36] Sandris Ručevskis, Pavel Akishin, and Aleksandrs Korjakins. Parametric analysis and design optimisation of PCM thermal energy storage system for space cooling of buildings. *Energy and Buildings*, 224, 10 2020.

[37] Taha K. Aldoss and Muhammad M. Rahman. Comparison between the single-PCM and multi-PCM thermal energy storage design. *Energy Conversion and Management*, 83:79–87, 2014.

[38] Tianhao Xu. *Integrating Latent Heat Storage into Residential Heating Systems.* PhD thesis, KTH Royal Institute of Technology, Stockholm, 2021.

[39] Changqing Xia, Guancong Chen, Jiaxing Shi, Xiaohua Bao, and Hongzhi Cui. Investigation of heat transfer characteristics in steel fiber-reinforced energy piles utilizing steel tubes for PCM encapsulation. *Energy*, 326:136273, 7 2025.

[40] Phase Change Material Products Limited. Thermal Storage Catalogue.

[41] Phase Change Material Products Limited. THERMAL ENERGY STORAGE (TES) DESIGN GUIDE, 2011.

[42] T. Kousksou, P. Bruel, A. Jamil, T. El Rhafiki, and Y. Zeraouli. Energy storage: Applications and challenges, 2014.

[43] Pluss Advanced Technologies. plussatOM08. Technical report, Haryana, India, 11 2022.

[44] Plussat Advanced Technologies. TECHNICAL DATA SHEET OF savE ® OM 18-P. Technical report, Haryana, India, 11 2021.

[45] I. Shamseddine, F. Pennec, P. Biwole, and F. Fardoun. Supercooling of phase change materials: A review, 4 2022.

[46] Md Hasan Zahir, Shamseldin A. Mohamed, R. Saidur, and Fahad A. Al-Sulaiman. Supercooling of phase-change materials and the techniques used to mitigate the phenomenon, 4 2019.

[47] Bard Skagestad and Peter Mildenstein. INTERNATIONAL ENERGY AGENCY IEA DISTRICT HEATING AND COOLING Programme of Research, Development and Demonstration on District Heating and Cooling District Heating and Cooling Connection Handbook. Technical report.

[48] Svend Frederiksen and Sven Werner. *Fjärrvärme och fjärrkyla.* Studentlitteratur AB, Lund, Sweden, 1 edition, 2014.

[49] Frank P. Incropera, Theodore L. Bergman, Adrienne S. Lavine, and David P. DeWitt. *fundamentals-of-heat-and-mass-transfer-incropera.*

[50] Maria Jangsten, Torbjörn Lindholm, and Jan Olof Dalenbäck. District cooling substation design and control to achieve high return temperatures. *Energy*, 251, 7 2022.

[51] Chengchu Yan, Xiuxiu Yang, and Yizhe Xu. Mathematical explanation and fault diagnosis of low delta-T syndrome in building chilled water systems. *Buildings*, 8(7), 6 2018.

[52] Maria Jangsten, Torbjörn Lindholm, and Jan Olof Dalenbäck. Analysis of operational data from a district cooling system and its connected buildings. *Energy*, 203, 7 2020.

[53] Nicole Burstein. Statistik: Fjärrkylestatistik, 6 2025.

[54] Maja Nyberg. Conversation With Expert. *Göteborg Energi AB*, 3 2026.

[55] ISO 5151:2017(en), Non-ducted air conditioners and heat pumps — Testing and rating for performance.

[56] Ángel Andrade, Álvaro Restrepo, and Juan E. Tibaquirá. EER or Fcsp: A performance analysis of fixed and variable air conditioning at different cooling thermal conditions. *Energy Reports*, 7:537–545, 11 2021.

[57] Understanding SEER and SCOP | Energy efficiency Eurovent Certita Certification.

[58] Göteborg Energi AB. Lokala anvisningar för fjärrkyla. Technical report.

[59] Göteborg Energi AB. Handbok för effektiv fjärrkyla. Technical report, Göteborg, 1 2024.

[60] fjärrkylecentralen utförande och installation. Technical report, 2013.

[61] Göteborg Energi AB. Fjärrkyla för ditt företag? Så mycket kostar det., 2026.

[62] Joseph Maria Jebamalai, Kurt Marlein, and Jelle Laverge. Influence of centralized and distributed thermal energy storage on district heating network design. *Energy*, 202, 7 2020.

[63] Sven Werner. International review of district heating and cooling, 10 2017.

[64] O. Angelidis, A. Ioannou, D. Friedrich, A. Thomson, and G. Falcone. District heating and cooling networks with decentralised energy substations: Opportunities and barriers for holistic energy system decarbonisation, 4 2023.

[65] Shang Mao, Yong Liu, Xuehong Wu, Leigang Zhang, Junjie Chen, and Tao Zhou. Thermal energy storage performance, application and challenge of phase change materials: a review, 9 2025.

[66] Stuart Mitchell. PuLP: A Linear Programming Toolkit for Python. Technical report, 2011.

[67] John Forrest and Robin Lougee-Heimer. CBC.

[68] Yifan Jiang, Shengli Liao, Xi Zhang, Zhou Fang, and Chuntian Cheng. Short-term peak-shaving model for hydro-wind-photovoltaic hybrid system coupled with complex ecological constraints. *Journal of Hydroinformatics*, 27(11):1784–1800, 11 2025.

[69] European Central Bank. Swedish Krona (SEK).

[70] APPLICATIONS OF THERMAL ENERGY STORAGE IN THE ENERGY TRANSITION BENCHMARKS AND DEVELOPMENTS Public Report of IEA ECES Annex 30. Technical report, 2018.

[71] Pepe Tan, Patrik Lindberg, Kaia Eichler, Per Löveryd, Pär Johansson, and Angela Sasic Kalagasidis. Thermal energy storage using phase change materials:

Techno-economic evaluation of a cold storage installation in an office building. *Applied Energy*, 276:115433, 10 2020.

[72] Elizabeth B Stein, Chris Holt, Peter Howard, and Jason A Schwartz. Applying Discount Rates in Energy Utilities' Benefit-Cost Analyses ISSUE BRIEF Present Value of a $1 Million Effect Occurring in the Future, at Different Discount Rates. Technical report, 2025.

[73] Effektiv användning av energi, effekt och resurser För att underlätta elektrifieringen.

[74] Bolåneräntor – jämför boräntor och snitträntor bolån – aktuella räntor bolån | Swedbank.

A

Appendix 1: Individual Customer Results Configuration 1

Customer 1

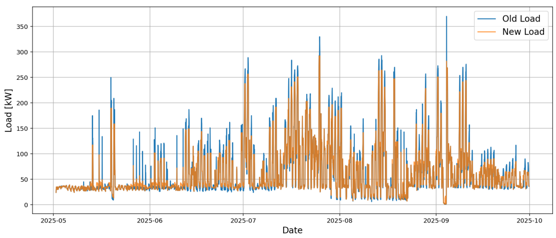

(a) Old vs new load.

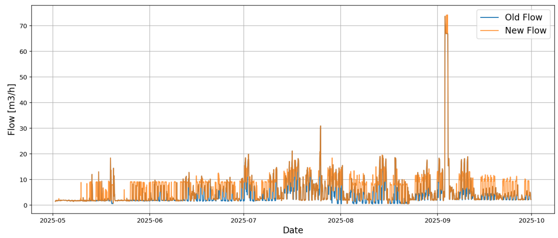

(b) Old vs new flow.

Customer 2

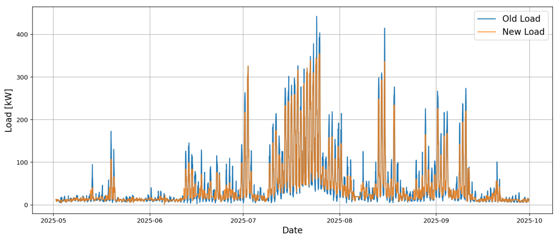

(a) Old vs new load.

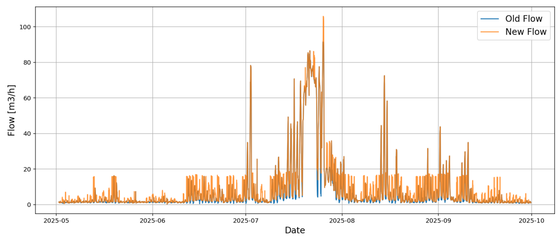

(b) Old vs new flow.

Customer 3

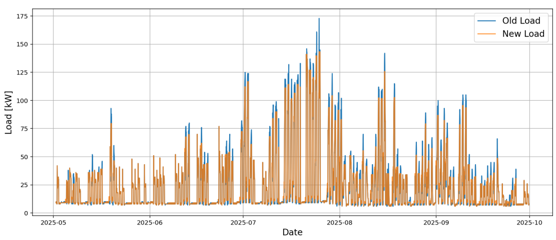

(a) Old vs new load.

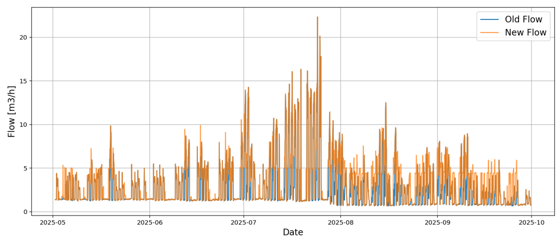

(b) Old vs new flow.

Customer 4

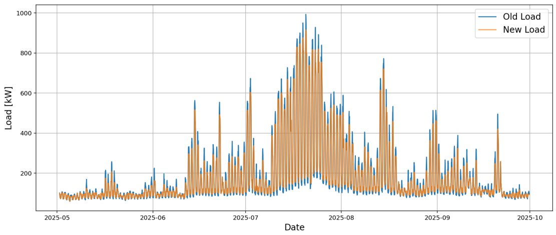

(a) Old vs new load.

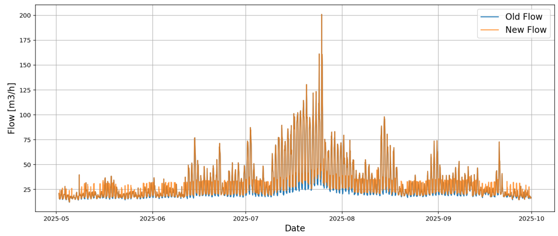

(b) Old vs new flow.

Customer 5

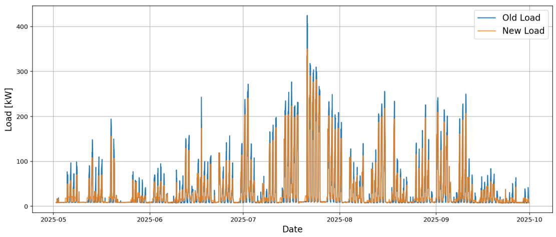

(a) Old vs new load.

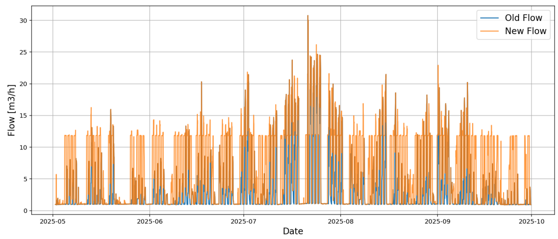

(b) Old vs new flow.

Customer 6

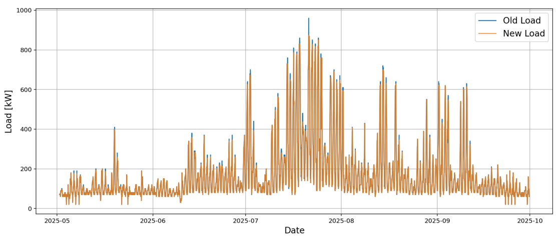

(a) Old vs new load.

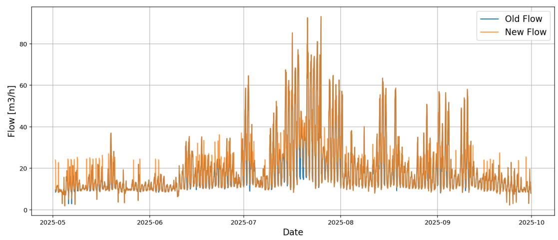

(b) Old vs new flow.

Customer 7

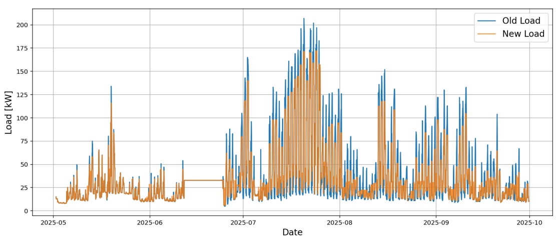

(a) Old vs new load.

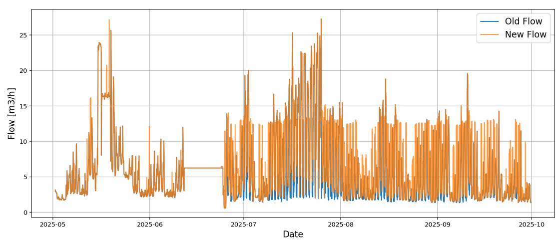

(b) Old vs new flow.

Customer 8

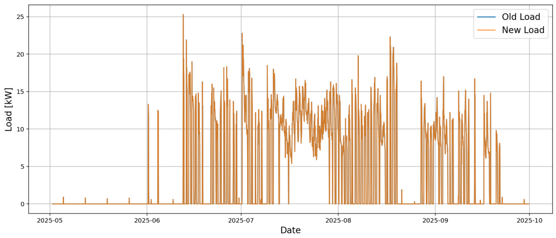

(a) Old vs new load.

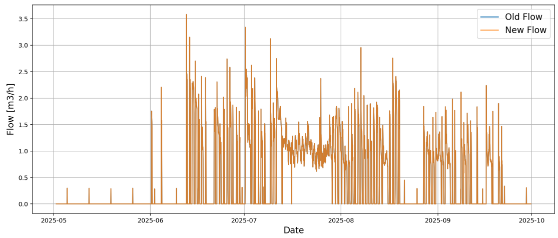

(b) Old vs new flow.

Customer 9

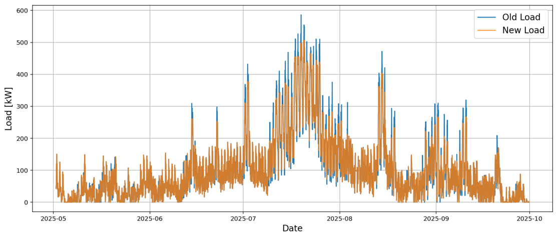

(a) Old vs new load.

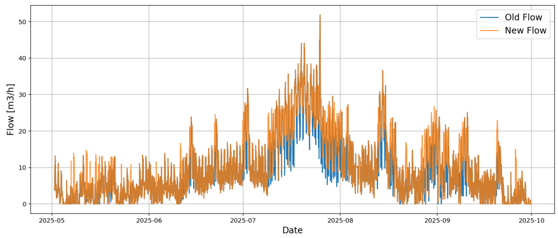

(b) Old vs new flow.

Customer 10

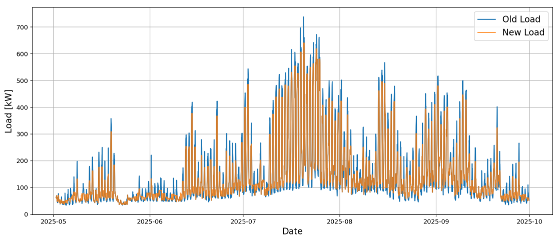

(a) Old vs new load.

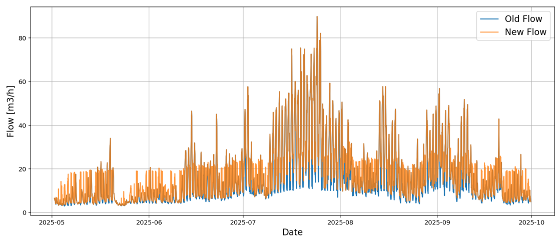

(b) Old vs new flow.

Customer 11

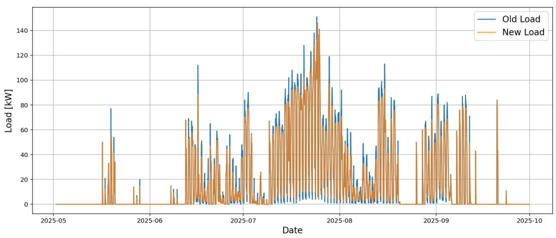

(a) Old vs new load.

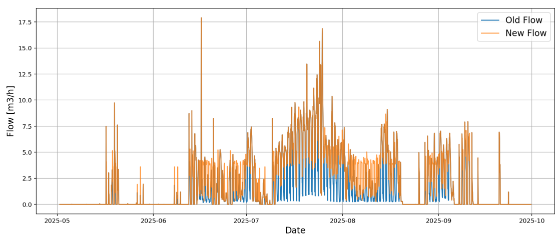

(b) Old vs new flow.

B

Appendix 2: Individual Customer Results Configuration 2

Customer 1

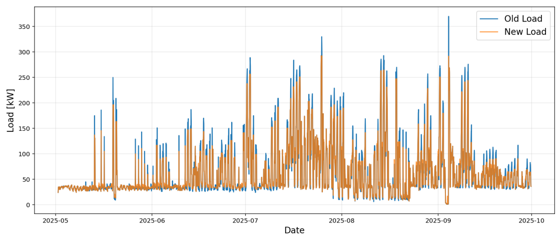

(a) Old vs new load.

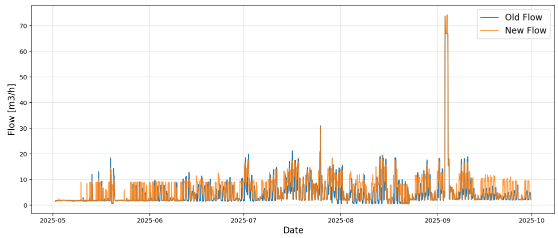

(b) Old vs new flow.

Customer 2

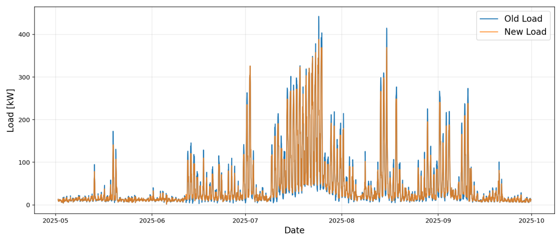

(a) Old vs new load.

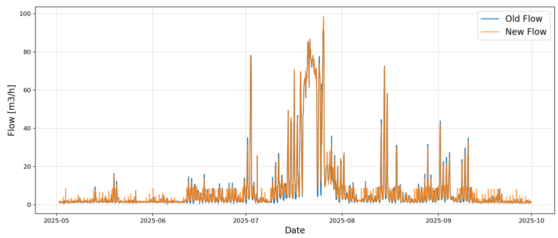

(b) Old vs new flow.

Customer 3

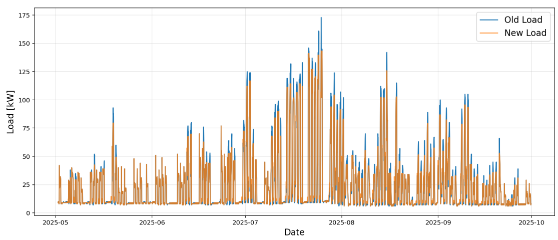

(a) Old vs new load.

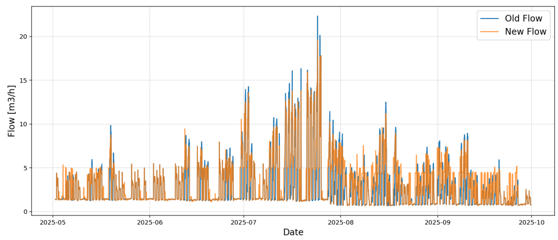

(b) Old vs new flow.

Customer 4

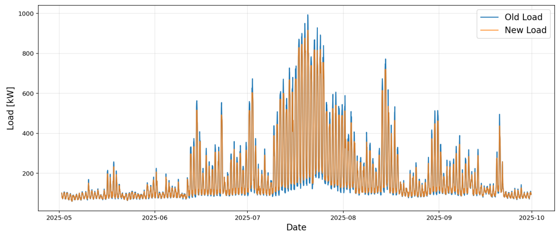

(a) Old vs new load.

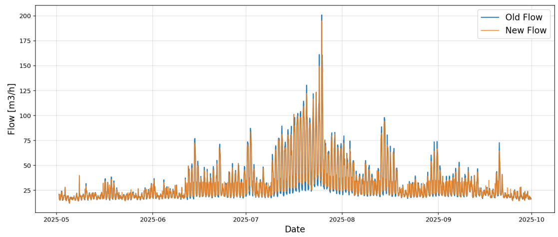

(b) Old vs new flow.

Customer 5

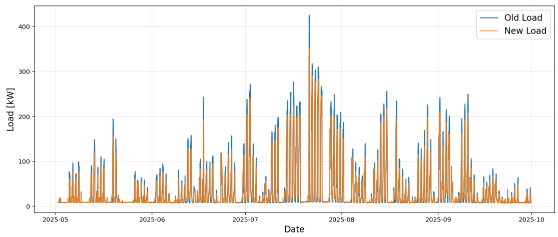

(a) Old vs new load.

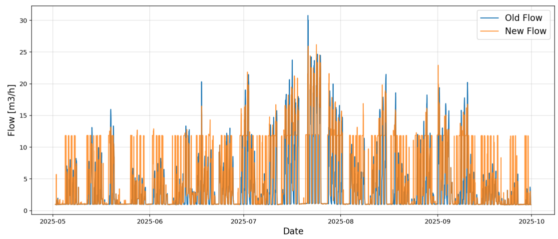

(b) Old vs new flow.

Customer 6

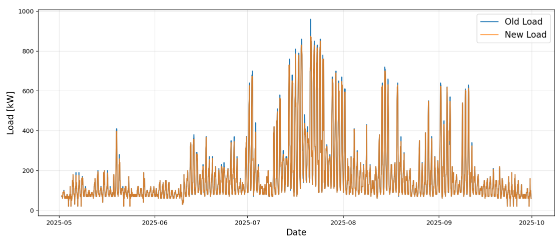

(a) Old vs new load.

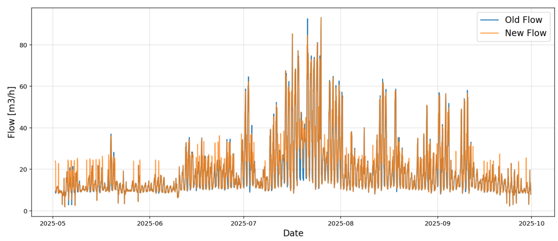

(b) Old vs new flow.

Customer 7

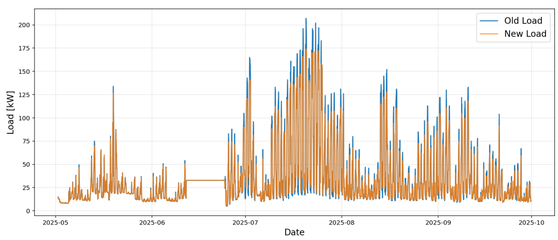

(a) Old vs new load.

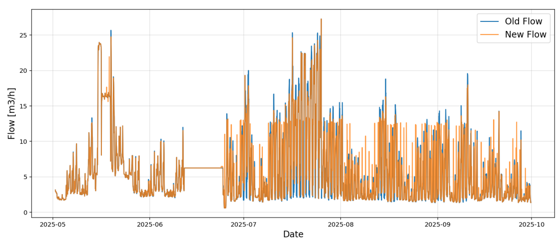

(b) Old vs new flow.

Customer 8

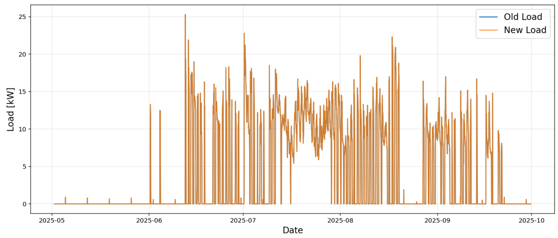

(a) Old vs new load.

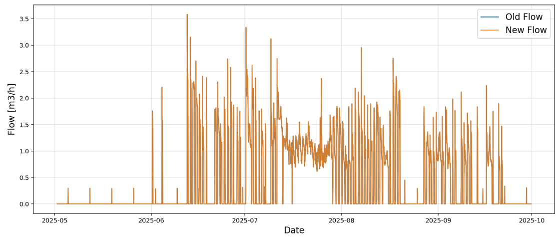

(b) Old vs new flow.

Customer 9

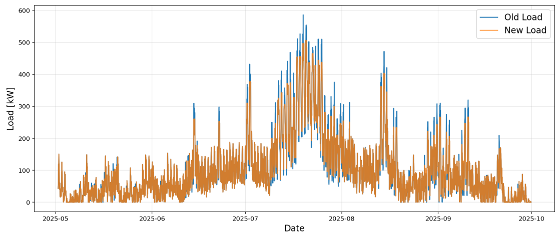

(a) Old vs new load.

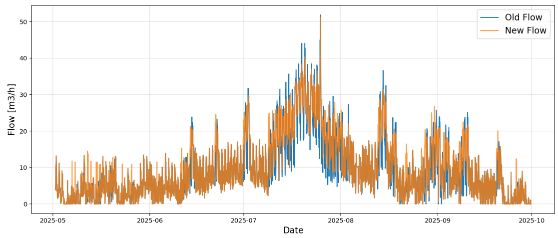

(b) Old vs new flow.

Customer 10

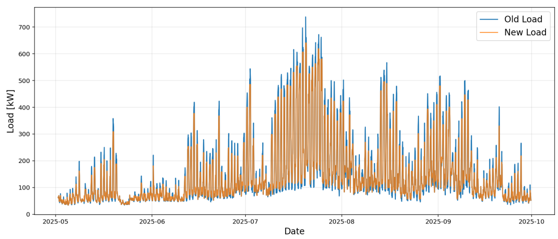

(a) Old vs new load.

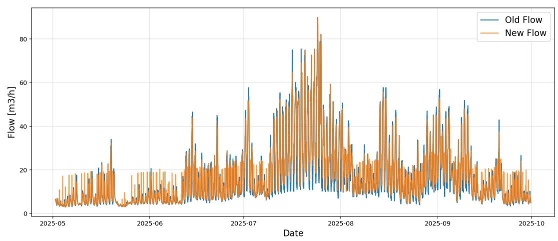

(b) Old vs new flow.

Customer 11

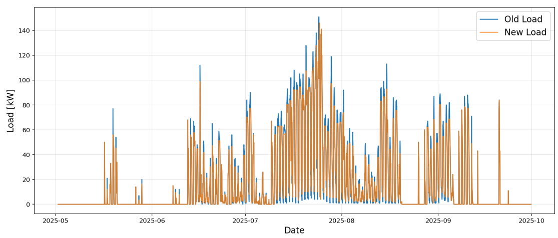

(a) Old vs new load.

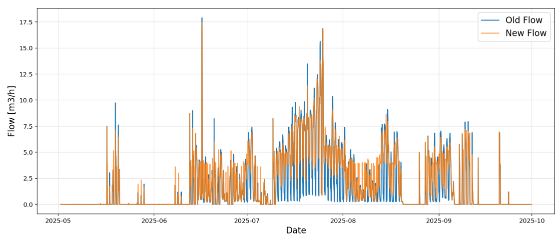

(b) Old vs new flow.

C

Appendix 3: Graphs

Model Validation Results

In the figures, the orange curve represents the new load, and the blue curve represents the original load.

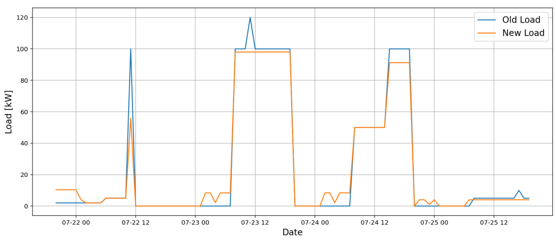

(a) Load profile for configuration 1.

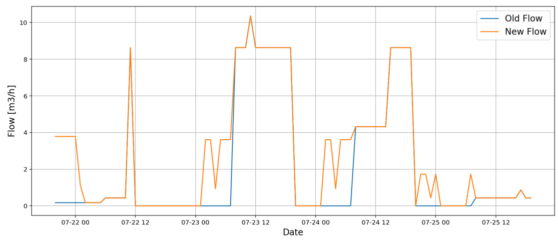

(b) Flow profile for configuration 1.

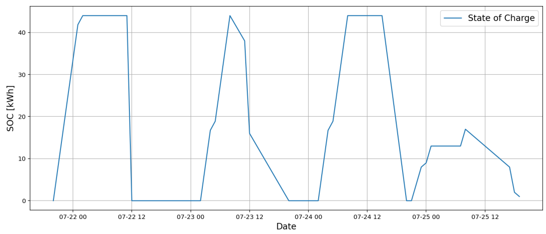

(c) SOC for configuration 1.

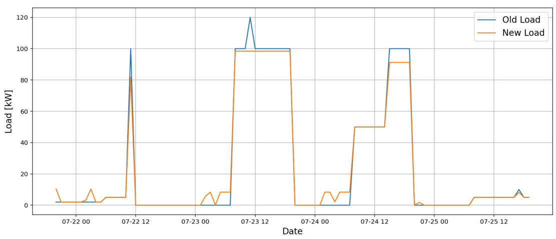

(a) Load profile for configuration 2.

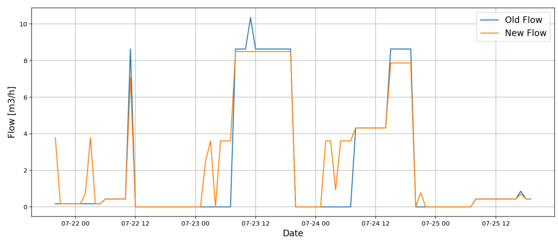

(b) Flow profile for configuration 2.

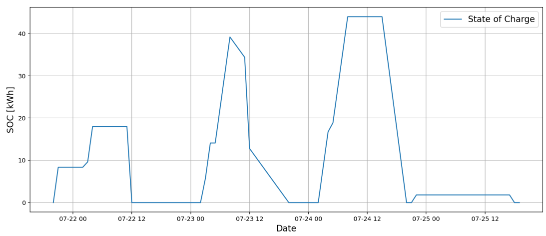

(c) SOC for configuration 2.

Theoretical Findings

The schematics uses the connection of configuration 1, although is still valid when considering configuration 2.

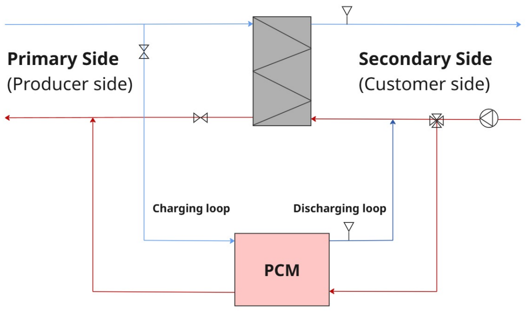

(a) No HX.

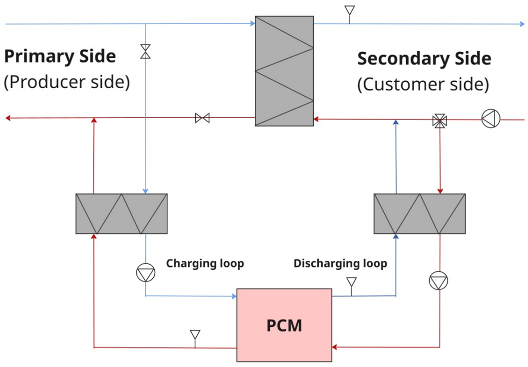

(b) HX on both sides.

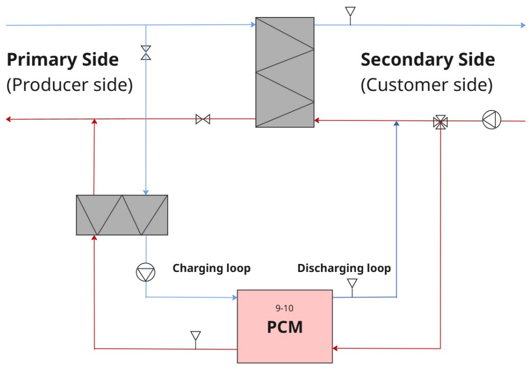

(c) HX on primary side.

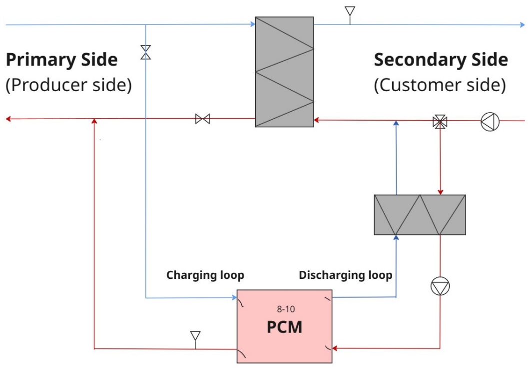

(d) HX on secondary side.

Figure C.3: Different PCM storage configurations.

Economical Evaluation for Customers

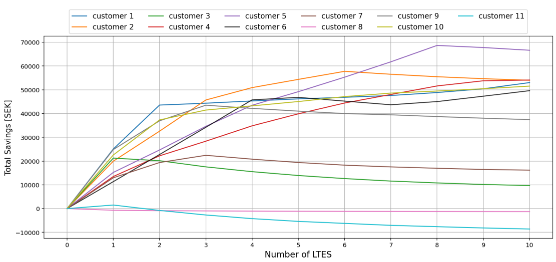

(a) Total savings per year dependent on the number of LTES, configuration 1.

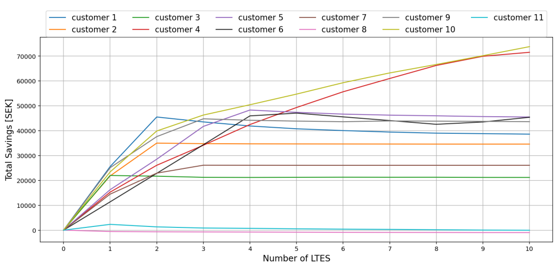

(b) Total savings per year dependent on the number of LTES, configuration 2.

Sensitivity Analysis: Loss Factor

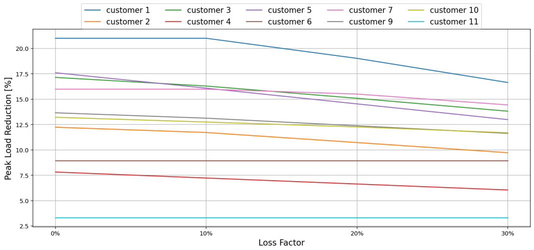

(a) Peak load reduction for selected customers at different loss factors.

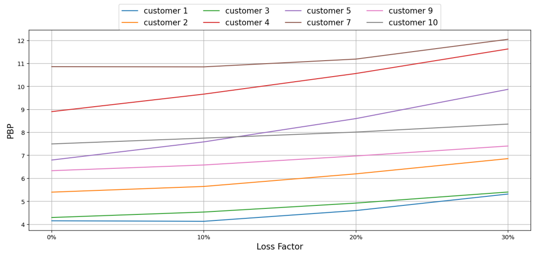

(b) Loss factor vs PBP for selected customers.

Sensitivity Analysis: Flow Fractions

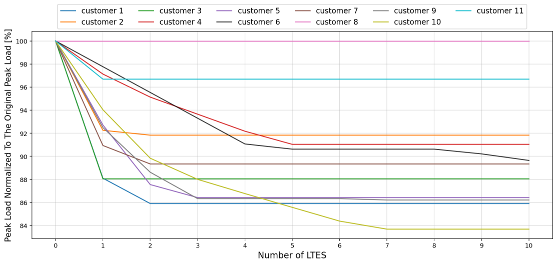

(a) Peak load reduction, $w^{max} = 0.2$.

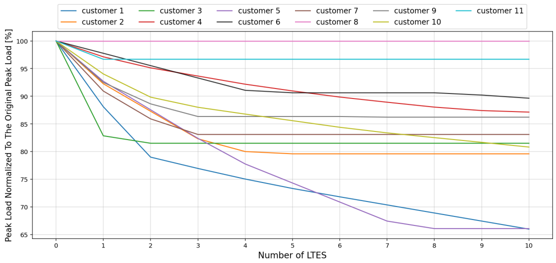

(b) Peak load reduction, $w^{max} = 0.5$.

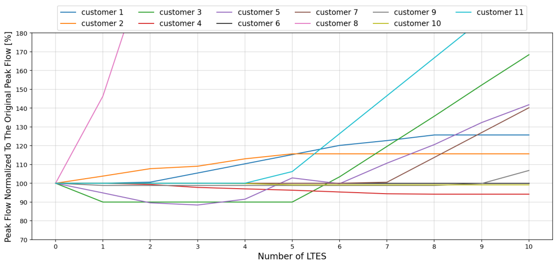

(a) Peak flow reduction, $w^{max} = 0.2$.

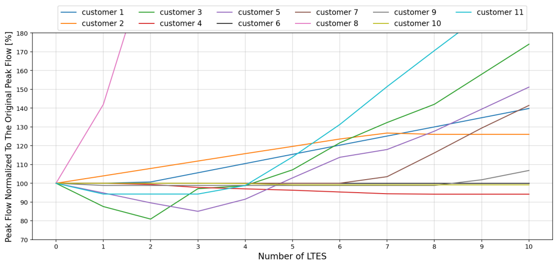

(b) Peak flow reduction, $w^{max} = 0.5$.

Calculation of Shared Investment Cost (r = 9%)

Willingness to pay for producer:

$$NPV = 0 = -(c^{inv} \ + \ (2000 \cdot \Delta load)) \ + \ ((1273 - 754) \cdot \Delta load) \cdot \frac{1 - (1 + 0.09)^{-10}}{0.09} \tag{C.1}$$

$$\frac{c^{inv}}{\Delta load} = 1\ 331 \quad \frac{SEK}{reduced\ kW} \tag{C.2}$$

Willingness to pay for customer:

$$NPV = 0 = -c^{inv} \ + \ (754 \cdot \Delta load) \ \cdot \ \frac{1 - (1 + 0.09)^{-10}}{0.09} \tag{C.3}$$

$$\frac{c^{inv}}{\Delta load} = 4\ 839 \quad \frac{SEK}{reduced\ kW} \tag{C.4}$$

Willingness to pay for both parties per installed kWh of LTES:

$$INV^{prod,0-7} = 1\ 331 \ \frac{SEK}{reduced\ kW} \ \cdot 0.72 \ \frac{reduced\ kW}{kWh\ LTES} = 958 \ \frac{SEK}{kWh\ LTES} \tag{C.5}$$

$$INV^{cust,0-7} = 4\ 839 \frac{SEK}{reduced\ kW} \cdot 0.72 \ \frac{reduced\ kW}{kWh\ LTES} = 3\ 484 \ \frac{SEK}{kWh\ LTES} \tag{C.6}$$

$$INV^{prod,8-60} = 1\ 331 \ \frac{SEK}{reduced\ kW} \ \cdot 0.17 \ \frac{reduced\ kW}{kWh\ LTES} = 226 \ \frac{SEK}{kWh\ LTES} \tag{C.7}$$

$$INV^{cust,8-60} = 4\ 839 \frac{SEK}{reduced\ kW} \cdot 0.17 \ \frac{reduced\ kW}{kWh\ LTES} = 822 \ \frac{SEK}{kWh\ LTES} \tag{C.8}$$

Minimum reduction to maintain profitable with the assumed investment cost:

$$1\ 331x \ + \ 4\ 839x \ = 2\ 149 \tag{C.9}$$

$$x = 0.35 \tag{C.10}$$

D

Appendix 4: Code/Model Configuration 1

```
    #%% main function

#Main Function, input of customer data frame, total production data
    frame and number of LTES units
def optimize_customer_config1(kund_df,df_totprod, n):
    # Start with importing parameters
    # ######## PARAMETERS ########
    cust_load = kund_df.iloc[:, 0].values # Load values of the
   customers
    cust_flow = kund_df.iloc[:,1].values # Flow of customer in kg/s
    comp_use = df_totprod.iloc[:,3].values # Compressor cooling
   each hour
    abs_use = df_totprod.iloc[:,2].values # Absorption Cooling each
    hour

    Tret_cust = kund_df.iloc[:,4].values + 2 # T return customer
    Tret_prod = kund_df.iloc[:,4].values # T return production

    Tsup_cust = kund_df.iloc[:,3].values +2 #T supply customer
    Tsup_prod = kund_df.iloc[:,3].values # T supply producer

    T = len(cust_load)
    D = T // 24 #// = gives no decimals, only integers

    # --- Charging and Discharging time windows ---
    start_charge = 20
    end_charge = 7
    start_discharge = 8
    end_discharge = 19

    Cp = 4184 # Assumed Constant for Water/HTF
    T_PCM_melt = 10 # Melting temperature for PCM
    numb_LTES = n # Number of LTES units


    m_prod= 1 * numb_LTES #maximal flow for charging in kg/s
    max_PCM_cap = 44 * numb_LTES  # How much storage capacity [kWh]
    44kWh = 1m3 (according to pcmproducts.net)

    flow_customer = cust_flow # Mass flow at customer assumed equal
    to producer
```

```

    T_PCM_out_charge = T_PCM_melt - 2 # Output temperature of charging
    T_PCM_out_discharge = T_PCM_melt + 2 # Output temperature of discharging

    SOC_current = 0                    # State of charge at hour 0
    total_SOC = [SOC_current]          # list with SOC /hour. Puts SOC_current as first hour
    total_new_load = np.zeros(T)       # array for optimized load, hourly
    total_charge = np.zeros(T)         # array for optimized charge, hourly
    total_discharge = np.zeros(T)      # array for optimized discharge, hourly
    total_peak = []                    # list with daily peak (after LTES installment)
    total_new_flow = np.zeros(T)       # array with new flow
    new_Tret_cust = []                 # list with new return temperature on customer side post LTES
    new_Tret_prod = []                 # list with new return temperature on producer side post LTES

# Define charge/discharge periods
# Function returns True if the hour is in charge/discharge window
    def is_charge_hour(h):
        return (h >= start_charge or h <= end_charge)

    def is_discharge_hour(h):
        return (h >= start_discharge and h <= end_discharge)


    # ######## Optimize Daily Peak ########

    for d in range(D):
        start = d*24 # Make sure the hour/index is correct
        end = start+24 # End of daily peak reduction 24h later

        day_load = cust_load[start:end] # Load of the day
        day_flow = flow_customer[start:end] # Flow of the day

        T_ret_cust = Tret_cust[start:end] # Return temperature on customer side
        T_sup_cust = Tsup_cust[start:end] # Supply temperature on customer side

        T_sup_prod = Tsup_prod[start:end] # Supply temperature on producer side
        T_ret_prod = Tret_prod[start:end] # Return temperature on producer side

        # ######## MODEL ########
        #State that the problem is a minimizing problem of daily peak
        model = pl.LpProblem(f"Day_{d}", pl.LpMinimize)

```

```python
    # Needs 25 in range to state SOC for hour zero of the coming day,
    # ######## VARIABLES ########
    # Dictionary with 25 positions of variable SOC, max = max_PCM_cap
    SOC = pl.LpVariable.dicts("SOC", range(25), lowBound=0, upBound=max_PCM_cap)
    # Dictionary with 24 variables of Charging and Discharging
    charge = pl.LpVariable.dicts("Charge", range(24), lowBound=0)
    discharge = pl.LpVariable.dicts("Discharge", range(24), lowBound=0)
    # Variable of the daily peak, that is to be optimized
    peak_day = pl.LpVariable("peak_day", lowBound=0)

    # ######## CONSTRAINTS ########
    # Optimal Function
    weight = 0.001 # state 0.0001 for optimal (10 factor)
    model += peak_day + (weight * pl.lpSum(charge[t] * day_load[t] for t in range(24)))

    # Initial SOC
    model += SOC[0] == SOC_current

    # Constraints per timme
    for t in range(24):

        hour = kund_df.index[start+t].hour # Get the correct date and hour

        # SOC-Dynamic (Checks for the uocoming hour)
        model += SOC[t+1] == SOC[t] + charge[t] - discharge[t]

        # Peak constraint
        model += peak_day >= day_load[t] + charge[t] - discharge[t]

        # Charging during night
        if not is_charge_hour(hour):
            model += charge[t] == 0

        # Discharging during daytime
        if not is_discharge_hour(hour):
            model += discharge[t] == 0

        # Customer Return Temperature Check (more than 12)
        if T_ret_cust[t] <= T_PCM_out_discharge:
            model += discharge[t] == 0
        else:
            model += discharge[t] <= ((day_flow[t] * Cp * (T_ret_cust[t] - T_PCM_out_discharge))/1000)

        # Producer Supply Temperature Check (less than 8)
        if T_sup_prod[t] >= T_PCM_out_charge:
            model += charge[t] == 0
        else:
```

```
            model += charge[t] <= ((m_prod * Cp * (T_PCM_out_charge - T_sup_prod[t]))/1000)

        # No negative load
        model += day_load[t] + charge[t] - discharge[t] >= 0


    # Solve LP
    #PULP_CBC_CMD = solver using Coin-or Branch and Cut
    #False is only referring to printing the solverlog or not
    solver = pl.PULP_CBC_CMD(msg=False)
    model.solve(solver) # model into solver

    # ######## EXTRACT DAILY RESULTS ########
    # Discharge and Charge
    charge_opt = np.array([pl.value(charge[t]) for t in range(24)])
    discharge_opt = np.array([pl.value(discharge[t]) for t in range(24)])
    # SOC
    SOC_opt = np.array([pl.value(SOC[t+1]) for t in range(24)])
    # New Load
    new_load = day_load + charge_opt - discharge_opt
    # Daily Peak
    peak = pl.value(peak_day)

    # Flow
    for a in range(len(day_flow)):
        if day_flow[a] == 0:
            new_Tret_cust.append(T_ret_cust[a])
            new_Tret_prod.append(T_ret_prod[a])

        else:
            Temp = (T_ret_cust[a] - (discharge_opt[a]*1000/(Cp * day_flow[a])))
            new_Tret_cust.append(Temp)
            new_Tret_prod.append(Temp - 2)

    mflow_charge = []
    for temp in range(len(T_sup_prod)):
        if charge_opt[temp] == 0:
            mflow_charge.append(0)
        else:
            mflow_charge.append((charge_opt[temp] * 1000) / (Cp * (T_PCM_out_charge - T_sup_prod[temp])))
    # New flow, adding the charging flow
    new_flow = day_flow + np.array(mflow_charge)

    # Add to lists/arrays created earlier
    total_new_load[start:end] = new_load
    total_charge[start:end] = charge_opt
    total_discharge[start:end] = discharge_opt
    total_SOC.extend(SOC_opt)
    total_peak.append(peak)
    total_new_flow[start:end] = new_flow

```

```
        # Set Current SOC to the last value of the dict (Hour 00:00)
        SOC_current = SOC_opt[-1]


    # ######## SUM ALL RESULTS ########
    PCM_opt = max(total_SOC)
    old_peak = max(cust_load)
    new_peak = max(total_new_load)

    old_flow_peak = max(cust_flow)
    new_flow_peak = max(total_new_flow)

    comp_charge = []
    abs_discharge = []

    total_SOC.pop(-1) #Remove Value 25

    dT_flow = (cust_flow - total_new_flow)
    dT_flow_max = max(dT_flow)

    for a in range(T):
        if comp_use[a] > 0 and total_charge[a] > 0: # Number of hours we charge while using compressor
            comp_charge.append(1)
        else:
            comp_charge.append(0)

        if comp_use[a] == 0 and total_discharge[a] > 0: # Number of hours we charge while using absorption
            abs_discharge.append(1)
        else:
            abs_discharge.append(0)


    # ######## EXTRACT ALL RESULTS AND RETURN ########
    #Gather Results in a DataFrame, each per hour wiht time index
    result_config1s_df = pd.DataFrame({
    "old_load": cust_load,                  # Old Load per hour
    "new_load": total_new_load,             # New Load per hour
    "charge": total_charge,                 # Total Charge
    "discharge": total_discharge,           # Total Discharge
    "SOC": total_SOC,                       # Total SOC
    "old_flow": cust_flow * 3600/997,       # Old Flow
    "new_flow": total_new_flow * 3600/997, # New Flow
    "T_sup_prod": Tsup_prod,                # T Supply Producer
    "T_ret_prod": Tret_prod,                # T Return Producer
    "T_sup_cust": Tsup_cust,                # T Supply Customer
    "T_ret_cust": Tret_cust,                # T Return Customer
    "new_Tret_cust": new_Tret_cust,         # New T return Customer
    "comp_charge": comp_charge,             # Compression Charge
    "abs_discharge": abs_discharge          # Absorption Discharge
    }, index=kund_df.index)

    # The Function Returns:
    return {
```

```
        "PCM_opt": PCM_opt,              # Value (PCM storage
   capacity)
        "number_LTES": numb_LTES,        # Number of LTES
        "old_peak": old_peak,            # Value (max peak old)
        "new_peak": new_peak,            # Value (max peak new)
        "old_flow_peak": old_flow_peak * 3600/997, # Convert kg/s
   -> m3/h, Value (max peak old)
        "new_flow_peak": new_flow_peak * 3600/997, # Convert kg/s
   -> m3/h, Value (max peak new)
        "charge": total_charge,          #ilst of charging per hour
        "discharge": total_discharge,    #list of discharging per
   hour
        "SOC": total_SOC,                #list of SOC per hour
        "new_load": total_new_load,      #list of new load per hour
        "old_load": cust_load,           #list of old load per hour
        "old_flow": cust_flow * 3600/997, # Convert kg/s -> m3/h,
   list of old flow
        "new_flow": total_new_flow * 3600/997, # Convert kg/s -> m3
   /h, list of new flow
        "dT_flow": dT_flow * 3600/997,   # Convert kg/s -> m3/h,
   list of increased new flow difference
        "dT_flow_max": dT_flow_max * 3600/997, # Convert kg/s -> m3
   /h, Value (max increased flow difference)
        "comp_charge": comp_charge,      # List of compression
   charge per hour
        "abs_discharge": abs_discharge, # List of absorption charge
    per hour
        "result_config1": result_config1s_df # Results Dataframe
   from above
    }
```

E

Appendix 5: Code/Model Configuration 2

```
 def optimize_customer_config2(kund_df,df_totprod,n):
 kund_load = kund_df.iloc[:, 0].values #load profiles customers
 kund_flow = kund_df.iloc[:,1].values #flow profiles customer

 Tret_cust = kund_df.iloc[:,4].values + 2 #return temperature
secondary side
 Tret_prod = kund_df.iloc[:,4].values #return temperature
primary side

 Tsup_cust = kund_df.iloc[:,3].values +2 #supply temperature
secondary side
 Tsup_prod = kund_df.iloc[:,3].values #supply temperature
primary side


 T = len(kund_load)
 D = T // 24 #// = integer division

 # charging and discharging windows
 start_charge = 20
 end_charge = 7

 start_discharge = 8
 end_discharge = 19

 Cp = 4184
 T_PCM_melt = 10 #mtelting temperature PCM

 e = 0.001 #small value connecting the binary variable to
discharging
 m_max = 0.3 #flow fraction
 eta = 1 #loss factor

 numb_PCM = n #number of LTES units

 m_charge = 1 * numb_PCM #maximum flow constraint
 max_PCM_cap = 44 * numb_PCM  # LTES capacity

 flow_customer = kund_flow #flow customer

 #Temperature constraints for charging and discharging
```

```
    T_PCM_out_charge = T_PCM_melt - 2
    T_PCM_out_discharge = T_PCM_melt + 2


    SOC_current = 0
    total_SOC = [SOC_current]
    total_new_load = np.zeros(T)
    total_charge = np.zeros(T)
    total_discharge = np.zeros(T)
    total_peak = []
    total_new_flow = np.zeros(T)
    new_Tsup_mix = []
    m_dis = np.zeros(T)
    total_new_flow_customer = []
    dT_overall = np.zeros(T)
    mflowcharge = np.zeros(T)


    #charging/discharging window constraints
    def is_charge_hour(h):
        return (h >= start_charge or h <= end_charge)

    def is_discharge_hour(h):
        return (h >= start_discharge and h <= end_discharge)


    for d in range(D):
        start = d*24
        end = start+24

        day_load = kund_load[start:end]
        cust_flow = flow_customer[start:end]

        T_ret_cust = Tret_cust[start:end]
        T_sup_cust = Tsup_cust[start:end]

        T_sup_prod = Tsup_prod[start:end]
        T_ret_prod = Tret_prod[start:end]

        M_dis = max(day_load)

        #Minimizes each day individually
        model = pl.LpProblem(f"Day_{d}", pl.LpMinimize)

        #Variables
        SOC = pl.LpVariable.dicts("SOC", range(25), lowBound=0, upBound=max_PCM_cap)
        charge = pl.LpVariable.dicts("Charge", range(24), lowBound=0)
        discharge = pl.LpVariable.dicts("Discharge", range(24), lowBound=0)
        peak_day = pl.LpVariable("peak_day", lowBound=0)
        m_dis_part = pl.LpVariable.dicts("m_dis_part", range(24), lowBound = 0, upBound = m_max)
        on_dis = pl.LpVariable.dicts("on_dis", range(24), cat="Binary")
```

```python

    #Objective function
    weight = 0.001 #weight for charging penalty
    model += peak_day + (weight * pl.lpSum(charge[t] * day_load[t] for t in range(24)))



    model += SOC[0] == SOC_current


    # Constraints (hourly)
    for t in range(24):
        hour = kund_df.index[start+t].hour


        # No negative load
        model += day_load[t] + charge[t] - discharge[t] >= 0

        # Peak constraint
        model += peak_day >= day_load[t] + charge[t] - discharge[t]

        # SOC constraint
        model += SOC[t+1] == SOC[t] + charge[t] - discharge[t]


        # Charging window constraint
        if not is_charge_hour(hour):
            model += charge[t] == 0

        # Discharging window constraint
        if not is_discharge_hour(hour):
            model += discharge[t] == 0

        #Temperature constraint discharging
        if T_ret_cust[t] <= T_PCM_out_discharge:
            model += discharge[t] == 0

        else:
            model += discharge[t] == ((cust_flow[t]*m_dis_part[t] * Cp * (T_ret_cust[t] - T_PCM_out_discharge))/1000)

        #Temperature constraint charging
        if T_sup_prod[t] >= T_PCM_out_charge:
            model += charge[t] == 0

        else:
            model += charge[t] <= ((m_charge * Cp * (T_PCM_out_charge - T_sup_prod[t]))/1000)

        #Flow fraction constraint
        model += discharge[t] <= M_dis * on_dis[t]
        model += m_dis_part[t] <= m_max * on_dis[t]
        model += discharge[t] >= e * on_dis[t]

```

```


    # Solver
    solver = pl.PULP_CBC_CMD(msg=False)
    model.solve(solver) #den skickar modellen in i solvern

    # Extract results
    charge_opt = np.array([pl.value(charge[t]) for t in range(24)])
    discharge_opt = np.array([pl.value(discharge[t]) for t in range(24)])
    SOC_opt = np.array([pl.value(SOC[t+1]) for t in range(24)])
    m_dis_part_opt = np.array([pl.value(m_dis_part[t]) if pl.value(m_dis_part[t]) is not None else 0 for t in range(24)])
    peak = pl.value(peak_day)

    new_flow_discharge = []

    for i in range(len(cust_flow)):
        if discharge_opt[i] == 0:
            new_flow_discharge.append(cust_flow[i])
            total_new_flow_customer.append(cust_flow[i]*3600/997)
        else:
            x = ((day_load[i] - discharge_opt[i])*1000) / (Cp * (T_ret_prod[i] - T_sup_prod[i]))
            new_flow_discharge.append(x)
            total_new_flow_customer.append((x + cust_flow[i]*m_dis_part_opt[i])*3600/997)

    flow_PCM = cust_flow * m_dis_part_opt

    Tsup_mixed = np.zeros(24)
    flow_dis = np.zeros(24)

    for h in range(len(cust_flow)):
        if T_ret_prod[h] != T_sup_prod[h]:
            flow_dis[h] = ((day_load[h] - discharge_opt[h])*1000) / (Cp * (T_ret_prod[h] - T_sup_prod[h]))
            Tsup_mixed[h] = ((flow_dis[h] *T_sup_cust[h]) + (flow_PCM[h] * T_PCM_out_discharge))/(flow_dis[h] + flow_PCM[h])
        else:
            flow_dis[h] = 0
            Tsup_mixed[h] = T_sup_cust[h]

    mflow_charge = []

    for temp in range(len(T_sup_prod)):

        if charge_opt[temp] == 0:
            mflow_charge.append(0)

        else:
            mflow_charge.append((charge_opt[temp] * 1000) / (Cp * (T_PCM_out_charge - T_sup_prod[temp])))

```

```
        new_flow = np.array(new_flow_discharge) + np.array(mflow_charge)


        new_load = day_load + charge_opt - discharge_opt

        dT_ov = T_ret_prod - T_sup_prod

        total_new_load[start:end] = new_load
        total_charge[start:end] = charge_opt
        total_discharge[start:end] = discharge_opt
        total_SOC.extend(SOC_opt)
        total_peak.append(peak)
        total_new_flow[start:end] = new_flow
        new_Tsup_mix[start:end] = Tsup_mixed
        m_dis[start:end] = m_dis_part_opt
        dT_overall[start:end] = dT_ov

        SOC_current = SOC_opt[-1]

        mflowcharge[start:end] = np.array(mflow_charge)

    PCM_opt = max(total_SOC)
    old_peak = max(kund_load)
    new_peak = max(total_new_load)

    total_SOC.pop(-1)

    dT_cust = new_Tsup_mix - Tsup_cust
    dT_flow = (kund_flow - total_new_flow) *3600/997
    dT_flow_max = max(dT_flow)
    old_flow_peak = max(kund_flow)
    new_flow_peak = max(total_new_flow)

    result_config2_df = pd.DataFrame({
    "old_load": kund_load,
    "new_load": total_new_load,
    "load_difference": kund_load - total_new_load,
    "charge": total_charge,
    "discharge": total_discharge,
    "SOC": total_SOC,
    "old_flow": kund_flow * 3600/997,
    "new_flow": total_new_flow * 3600/997,
    "dT_flow": dT_flow,
    "T_sup_prod": Tsup_prod,
    "T_ret_prod": Tret_prod,
    "dT_overall": dT_overall,
    "T_sup_cust": Tsup_cust,
    "T_ret_cust": Tret_cust,
    "dT_cust": dT_cust,
    "new_T_sup_mixed": new_Tsup_mix,
    "m_dis_part": m_dis,
    "new_customer_flow": total_new_flow_customer,
    "mflow_charge": mflowcharge *3600/997
    }, index=kund_df.index)

```

```
    return {
        "PCM_opt": PCM_opt,
        "number_PCM": numb_PCM,
        "old_peak": old_peak,
        "new_peak": new_peak,
        "old_flow_peak": old_flow_peak * 3600/997,
        "new_flow_peak": new_flow_peak * 3600/997,
        "charge": total_charge,
        "discharge": total_discharge,
        "SOC": total_SOC,
        "new_load": total_new_load,
        "old_load": kund_load,
        "old_flow": kund_flow * 3600/997,
        "new_flow": total_new_flow * 3600/997,
        "dT_flow": dT_flow,
        "dT_flow_max": dT_flow_max,
        "result_config2_with_time": result_config2_df,
        "dT_overall": dT_overall
    }
```

DEPARTMENT OF ARCHITECTURE AND CIVIL ENGINEERING
CHALMERS UNIVERSITY OF TECHNOLOGY
Gothenburg, Sweden
www.chalmers.se

CHALMERS